Lamie, Nathan. 2020. Experiments on a Linear Augmented Fire Boom Configuration to Increase Burn Removal Efficiency and Reduce Emissions of OCS In Situ Crude Oil Burns. (Bureau of Safety and Environmental Enforcement Oil Spill Response Research Project # 1093).

Bureau of Safety and Environmental Enforcement (BSEE) Report: Experiments on a Linear Augmented Fire Boom Configuration to Increase Burn Removal Efficiency and Reduce Emmissions of OCS In Situ Crude Oil Burns

Nathan Lamie, David Cooper, Ian Buist

Final Report

To

Bureau of Safety and Environmental Enforcement (BSEE)

Experiments on a Linear Augmented Fire Boom Configuration to Increase Burn Removal Efficiency and Reduce Emissions of OCS In Situ Crude Oil Burns

(BSEE Oil Spill Response Research Project E17PG00032)

Nathan Lamie

U.S. Army Engineer Research and Development Center

Cold Regions Research and Engineering Laboratory

David Cooper and Ian Buist

SL Ross Environmental Research Ltd.

October 2020

Table of Contents

List of Figures

Acknowledgements

This study was funded by the Bureau of Safety and Environmental Enforcement (BSEE), U.S. Department of the Interior, Washington, D.C., under Contract E17PG00032. The U.S. Environmental Protection Agency (EPA), Washington D.C., conducted the emissions and residue analysis and was funded by BSEE under the Contract E17PG00035.

Disclaimer

This final report has been reviewed by the BSEE and approved for publication. Approval does not signify that the contents necessarily reflect the views and policies of the BSEE, nor does mention of the trade names or commercial products constitute endorsement or recommendation for use.

Summary

The objective of the project was to increase burn and combustion efficiencies for *in situ* burning of crude oil by changing the geometry of the oil slick and supplementing the burn with compressed air. The first technological advancement investigated *in situ* burns in long, narrow, parallel fire boom configurations. This arrangement may allow better penetration of air into the burn zone to both reduce soot yields and increase radiant heat feedback to the burning slick to increase oil removal efficiency. The second technology advancement investigated augmenting the linear burns using compressed air injected into the flames to promote better mixing of fuel and naturally entrained air, multiply burning rates, and further reduce smoke yield. The influence of boom configuration on *in situ* burn efficiencies were characterized by assessing burn efficiencies using oil mass in mass-mass out data. Additionally, through a collaboration with the U.S. Environmental Protection Agency (EPA), combustion efficiencies and chemical analysis of burn residues were performed. Results were used to determine the amount of pollutant and residue constituent per amount of oil burned and compared across boom configurations.

To systematically explore the effect of boom geometry and air injection on burning efficiency (i.e, burning rate enhancement and emission reduction), experiments were performed in rectangular oil slicks of varying aspect rations (1:1 to 9:1, length to width) and air volumes. The experiments were divided into 2 phases based on scale: intermediate-scale (1.2 m wide by 11 m long SL Ross wave tank), and large-scale (2.4 m wide,14.3 m long, 2 m deep CRREL wave tank).

Small-scale *in situ* burn tests with different aspect ratios, and air injection configurations were conducted in the SL Ross wind/wave tank. The goal of the experiments was to measure the effects of the various configurations and compressed air injection on the burn characteristics under controlled conditions, and identify the most promising combinations of burn layout and air injection settings. A total of 38 experiments were conducted in small metal fire boom models (burn area of 0.16 m^2) varying boom aspect ratio, wave height (calm and a sinusoidal wave of 3 cm amplitude with a 0.8 s period), air injection nozzle angle (45° and 90° from vertical upwards) and air flow rate (0, 2 and 3 scfm).

The small-scale experimental results showed that

1. There appears to be little or no appreciable change in burn efficiency with increasing aspect ratio (the ratio of length to width of the model fire boom) at this scale;
2. Calm conditions generally result in higher burn efficiency at this scale;
3. Increased air injection increases burn efficiency at this scale;
4. 90° nozzles generally result in higher efficiency than 45° nozzles at this scale;
5. Increasing aspect ratio (longer, narrower burns) results in declining burn rate;
6. Calm conditions generally result in higher burn rates;
7. Increased air injection increased burn rate; and,
8. 90° nozzles generally result in higher burn rate than 45° nozzles at this scale.

Using the results of the small-scale test burns, particularly the configurations that produced the most efficient burns, a detailed design for the full-scale linear augmented fire boom was produced. The design was based on enhancing a 50-foot section of commercially-available DESMI PyroBoom® fire boom with:

i. adjustable structural components to hold the fire boom in rectangular shapes of different aspect ratios in waves, and
ii. angled compressed air nozzles and compressed air supply hoses.

A 50-foot section of the modified fire boom was positioned to contain the experimental burns in the CRREL wave tank. The aspect ratio of the burn area in the modified fire boom was varied from 1:1 to 9:1, length to width. The area encompassed by the boom was kept constant at approximately 3.4 m^2.

In general, the data from the large-scale experiments in the CRREL wave tank showed that:

1. All the experiments produced a high oil removal efficiency (> 88%);
2. There appears to be a slight increase in burn efficiency with increasing aspect ratio in calm conditions (due to better aeration of the flames);
3. Calm conditions generally result in higher burn efficiency than burning in waves, as one might expect (waves cause gentle mixing of the slick, which likely increases heat transfer through the burning oil which in turn causes earlier extinction); however, the presence of waves, regardless of air or boom ration condition, always lowers the oil weight. Higher boom rations have higher MCE values than lower room rations. This is true for oil with loss, but only in the absence of waves. The boom ratio effect is possibly due to more efficient air penetration into the flame zone due to the thinner oil slick configuration;
4. Increased air injection does not seem to significantly affect burn efficiency (variability in the data masks any effects);
5. The lowest measured burn efficiency (88.8% mass removed) was measured with the 4:1 aspect ratio, in waves with the nozzles pointed at 135° (45° down towards the slick). This was potentially due to turbulent mixing of the burning oil layer by the jets of compressed air causing earlier onset of the vigorous burn phase and extinction than in the case of a quiescent burning oil layer;
6. The highest burn efficiency recorded (99.6% mass removed) was with a 9:1aspect ratio in calm conditions with no air injection (probably because of the additional aeration from the long, narrow fire, but no turbulence induced by compressed air nozzles).The estimated burn rate at an aspect ratio of 9:1 is lower than at an aspect ratio of 1:1 or 4:1 (because the longer narrower burn shape reduces the unit heat radiation back to the surface of the slick);
7. Waves reduce burn rate slightly;

8. There appears to be a slight increase in burn rate with air injection;
9. The lowest measured burn rate (1.6 mm/min) was measured with the 9:1 aspect ratio, in calm conditions with no air injection (as noted above, due to reduced radiant heat transfer to the slick); and,
10. The highest burn rate estimated (3.2 mm/min) was with a 4:1aspect ratio in waves with air injected at 135° from vertical up (i.e., 45° downward toward the burning slick). This is because the turbulent mixing energy of the compressed air impinging on the burning slick increases the convective heat transfer to the slick and thus increases the vaporization rate of the hot oil).
11. The narrow boom configuration (9:1, red points) has the lowest $PM_{2.5}$ emission factors and the highest combustion efficiency, but not necessarily the greatest amount of oil consumed,
12. The highest $PM_{2.5}$ emission factor is 160 g/kg oil consumed for the 1:1 aspect ratio control burn (no waves, no compressed air). The lowest emission factor is 60 g/kg for the case of the 9:1 aspect ratio fire boom, in waves, with air injected by 12 nozzles pointed up at 45°.
13. Combustion efficiencies increased at the boom aspect ratio increased (making the oil slick more linear), independent of air and wave treatments.
14. The 9:1 aspect ratio showed the best combustion efficiencies across all treatment, even though burn efficiencies were decrease with wave action.

Based on the results of the experiments, the following recommendations are made:

1. Further testing at CRREL is warranted to assess whether additional compressed air would reduce soot emission factors.
2. The system as tested, with a 185 scfm compressor, supplies about 100 g/s of compressed air to a fire burning about 100 g/s of crude oil. Stoichiometric air requirement is about 15 g air/g crude oil. Additional tests to determine how much more compressed air would be required to virtually eliminate soot would be useful.
3. Redesign compressed air system with field use in mind (i.e., use common air header built into boom floatation or skirt, like Hydro Fire Boom concept) and tow test at Ohmsett.
4. Consider use of central compressed air nozzles placed just above the fuel surface to allow wider aspect ratios (i.e., feed combustion air into central area of fire that is usually starved of combustion air).
5. Consider using multiple spouts with the optimum aspect ratio obtained from this study (9:1). A recent study (Wan et al., 2019) demonstrated that the interaction of multiple pool fires might lead to higher burning rate and flame height than single pool fire. The flame of the optimally spaced multiple spouts will couple and result a higher heat feedback to the pool surface. The spacing between the spouts will drag air into flame and reduce the soot production. By changing the length of the adjacent spouts (one short, one long spout) a fire whirl can be created to further enhance the burn efficiency.

1. Outline

This report is organized as:

- Section 2 present the background of the current study.
- Section 3, and 4 present experimental results for the small, and large-scale experiments.
- Section 5 presents the conclusions and future work.
- Appendices A to E further discusses the below topics;
  Appendix A: Small-scale Test Protocol.
  Appendix B: Test Plan, Data Sheets and Spreadsheets for Small-scale In-situ Burn Experiments.
  Appendix C: Test Plan, Data Sheets and Spreadsheets for CRREL Wave Tank In-situ Burn Experiments.
  Appendix D: Large-scale Test Protocol.
  Appendix E: EPA report "Analysis of Emissions and Residue from Methods to Improve Combustion Efficiency of In Situ Oil Burns".

2. Introduction

In situ burning is an effective response option for oil spills; however, the smoke plume, burn residues and black carbon soot from unburned oil and incomplete combustion are known drawbacks. The dramatic appearance of a large column of dark smoke rising from a burning slick can lead to significant public criticism. In situ burning has been discounted or curtailed due to concerns over the appearance of a smoke plume, despite the scientifically proven net environmental benefits of removing oil from the water surface. Improvements in technology to achieve a cleaner in situ burn would allow Federal On-Scene Commanders (FOSCs) to use the technique in more situations, with less worry about perceived negative environmental effects and potential public reaction.

2.1 Background

It is known that the rates of oil consumption and soot production are functions of the surface area of the burning slick. The generally accepted burn rate correlation with size for circular in situ crude oil fires (1) is:

$$\dot{r}'' = 3.5(1 - e^{-D}) \quad (1)$$

Where:

$\dot{r}''$ is the burning oil slick regression rate (mm/min)

D is the pool diameter (m)

The crude oil burn rate increases with pool diameter until it reaches about 3 m, at which point oil consumption levels off at around 3.5 mm/min. The oil consumption rate is limited by the radiant heat transfer back to the burning slick.

Smoke is produced by the incomplete combustion of crude oil, which is largely because of a lack of oxygen, or the inability to supply sufficient air to the center of the fire. Large in situ oil fires draw in large amounts of air and most of this entrained air is drawn upwards by the rising column of hot combustion gases. These gases do not penetrate to the middle of the burning slick. Fig. 1 shows the measured smoke yield for in situ burns of crude oil over a range of pool sizes (Koseki, 2000). The smoke yield increases with the pan diameter until about 3 m (e.g., from 0.055 kg smoke/kg oil burned in a 0.09-m pan to about 0.2 kg smoke/kg oil burned in a 3-m pan), but does not increase with further increases in diameter. Large-scale in situ burns of crude oil in fire booms at sea have diameters on the order of 40 m, will burn at about 3.5 mm/min and produce a yield of approximately 0.2 kg smoke/kg oil burned.

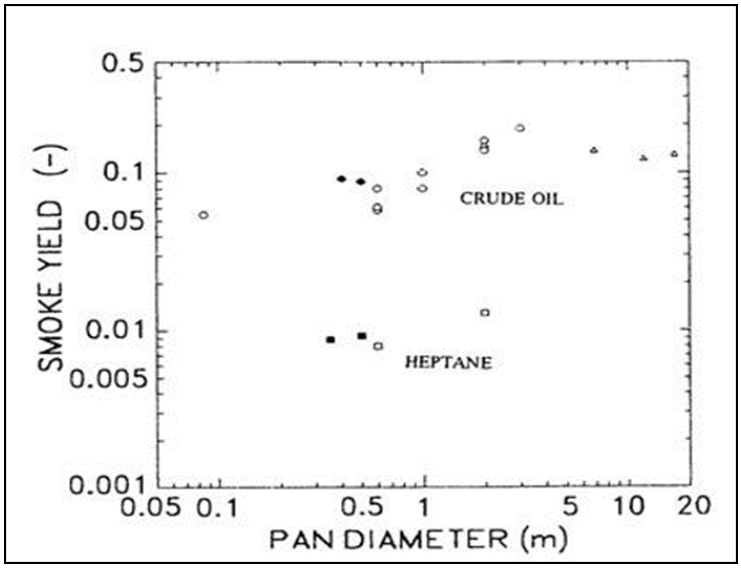

Figure 1: Smoke yield vs. in situ fire diameter (Koseki, 2000).

A considerable amount of research has already gone into ways to supplement the natural aeration of in situ burns to increase burn efficiency and rate and reduce soot emissions. A succinct summary of the earlier R&D was provided by the NRT Science and Technology Committee (NRT 1995). An update on recent studies is also available (Buist et al., 2013). A summary of the most relevant research follows:

2.1.1 University of Arizona Burners

In the early 1990s, research was undertaken on methods to enhance in-situ combustion of oil on water (Franken et al., 1992) by mechanically enhancing air entrainment into the combustion zone. Any buoyant column of heated rising air or hot combustion gases tends to have a swirl component, commonly referred to as the "Fire Whirl". This is a desirable effect as it encourages the entrainment of surrounding air and thereby increases aeration at the center of the flames. Several approaches to augmenting this fire whirl have been studied.

One method involved deploying sheet metal vanes around the perimeter of a burning pool to guide the in-flowing air into a cyclonic pattern (Fig. 2). Experiments performed in pools up to 2.4 m in diameter indicated that the addition of vanes increased the flame height by 200%, produced 50% less smoke, and burned faster and more efficiently than control experiments performed without the vanes (Franken et al., 1992). Tests were also carried out with different vane configurations (semi-circular and straight vanes), but no significant differences in burn rate or smoke production were found. It was determined that the vanes augmented the combustion by directing additional air to the center of the blaze, but the configuration or shape of the vanes seemed to have little impact on the combustion rate.

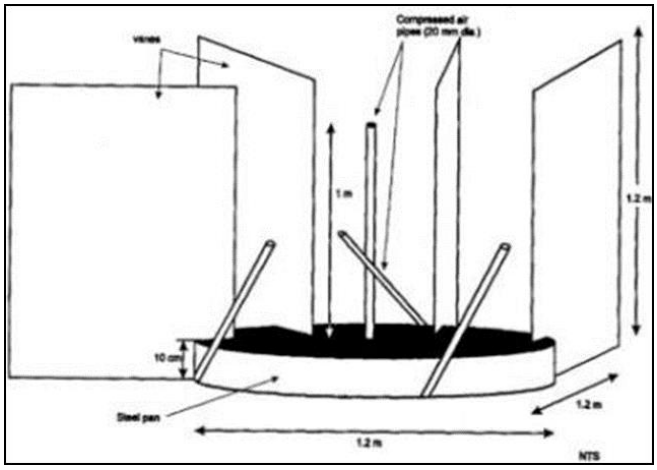

Figure 2: Burn pool showing vanes and compressed air jets.

Alaska Clean Seas tested the use of vanes around a larger-scale burn test of fire resistant boom in a large tank (ACS 1991) and found no induced vortex and no reduction in smoke. The increase in the size of the fire reduced the relative effectiveness of the vanes, and it was concluded that vanes alone may not be sufficient to significantly affect the flow of air into the combustion zone when ambient wind effects were present.

Subsequent experiments were designed to research an effective method of augmenting the vane ducting effect described above by supplying more air to the combustion zone. It was concluded that it was not effective in practice to supply all the stoichiometric air needed for combustion using low velocity, high volume air blowers; rather, "the addition of a few hundred cfm of compressed air is more utilitarian than the addition of more than 50,000 cfm of low velocity streams" (Franken et al., 1992).

An effective arrangement for the 1.2 m diameter pool with the vane structure, as described above, was to employ four high pressure air jets, with one placed about 1 m above the liquid surface, aimed straight up the axis of the flames, and the remaining three each placed about 0.6 m from the central axis, a few feet above the liquid and canted by some 30° from vertical (Fig. 2). These jets produced a "cyclonic" or "whirling" action within the flame in the same rotational sense as produced by the external vanes. The addition of the high velocity air increased the burning rate by about three- and one-half times, over that of the vanes alone.

2.1.2 **Marine Spill Response Center Burns**

In June 1995, MSRC conducted a series of large-scale pan burn tests to evaluate the effectiveness of several air injection techniques at reducing smoke emissions from in situ burning (Nordvik et al., 1995):

High Volume/Low Velocity Diffusers: Heavy industrial blowers were used to provide up to 150% of the stoichiometric air requirement (which for liquid petroleum oils is approximately 16 pounds of air per pound of oil). The air was delivered to the test pool via four ducts positioned outside the burn perimeter, aimed across the surface of the oil. This arrangement reduced smoke production, doubled the natural free burn rate and increased flame temperatures; however, much of the supplemental air was carried away by the rising hot air at the periphery of the flames, preventing the necessary aeration at the center of the burn. Also, the duct equipment was cumbersome and prone to failure in the high-temperature environment (Kupersmith, 1995).

Subsurface air bubblers: Adding air from underneath the burning zone was attempted. The use of a submerged bubbler did reduce smoke emissions; however, it also greatly reduced the burn rate and increased residue mass because the mixing and turbulence from the rising air bubbles disrupted the oil surface and reduced the temperature and volatilization rate of the slick.

Compressed Air Injection: The most successful was the compressed air injection system. Fig. 3 shows a pan burn with no air injected on the left, and with 66 m^3/min of compressed air injected into the fire from five 4-cm diameter nozzles (four canted 45° in a clockwise direction and one straight up in the center of the burn) on the right. The burn rate was increased from 3.5 to almost 5 mm/min using this technique; however, the system was very susceptible to wind. Even a slight breeze would move the fire away from the influence of the compressed air nozzles and cause an increase in smoke and decrease in burn rate.

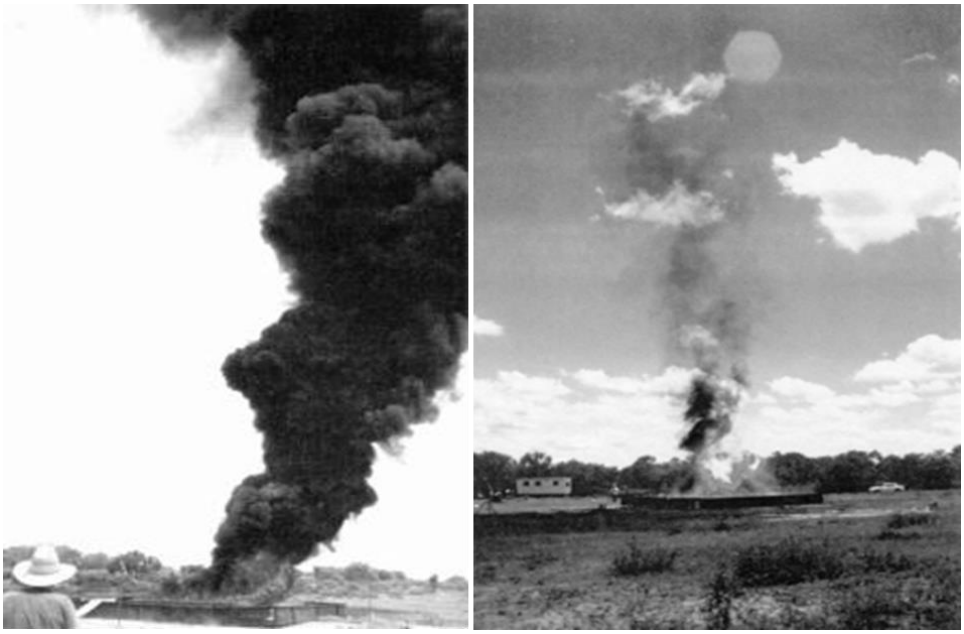

Figure 3: MSRC burn tests without and with aeration.

2.1.3 ExxonMobil Floating Burner

A recently-developed floating burner designed to combust crude oil recovered by skimmers on smaller recovery vessels has been based on the canted compressed air injection concept, among other enhancement techniques (Zhang et al, 2014). Figure 4 shows a test of the prototype burner at CRREL burning oil from a pan at a rate equivalent to about 15 mm/min.

Figure 4: Floating burner tests at CRREL.

2.2 Experimental Rationale

This project was in response to a BSEE Broad Agency Announcement (BAA) E174PS00024 under topic 3: Improved efficiency of burns by minimizing burn residue and/or soot. Although *in situ* burning of crude oil on water is effective at removing oil from marine environments it results in residues and black soot from incomplete combustion. To achieve a cleaner *in situ* burn, more air must reach the burning oil. The research completed to date suggests that there is significant potential for increased burn rate and efficiency, and reduced smoke emissions, by altering the burn geometry and layout, and supplementing the air supply during in situ burning. There is sufficient past research (summarized above) to conclude that the concept is at Technology Readiness Level 2, technology concept and speculative application formulated (Panetta and Potter, 2016).

It was decided to build on the existing research and investigate techniques to change the shape of the burning slick and supplement the air to the burn using simple, practical enhancements to existing spill response equipment. The design for such a system was determined through a work plan consisting of scaled tests in two wave tanks using crude oil and varying burn geometries, culminating in the burn testing of a near-full-scale prototype in relevant conditions at CRREL in a newly-refurbished outdoor wind/wave tank.

The first technology advancement that was investigated was in situ burns in long, narrow, parallel fire boom configurations (denoted as linear fires). This arrangement would allow better natural penetration of air into the burn zone to both reduce soot yields and increase radiant heat

feedback to the burning slick to increase oil removal efficiency. The existing research suggests that using linear burn geometry with a width of 2 m instead of semi-circular or semi-ellipsoidal burns could reduce soot yields by half (from 0.2 to 0.1). Concomitantly, the overall burn rate would naturally reduce slightly, to approximately 3 mm/min, due to the reduction in heat transfer back to the narrower burn area.

The second technology advancement investigated was to augment the linear burns using compressed air injected into the flames to promote better mixing of fuel and naturally entrained air, multiply burning rates, and further reduce smoke yield.

2.3 Objective and Goals

The objective of the project was to develop and test prototype technology and operational methods to significantly enhance in situ burning and improve burn efficiencies.

The goals of the project were as follows:

1. Demonstrate proof-of-concept and refine operational parameters through lab-scale testing in waves with burning crude oil.
2. Design and assemble a prototype in situ burning enhancement system that can be used with existing oil spill response equipment, such as commercially available fire booms.
3. Demonstrate the prototype full-scale enhanced in situ burning system under realistic conditions.
4. Use sophisticated real-time air emissions sensors for soot monitoring and residue characterization to assess the prototype in realistic burn conditions.

3. Small-Scale In-situ Burn Tests

Small-scale (i.e., approximate burn area of 1650 cm^2) in situ burn tests with different aspect ratios, and air injection configurations were conducted in the SL Ross wind/wave tank (Fig. 5). The objective of the small-scale experiments was to measure the effects of the various configurations and enhancements on the burn characteristics under controlled conditions, and identify the most promising combinations of burn layout and air injection settings.

The goals of these initial small-scale experiments were to:

1. Design and assemble lab-scale prototype augmented linear burn concepts for testing in the SL Ross wind/wave tank.
2. Conduct small-scale in-situ burn experiments with crude oil in the SL Ross wind/wave tank to determine the efficacy of each of the augmented linear burn concepts in reducing burn residue.
3. Conduct small-scale in-situ burn experiments with crude oil in the SL Ross laboratory wind/wave tank to determine the efficacy of each of the augmented linear burn concepts in reducing soot emissions.
4. Select the most promising fire boom layouts for larger scale tests at CRREL.

3.1 Equipment and Methods

The SL Ross laboratory wind/wave tank measures 1.2 m wide by 11 m long; water depth can be up to 1.2 m. For these tests the working water depth was 85 cm. For in situ burn tests, metal heat shields are installed along the sides of the tank and a metal fume hood is positioned over the burn area. Smoke from the burns is removed with a 200-m^3/min fan, through a 60-cm metal duct that is connected to the fume hood (Fig. 5).

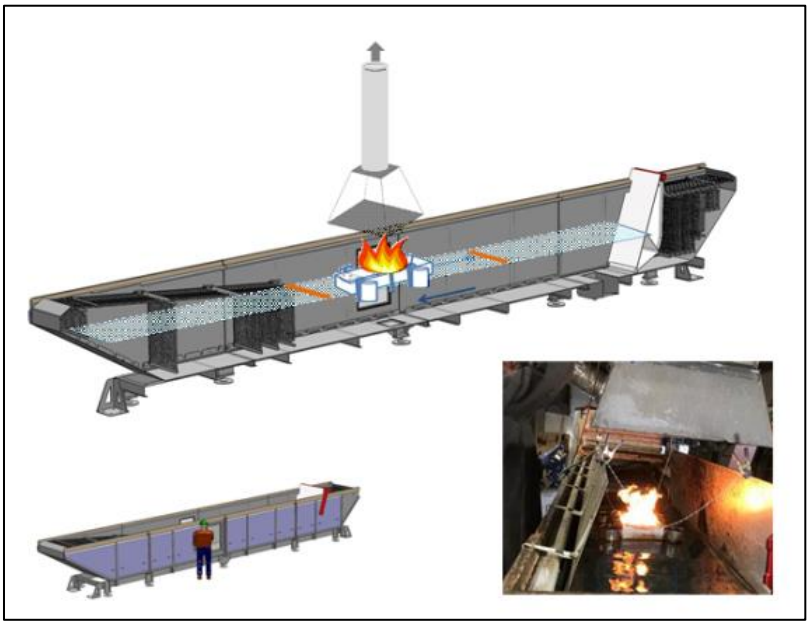

Figure 5: SL Ross Wind/Wave Tank.

Floating sheet metal models (Fig. 6) were fabricated and placed in the tank to simulate fire booms to contain the experimental burns. Three rectangular model fire booms were constructed. Each had an area of approximately 0.16 m^2, but with different length to width aspect ratios of 1.5:1, 3:1 and 6:1. The model dimensions are given in Table 1 and illustrated in Fig. 7. An aspect ratio of 6:1 was the longest that would fit completely under the wave tank's fume hood given the targeted working area.

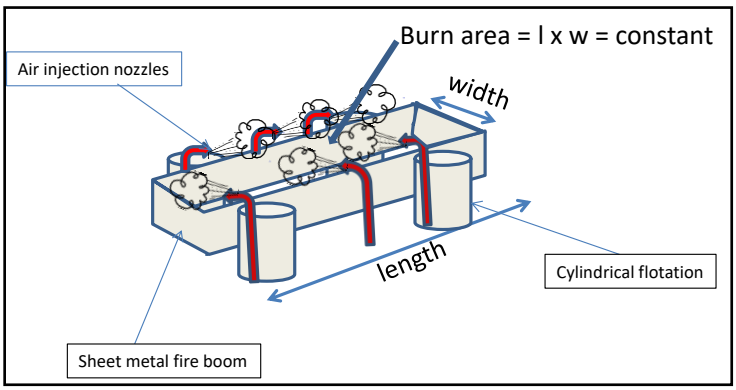

Figure 6: Schematic layout of sheet metal fire boom.

Table 1. Boom Model Dimensions

Aspect Ratio	Width (cm)	Length (cm)	Area (m^2)	Height
1.5:1	33.3	50	0.1665	20.3
3:1	23.3	70	0.1631	20.3
6:1	16.7	100	0.1670	20.3

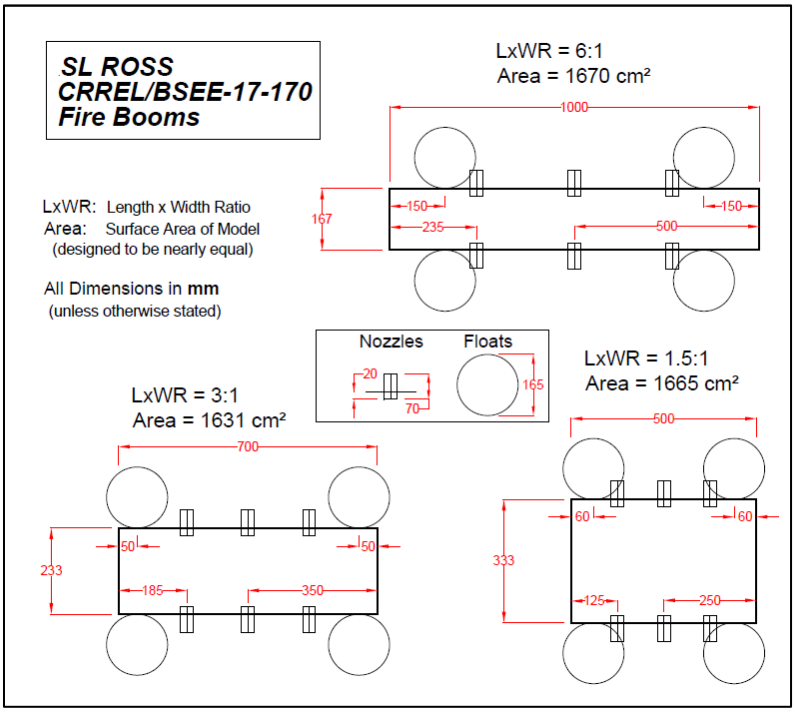

Figure 7: Schematic of fire boom model designs.

The booms were constructed of 18-gauge galvanized steel. Sheets were purchased and formed in-house. Each boom was constructed with two copper pipe cross braces placed under the water line (three cross braces for the 6:1 boom model). Floats were fashioned from 3.75-L paint cans.

Six compressed air nozzles that could be repositioned to direct air into the burn at two different angles were mounted in various positions along the top of the simulated fire boom to augment the natural combustion air. The air injection nozzles were assembled using ½" pipe and were attached to a 6-outlet manifold by flexible rubber hose positioned underwater (Fig. 8). The air nozzles consisted of stainless steel Spraying Systems nozzles with a diameter of 1.6 mm and a 0° spray angle mounted to the elbow fitting (e.g., Fig. 9). The angle of the nozzles from vertical could be altered between 90° and 45° by changing the elbow fitting on the top of the steel pipe (compare Figures 8 and 9). An Omega model FL4513 (range 0-8 SCFM) air rotameter was used to adjust and record the total air flow supplied to the six nozzles by a Husky Model: VT631505AJ(AGM05) 30-gallon 5.5 scfm compressor capable of producing 90 psig.

Figure 7 also shows the positioning of the compressed air nozzles. Figure 8 is a picture of the completed 6:1 aspect ratio model and Figure 9 compares the three models.

Figure 8: Photo of 6:1 fire boom model for SL Ross tank tests.

Figure 9: Comparison of fire boom models with different aspect ratios.

The burns were conducted with fresh (unweathered) ANS crude oil. The density of this crude was 0.863 g/cm^3 at 15°C and its viscosity was 11 cP at 15°C at a shear rate of 500 s^{-1}. The use of a crude oil (as opposed to a refined product) was necessary to simulate conditions at a US OCS spill, and for the residue characteristics to be relevant to field situations. The mass of oil initially added to the containment area and residue recovered was measured to allow burn removal efficiency to be calculated using Equation 2. The burns were videotaped and manually timed to permit estimates of burn rate using Equation 3.

Burn efficiency is the ratio of the mass of oil burned to the initial oil mass:

$$Burn\ Efficiency\ (vol\%) = \left[\frac{(Initial\ Oil\ Mass)\rho_{oil} - Residue\ Mass}{(Initial\ Oil\ Mass)\rho_{oil}}\right] \times 100 \quad (2)$$

The burn rate is calculated by dividing the volume of oil burned by the area of the fire and the burn time, as given below.

$$Burn\ Rate\ (mm/min) = \left[\frac{Initial\ Oil\ Mass - Residue\ Mass}{(Burn\ Time)(Burn\ Area)\rho_{oil}}\right] \quad (3)$$

Soot from each burn was collected by simple isokinetic stack sampling, using a vacuum pump to draw soot and gases from the fume hood through a stainless steel tube oriented parallel to the flow in the duct. Air and smoke from each experimental burn were passed through a pre-weighed filter paper to collect the particulate matter (Fig. 10).

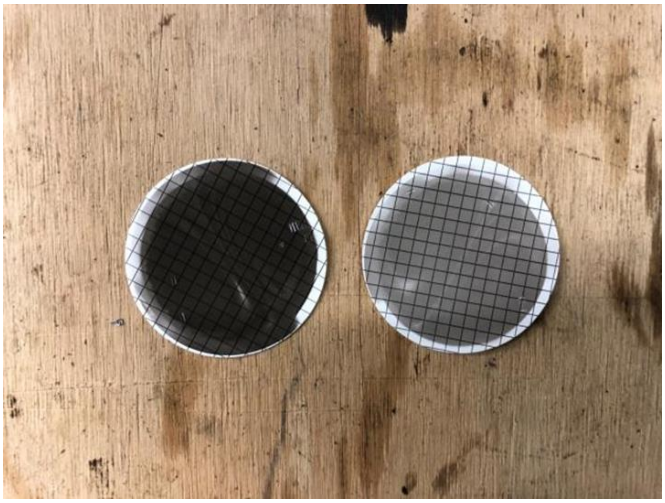

Figure 10: Soot collected on filter in the stack samples taken during small-scale burns.

The test protocol is explained in Appendix A. The test matrix is provided in Table 2. Three duplicate experiments were performed with each of the best combination of aspect ratio and compressed air to permit statistical analysis of the enhancements to the burn (i.e., soot and residue reduction) compared to three duplicates of the Base Case (Aspect Ratio 1.5:1 with no air injection in waves). A total of 36 experiments were conducted. The test plan can be found in Appendix B.

Table 2. Test Matrix

Fire Boom Aspect Ratio	Air Injection Configuration	Air Flow Rate	Waves
1.5:1	Base Case (No air)	0	Off On x 3
	Nozzle Configuration 1	2 scfm	Off On

		3 scfm	Off On
	Nozzle Configuration 2	2 scfm	Off On
		3 scfm	Off On
3:1	Base Case (No air)	0	Off On
	Nozzle Configuration 1	2 scfm	Off On
		3 scfm	Off On
	Nozzle Configuration 2	2 scfm	Off On
		3 scfm	Off On
6:1	Base Case (No air)	0	Off On
	Nozzle Configuration 1	2 scfm	Off On
		3 scfm	Off On
	Nozzle Configuration 2	2 scfm	Off On
		3 scfm	Off On

3.2 Results and Discussion

A total of 38 experiments were conducted varying boom aspect ratio, wave height (calm and a sinusoidal wave of 3 cm amplitude with a 0.8 s period), air injection nozzle angle (45° and 90° from vertical) and air flow rate (0, 2 and 3 scfm). Table 3 summarizes the key data from these tests. Key runs were repeated three times (see the colored highlighted rows in Table 3). Spreadsheets with all the data collected are given in Appendix B. Data sheets for each experiment can be found in Appendix B as can the spreadsheets used to analyze the data.

Table 3. Small-scale Experimental Results Summary (similarly-shaded rows are repeats)

Run	Date	Air Flow (SCFM)	Wave (h=3 cm; P= 0.8 s)	Nozzle Angle.	Boom Aspect Ratio (L:W)	Air Temp (C)	Water Temp (C)	Burn Area (cm^2)	Mass of Soot (g/hr)	Average Burn Rate (mm/min)	Burn Efficiency (mass %)
1	27-Jun-18	No	No	NA	1.5:1	24.9	21	1665	0.01	1.31	83.7

2	27-Jun-18	2	No	45	1.5:1	25.1	21	1665	0.01	1.23	82.6
3	27-Jun-18	2	Yes	45	1.5:1	25.3	21	1665	-0.24	1.00	64.0
4	27-Jun-18	No	Yes	NA	1.5:1	25.9	21	1665	0.00	1.03	59.6
5	27-Jun-18	3	No	45	1.5:1	26	21	1665	0.01	1.24	79.7
6	27-Jun-18	No	Yes	NA	1.5:1	26.6	21	1665	0.00	0.93	62.9
7	28-Jun-18	3	Yes	45	1.5:1	25.1	22	1665	0.01	0.84	61.6
8	28-Jun-18	No	Yes	NA	1.5:1	25.5	22	1665	0.01	0.99	64.8
9	29-Jun-18	2	No	90	1.5:1	26.3	22	1665	0.00	1.60	92.0
10	29-Jun-18	3	No	90	1.5:1	26.5	22	1665	0.01	2.75	93.6
11	29-Jun-18	3	Yes	90	1.5:1	26.9	22	1665	0.01	2.76	88.9
12	29-Jun-18	2	Yes	90	1.5:1	27.1	22	1665	0.00	1.25	79.3
13	03-Jul-18	No	No	NA	3.0:1	29.9	25	1631	0.01	1.09	79.1
14	03-Jul-18	2	No	90	3.0:1	29.6	25	1631	0.01	1.58	87.8
15	03-Jul-18	3	No	90	3.0:1	29.7	26	1631	0.01	2.44	92.2
16	03-Jul-18	2	Yes	90	3.0:1	29.8	26	1631	0.00	1.34	78.3
17	03-Jul-18	3	Yes	90	3.0:1	29.9	26	1631	0.00	1.94	87.0
18	03-Jul-18	No	Yes	NA	3.0:1	30.1	26	1631	0.00	1.12	66.9
19	04-Jul-18	2	Yes	45	3.0:1	30	26	1631	0.00	0.95	73.9
20	04-Jul-18	3	No	45	3.0:1	30.5	26	1631	0.00	1.01	76.4
21	04-Jul-18	3	Yes	45	3.0:1	31	26	1631	0.00	1.01	69.9
22	04-Jul-18	2	No	45	3.0:1	31.5	26	1631	0.00	1.13	79.1
23	05-Jul-18	2	No	45	6.0:1	30.1	26	1670	0.00	0.86	76.6
24	05-Jul-18	2	Yes	45	6.0:1	31	26	1670	0.00	0.56	62.5
25	05-Jul-18	3	No	45	6.0:1	31.5	26	1670	0.00	0.88	76.0
26	05-Jul-18	3	Yes	45	6.0:1	31.7	26	1670	0.00	0.66	67.2
27	06-Jul-18	No	No	NA	6.0:1	28	27	1670	0.01	0.83	77.5
28	06-Jul-18	No	Yes	NA	6.0:1	27.4	26	1670	0.00	0.71	68.8
29	06-Jul-18	2	No	90	6.0:1	27.2	26	1670	0.01	1.35	84.6
30	06-Jul-18	2	Yes	90	6.0:1	27.1	26	1670	0.00	0.88	72.7
31	06-Jul-18	3	No	90	6.0:1	27.1	26	1670	0.00	1.57	91.2

32	06-Jul-18	3	Yes	90	6.0:1	27	26	1670	0.00	1.22	82.1
33	12-Jul-18	3	Yes	90	6.0:1	27.6	24	1670	-0.01	1.35	84.3
34	12-Jul-18	3	Yes	90	6.0:1	27.9	24	1670	0.00	1.41	84.4
35	13-Jul-18	3	Yes	90	3.0:1	27.9	24	1631	0.01	1.97	86.5
36	13-Jul-18	3	Yes	90	3.0:1	27.9	24	1631	-0.01	1.92	87.1
37	13-Jul-18	3	Yes	90	1.5:1	28.7	24	1665	0.00	2.15	85.7
38	13-Jul-18	3	Yes	90	1.5:1	29.1	24	1665	0.00	2.16	86.1

3.2.1 Burn Efficiency

Figure 11 shows the effects of the experimental variables on burn efficiency. Note that the Y-axis extends only from 55 to 95% mass removal efficiency, in order to magnify the differences in the data. The burn efficiencies measured in calm conditions are shown with different shades of blue-filled diamond markers and lines; those measured in waves are shown with different shades of orange filled square markers and lines. Data points for runs with no additional compressed air are shown with the darkest shading; those with 2 scfm of compressed air added are moderately shaded; and, those with 3 scfm added are the lightest shading. Data points from experiments with the air nozzles at 45° are connected with single dashed lines while those with the nozzles at 90° are connected with double dashed lines.

For a circular burn with an initial thickness of approximately 6 mm (1 L of crude oil over an area of approximately 0.165 m^2) the expected removal efficiency would be 83% or, 1mm remaining at extinction (Buist et al, 2013).

In general, the data shows that:

- There appears to be little or no appreciable change in burn efficiency with increasing aspect ratio (the ratio of length to width of the model fire boom) at this scale (The error bars shown on select data points on Figure 10 indicate one standard deviation);
- Calm conditions generally result in higher burn efficiency at this scale;
- Increased air injection increases burn efficiency at this scale; and,
- 90° nozzles generally result in higher efficiency than 45° nozzles at this scale.

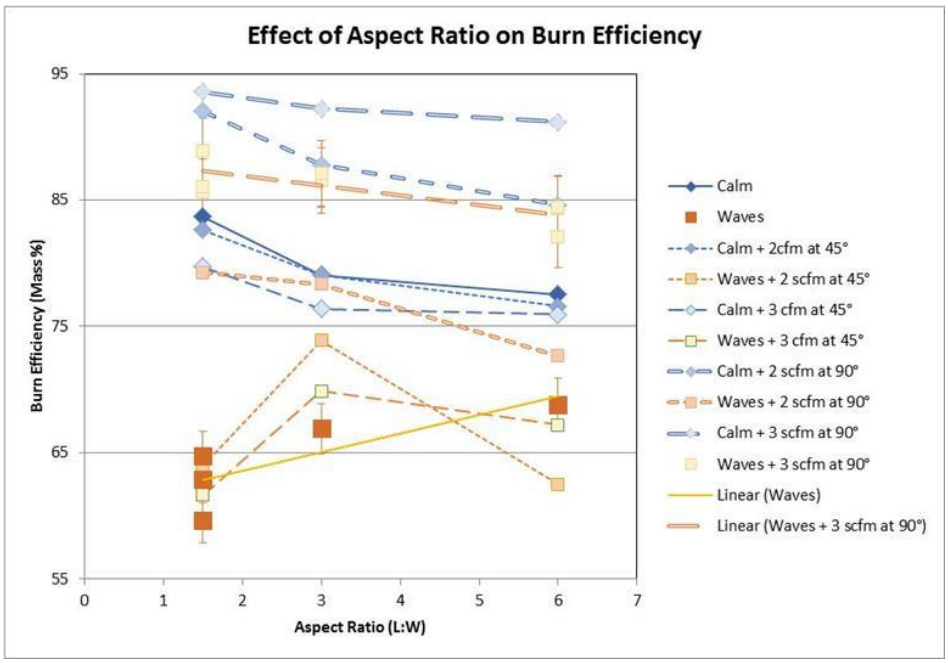

Figure 11: Effect of aspect ratio on burn efficiency at different air flow rates.

3.2.2 Burn Rate

Figure 12 shows the effects of the experimental variables on burn rate (oil removal rate). Note that the Y-axis extends only from 0.5 to 3 mm/min burn rate. The burn rates measured in calm conditions are shown with different shades of blue-filled diamond markers and lines; those measured in waves are shown with different shades of orange filled square markers and lines. Data points for runs with no additional compressed air are shown with the darkest shading; those with 2 scfm of compressed air added are moderately shaded; and, those with 3 scfm added are the lightest shading. Data points from experiments with the air nozzles at 45° are connected with single dashed lines while those with the nozzles at 90° are connected with double dashed lines.

For a circular crude oil burn with an area of approximately 0.165 m^2 (an equivalent diameter of approximately 46 cm) and an initial thickness of 6 mm (1 L of crude oil over an area of approximately 0.165 m^2) the normal burn rate would be approximately 1.1 to 1.3 mm/min (Buist et al. 2013).

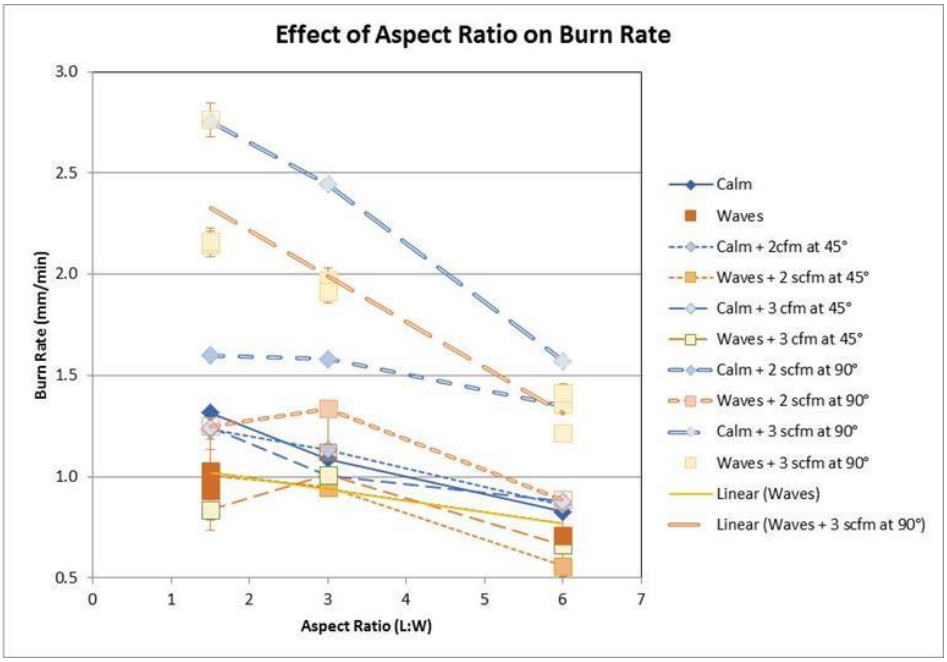

Figure 12: Effect of aspect ratio on burn rate at different air flow rates.

In general, the data shows that, at this scale:

- Increasing aspect ratio (longer, narrower burns) results in declining burn rate (The error bars shown on select data points on Fig. 11 indicate one standard deviation);
- Calm conditions generally result in higher burn rates;
- Increased air injection increases burn rate; and,
- 90° nozzles generally result in higher burn rate than 45° nozzles.

3.2.3 Soot Production

The weights of soot samples collected over the short burn times were very small compared to the initial weights of the filter and no significant trends could be determined due to accumulated errors.

3.3 Design of Full-scale Prototype Augmented Fire Boom

Using the results of the small-scale test burns, particularly the configurations that produced the most efficient burns, a detailed design for the full-scale linear augmented fire boom was produced. The design was based on enhancing a 50-foot section of commercially-available DESMI PyroBoom® fire boom with:

1. adjustable structural components to hold the fire boom in rectangular shapes of different aspect ratios in waves, and
2. canted compressed air nozzles and compressed air supply hoses.

Figure 13a shows the construction features of a stock PyroBoom® and Fig. 13b shows the as-built dimensions. Figure 14 shows the layout of the three boom rectangles with aspect ratios (L x W) of 1:1, 4:1, and 9:1 that fit into the working surface area of the CRREL wave tank (6 m x 2.4 m). Figure 15a shows how the compressed air nozzles were to be laid out, with one 3/8" pipe attached by the side bolts of each hemispherical float, and Fig. 15b shows the detailed plumbing layout to connect the 12 nozzles to a CPS 185 scfm air compressor. Figure 16 shows the modified PyroBoom® deployed in the wave tank in a 1:1 aspect ratio configuration.

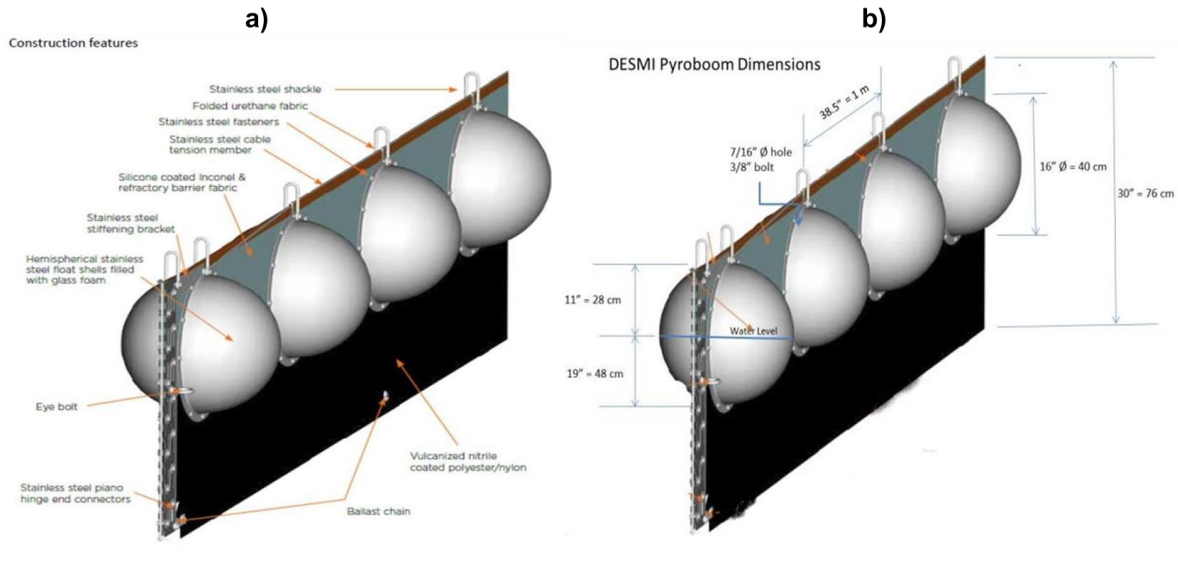

Figure 13: PyroBoom® a) Construction features, b) Key dimensions.

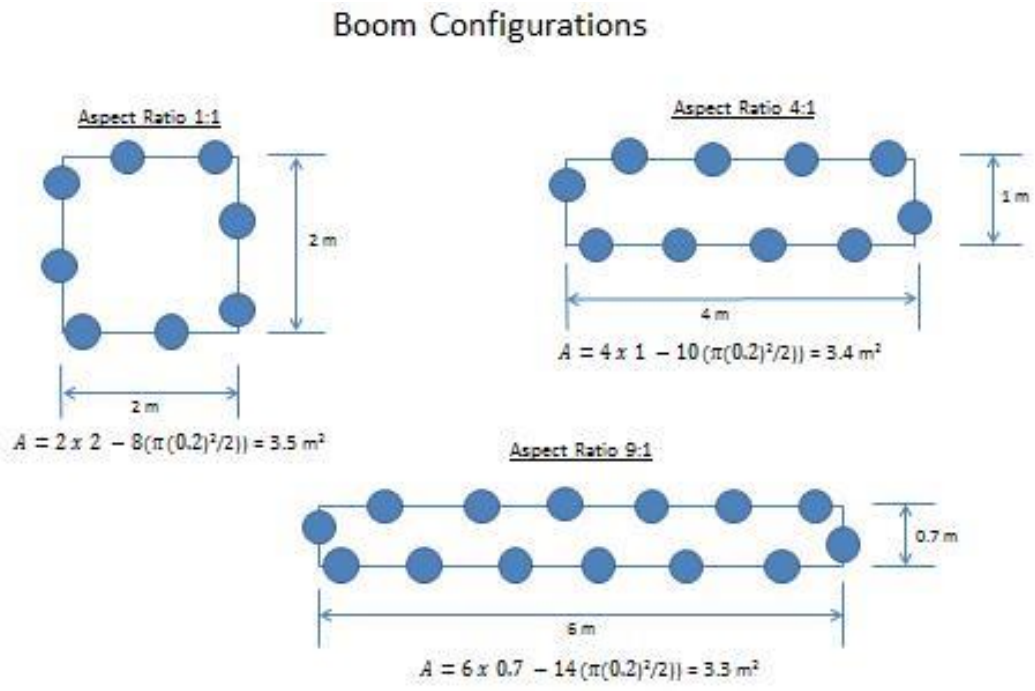

Figure 14: Boom configurations to fit CRREL wave tank with target aspect ratios.

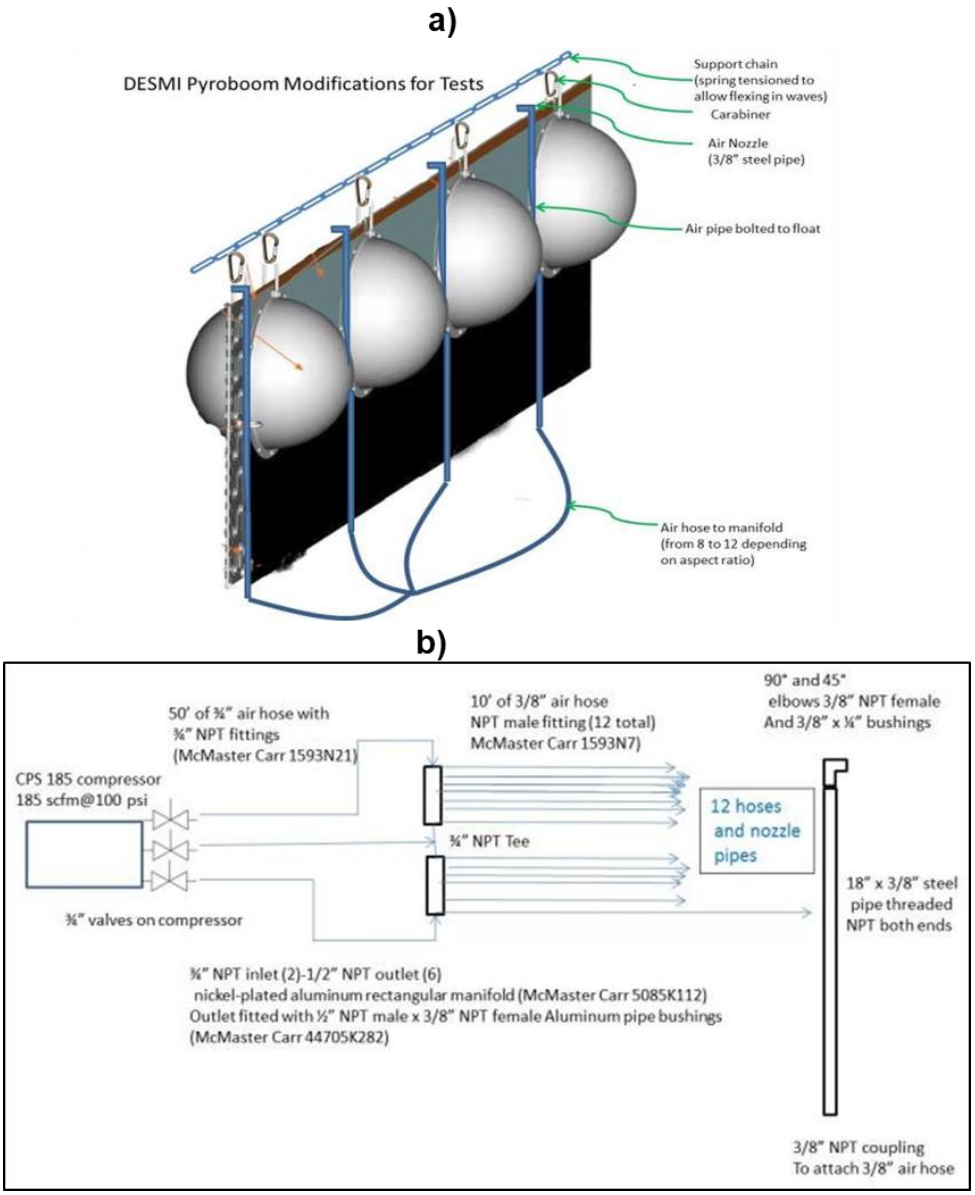

Figure 15: a) Compressed air nozzle layout, b) Compressed air plumbing design and hookup to 185 scfm compressor.

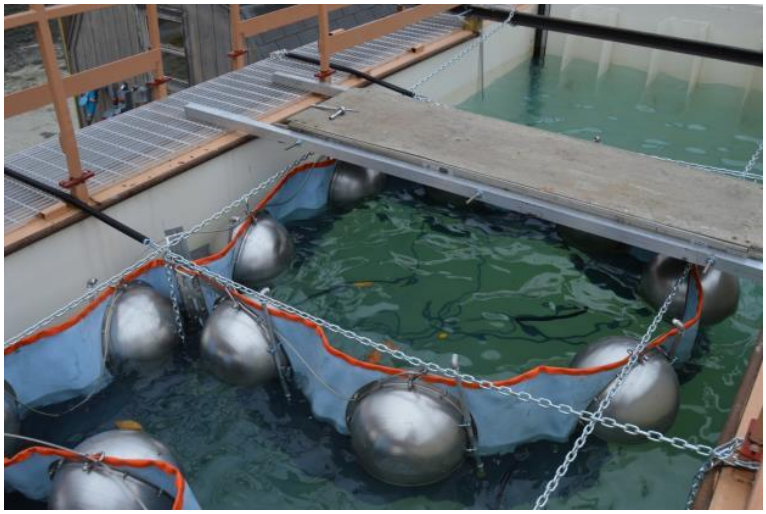

Figure 16: PyroBoom® with air nozzles deployed in CRREL wave tank. Note chains attached to large springs to hold PyroBoom test section in place yet allow movement in waves. Also note compressed air hoses retained underwater.

4. Large-Scale In-situ Burn Tests at CRREL

Full-scale prototype in situ burn tests on water with different geometries (aspect ratios) were conducted in the CRREL wave tank with the modified PyroBoom® fire boom system in November 2018. The tank and ancillary equipment were located outdoors at the south end of the Frost Effects Research Facility (FERF) at the CRREL grounds in Hanover, NH. The full test plan can be found in Appendix C.

The goal of the experiments was to measure the effects of the various boom configurations and air injection enhancements on the burn characteristics under controlled conditions in both calm water and waves, and identify the most promising combinations of burn layout and air injection.

The CRREL wave tank measures 2.4 m wide by 14.3 m long (its working length is 6 m); and, the water depth can be up to 2 m (Fig. 17). A water depth of 1.8 m (72 inches) was used for these experiments. For in situ burn experiments, water deluge pipes are installed along the top of the inside walls of the tank to provide protection against radiant heat and flame impingement on the tank walls above the waterline. The tank was filled with fresh water to simplify the experiments and disposal.

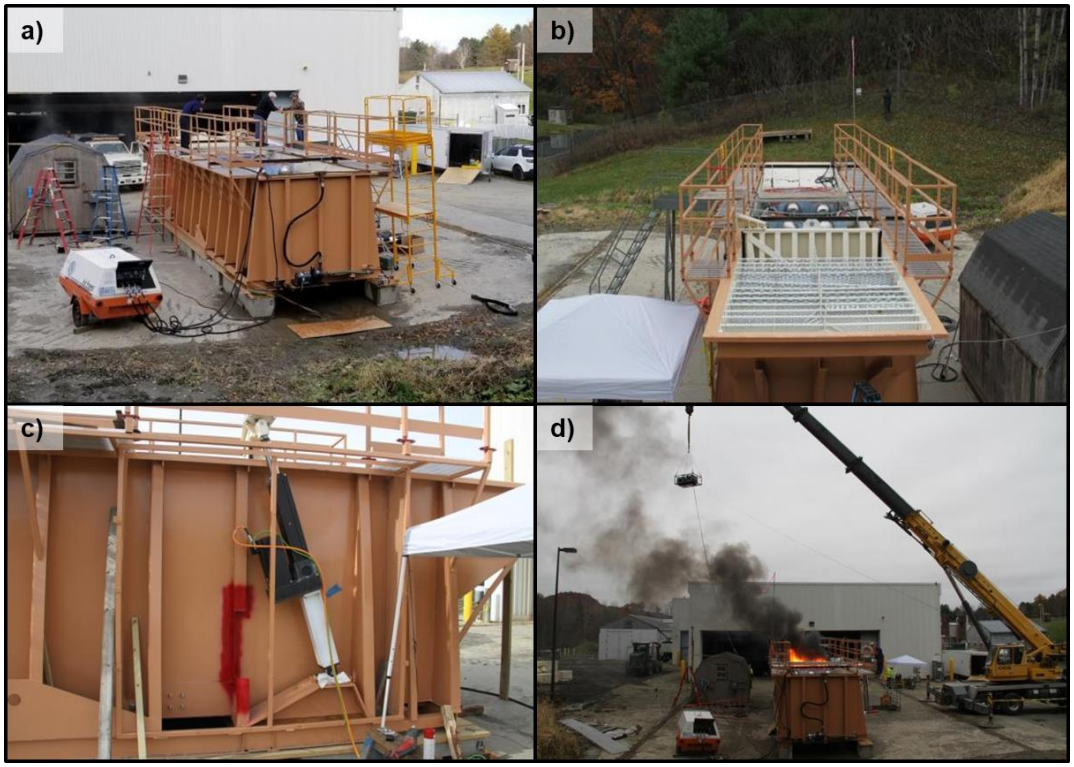

Figure 17: CRREL wave tank a) Air compressor and deluge water cooling pump, b) View from wave paddle end, c) Wave actuator, d) EPA smoke sampling package suspended by crane being moved into position.

A 50-foot section of DESMI PyroBoom® was modified as described in Section 3 and positioned in the wave tank to contain the experimental burns (Fig. 16 and Fig. 18). The aspect ratio of the burn area in the modified fire boom was varied from 1:1 to 9:1 (9:1 being the longest that will fit into the working length of the wave tank) by repositioning the boom on the elevated chain system. This was accomplished by releasing and reattaching the Carabiner clips holding the shackles on top of the floats to the chain. The area encompassed by the boom was kept constant at approximately 3.4 m^2. This burn area is equivalent to a circular burn of 210 cm diameter.

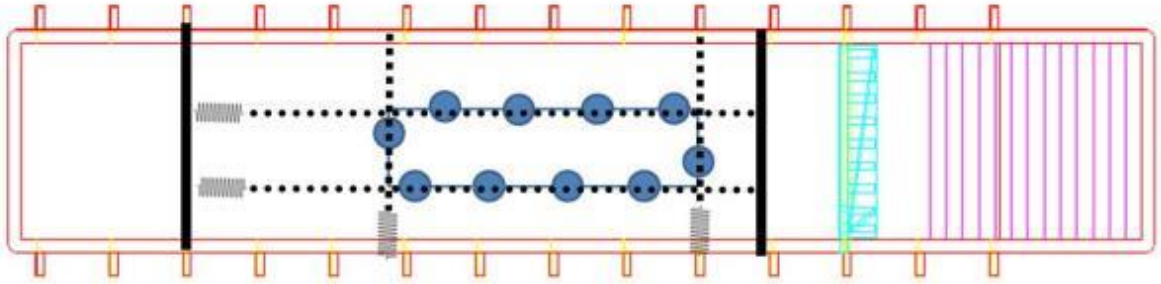

Figure 18: Planned positioning of PyroBoom® in working area of CRREL wave tank with chains and extension springs.

4.1 Materials and Methods

The burns were conducted with ANS crude oil provided by BSEE to ensure consistency with the small-scale experiments. Each burn required 35 L (9.25 gallons) of fresh crude. The mass of oil added and residue recovered were measured to allow burn removal efficiency (see Equation 2) to be calculated: the burns were videoed from several positions and manually timed to permit estimates of burn rate (see Equation 3). Soot emissions were estimated visually and from digital photos and video using the Ringlemann scale. In addition to visual estimates of the soot emissions, the Virtual Ringlemann App (http://virtualringelmann.com/app/en) was installed on an Android-based cell phone and used to estimate the Ringlemann number of the smoke plume. An example screenshot from Run 15 is given in Fig. 19.

The smoke plume was also directly sampled using an EPA instrument system suspended from a crane and maneuvered into the plume (Fig. 19). Target compounds included CO, CO_2, $PM_{2.5}$, black/brown carbon, elemental/organic carbon, total carbon, PAHs, PCDD/PCDF, and volatile organics including carbonyls (see Appendix E for further details).

Figure 19: Example screenshot of Virtual Ringlemann App.

A test program consisting of 15 individual burns on water varying burn geometry (aspect ratio), air injection angle and waves was planned. Sixteenth test was conducted looking at the effect of pointing the air injection nozzles mounted at the top of the freeboard portion of the boom 45° downwards towards the contained oil slick. The test matrix is provided in Table 4. The order that the tests were conducted in was dictated by the state of the fire boom after each experiment.

Table 4. Planned Test Matrix

Test	Date	Waves (h=12 cm; P= 1.5 s)	Air Flow into Fire (SCFM)	Nozzle angle (° from Vertical up)	Boom Aspect Ratio (L:W)
1	05/11/2018	No	0	90	1:1
2	05/11/2018	No	123	90	1:1
3	05/11/2018	Yes	0	90	1:1
4	06/11/2018	Yes	123	90	1:1
5	06/11/2018	Yes	123	45	1:1
6	07/11/2018	No	0	45	9:1
7	07/11/2018	No	199	45	9:1
8	07/11/2018	Yes	0	45	9:1
9	07/11/2018	Yes	196	45	9:1
10	08/11/2018	No	0	45	4:1
11	08/11/2018	No	166	45	4:1
12	08/11/2018	Yes	0	45	4:1
13	08/11/2018	Yes	169	45	4:1
14	08/11/2018	Yes	168	135	4:1
15	09/11/2018	Yes	205	45	9:1
16	09/11/2018	Yes	205	45	9:1

Each burn was digitally videoed, and photographed while observations were noted. As well, each experiment was made available in real time by web broadcast of still photographs of the wave tank from the roof of a nearby building (Fig. 26).

Fresh ANS crude oil, supplied by BSEE, was used in the full-scale prototype test, to ensure consistency with the small-scale tests.

Air flowrates were measured at the three outlet pipes from the CPS 185 air compressor receiver tank with three Model H771-150-EG Hedland Variable Area Air Flowmeters tapped off of a common manifold, one with a pressure gauge attached. Figure 20 shows the arrangement.

Figure 20: Hedland Air Flow rotameters mounted on air compressor.

4.2 CRREL Wave Tank Experimental Results and Discussion

A total of 16 experiments were conducted varying boom aspect ratio, wave height (calm, and sinusoidal waves with 12 cm amplitude and a 1.5 s period), air injection nozzle angle (45° and 90° from vertical upwards, with one test at 135°) and nominal air flow rates of (0 and 185 scfm). The experiments with a 9:1 aspect ratio in waves with the compressed air injected into the flames were repeated three times (see the color highlighted rows in Table 6). Spreadsheets with all the data collected are given in Appendix E. The slight differences in nominal surface area between boom aspect ratios (Table 5) resulted in slick thicknesses of approximately 1.0 cm, 1.03 cm, and 1.06 cm for the 1:1, 4:1, and 9:1, respectively. These variations are very slight and are not expected to have a significant influence on the results of the *in situ* burn tests.

4.2.1 Burn Efficiency

Table 5 summarizes the key data from these tests.

Table 5. CRREL Wave Tank Experimental Results Summary

Run	Waves (h=12 cm; P= 1.5 s)	Air Flow into Fire (SCFM)	Number of Nozzles in Fire	Nozzle angle (° from Vertical up)	Boom Aspect Ratio (L:W)	Air Temp (C)	Water Temp (C)	Wind Speed (m/s)	Nominal Burn Area (m^2)	Visually Observed Ringlemann Smoke Number	Video Observed Ringlemann Smoke Number	Smoke Photo Montage Link	$PM_{2.5}$ Emission Factor (g soot/kg oil consumed)	Average Burn Rate (mm/min)	Burn Efficiency (mass %)
1	No	0	0	90	1:1	NR	NR	1.25	3.5	NR	5	Web Photo Montage\Run1.docx	163	2.4	94.3
2	No	123	8	90	1:1	5.1	NR	1.7	3.5	3 to 4	3 to 4	Web Photo Montage\Run2.docx	130	2.8	95.5
3	Yes	0	0	90	1:1	5.5	NR	1	3.5	5	5	Web Photo Montage\Run3.docx	146	2.3	91.5
4	Yes	123	8	90	1:1	11.8	6.5	0	3.5	3 to 4	4 to 5	Web Photo Montage\Run4.docx	115	2.7	94.4
5	Yes	123	8	45	1:1	9.9	7	1.5	3.5	3 to 4	3 to 4	Web Photo Montage\Run5.docx	110	2.2	95.0
6	No	0	0	45	9:1	13.3	7.2	0.5	3.3	2 to 3	3 to 4	Web Photo Montage\Run6.docx	102	1.6	99.6
7	No	199	12	45	9:1	13.3	7.9	0.75	3.3	2 to 3	2 to 4	Web Photo Montage\Run7.docx	76	1.7	98.7
8	Yes	0	0	45	9:1	14.6	9.9	0	3.3	2 to 5	2 to 5	Web Photo Montage\Run8.docx	75	1.8	94.9
9	Yes	196	12	45	9:1	13.8	9.3	1.3	3.3	1 to 4	2 to 4	Web Photo Montage\Run9.docx	74	1.6	89.2
10	No	0	0	45	4:1	12.9	8.9	0.5	3.4	5	5	Web Photo Montage\Run10.docx	108	2.7	97.1
11	No	166	10	45	4:1	9.3	8.9	0.5	3.4	4 to 5	4 to 5	Web Photo Montage\Run11.docx	99	2.7	96.4
12	Yes	0	0	45	4:1	9.4	11.7	1.25	3.4	5	5	Web Photo Montage\Run12.docx	129	2.4	89.2
13	Yes	169	10	45	4:1	8.4	10.7	1.5	3.4	2 to 4	2 to 4	Web Photo Montage\Run13.docx	93	2.7	90.5
14	Yes	168	10	135	4:1	8.6	10.5	0.5	3.4	2 to 3	4 to 5	Web Photo Montage\Run14.docx	110	3.2	88.8
15	Yes	205	12	45	9:1	2.2	8.2	0.4	3.3	2 to 3	2 to 4	Web Photo Montage\Run15.docx	72	2.0	89.5

16	Yes	205	12	45	9:1	3.3	8.8	0.6	3.3	2 to 4	2 to 4	Web Photo Montage\Run16.docx	62	1.9	91.8

Figure 21 shows the effect of aspect ratio on burn efficiency.

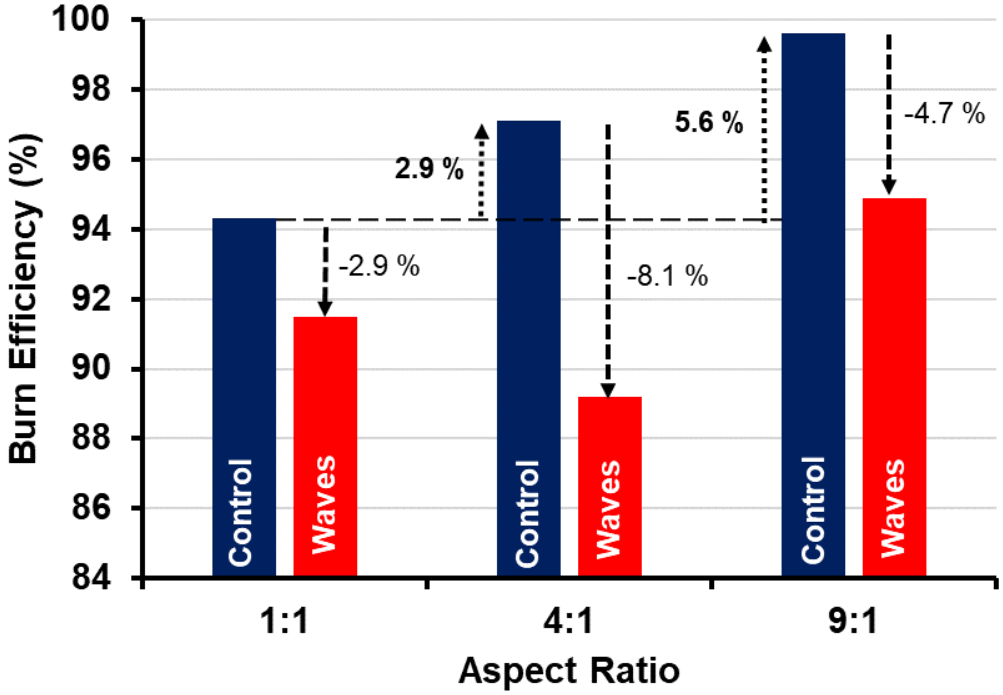

Figure 21: Effect of Aspect Ratio on Burn Efficiency – Control and wave tests

As shown in Fig. 21, the burn efficiency for the control experiment with 1:1 equals 94% which is characteristic of ISB of crude oil (Buist et al, 2013). With the increase of the aspect ratio to 4:1 and 9:1, the burning efficiency increases about 3% and 6%, respectively (Fig. 21). This is because the better aeration of flames that promotes hotter and more complete combustion. In wave conditions, the mixing action increased the heat transfer from hot oil to the cold water which in turn caused earlier extinction. It should be noted that the efficiency decrease caused by the waves is more significant for the higher aspect ratio. The fuel surface in the longer boom configuration was subjected to more wave cycles. For example, in 1:1 ratio with a wave amplitude of 12 cm, the fuel surface had 4 crests and 4 troughs, while there were 12 crests and 12 troughs in 9:1 ratio. Disturbance of the fuel surface and increase in mixing action caused a larger drop in burn efficiency in longer boom configurations. Figure 22 shows the effect of air injection on burn efficiency.

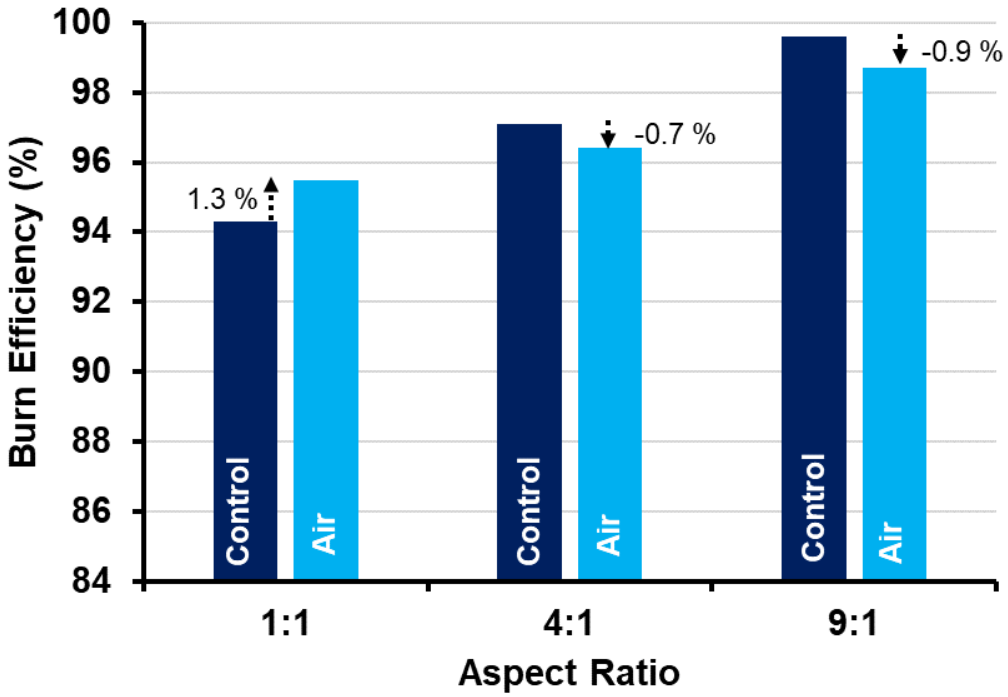

Figure 22: Effect of Aspect Ratio on Burn Efficiency – Control and air injection tests

Experiments demonstrated that the air injection did not significantly affect the burn efficiency at stagnant water conditions. Air injection promoted a 1.3% increase in 1:1 ratio, while caused 0.7% and 0.9% decrease in 4:1 and 9:1 ratio, respectively. However, when the emitted particulate matters are compared, a significant decrease in $PM_{2.5}$ emission factor with air injection is observed (Appendix E, Fig. 4-9). In 9:1 aspect ratio with air injection, the emitted $PM_{2.5}$ per initial oil mass was 40% less than the 1:1 case. Figure 23 shows the effect of and air injection on burn efficiency in wave conditions.

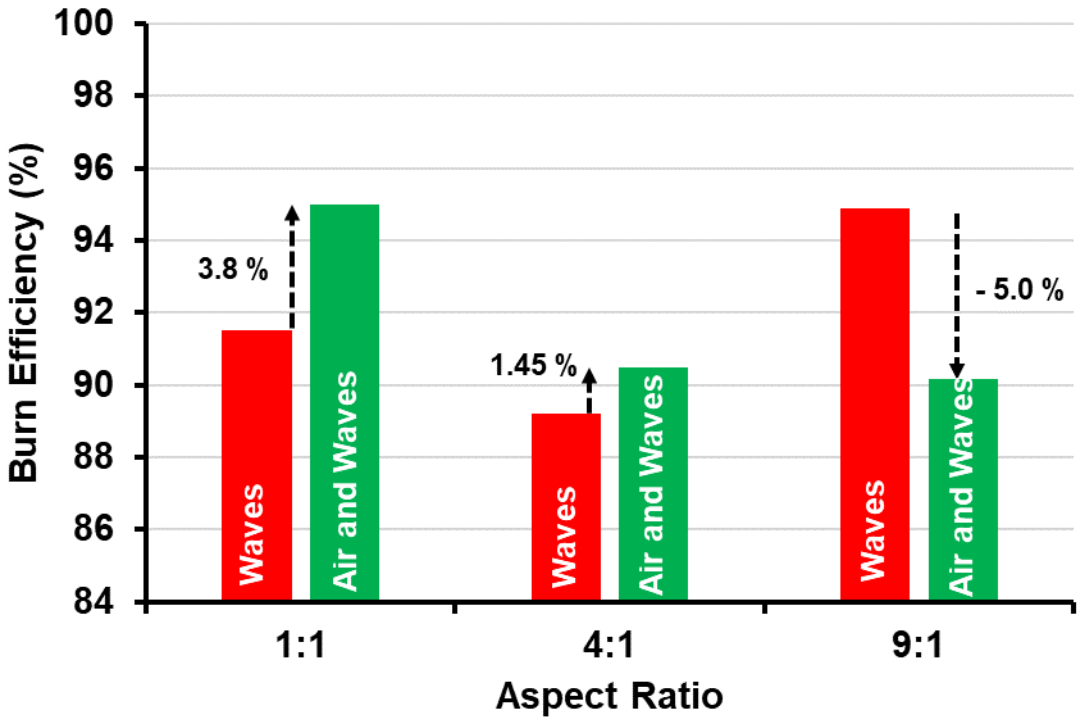

Figure 23: Effect of Aspect Ratio on Burn Efficiency – waves and air injection tests

Injecting air during waves increased the burning efficiency about 4% and 1.5% for the 1:1 and 4:1 aspect ratio. With the further increase of aspect ratio, the burn efficiency decreased about 5%. As discussed before, 9:1 case promoted the highest aeration due to its geometry. Injection additional air might cool down the flame temperate which in turn caused lower burn efficiency.

Figure 24 shows the summary of the all experimental data. Data points for experiments in calm conditions are shown with diamond-shaped markers: those in waves are shown with square markers. Data from experiments with no additional compressed air are shown with solid shading; those with compressed air added are hashed – horizontal hash marks indicate 90° air nozzles; angled up to the right hash marks indicate 45° air nozzles and one data point (Test 14 = 4:1, waves and air, 45^{o} down) has hash marks down to the right indicating a 135° nozzle angle. Data points from experiments with the air nozzles at 45° are connected with single dashed lines.

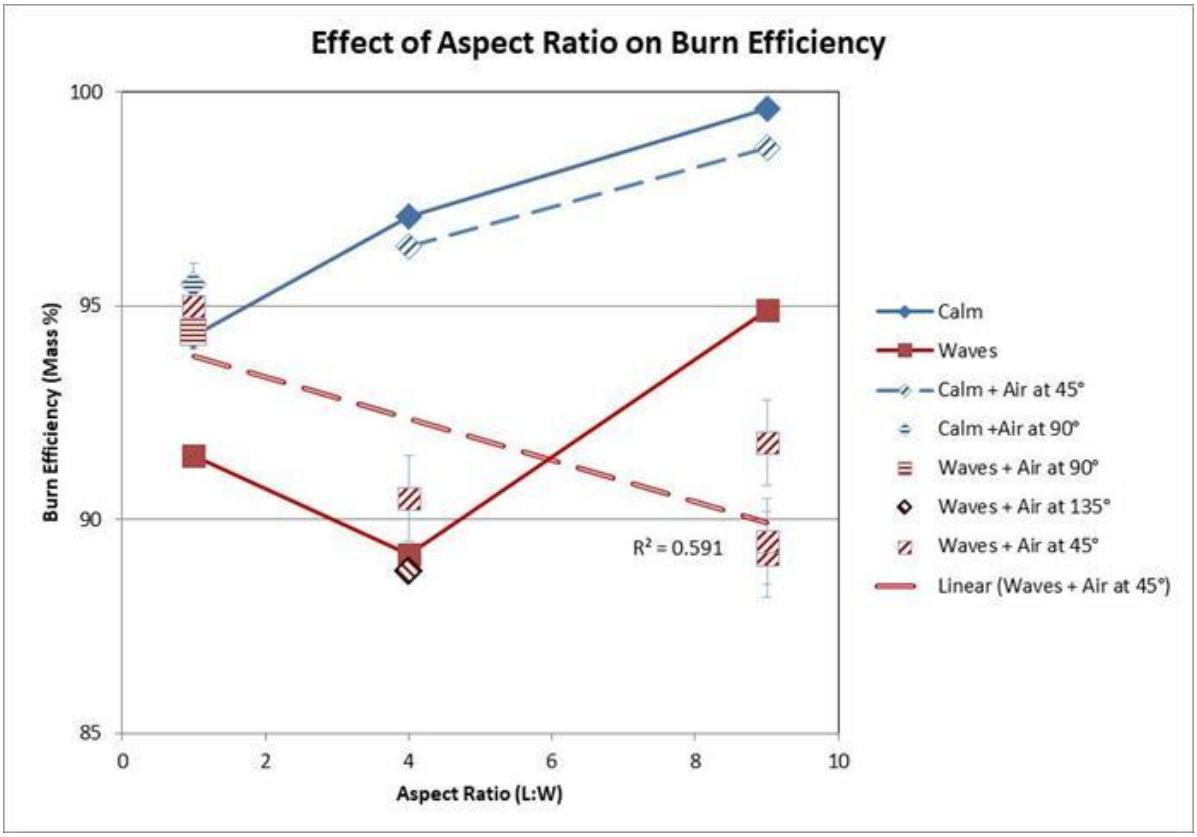

Figure 24: Effect of Aspect Ratio on Burn Efficiency – Magnified Y-Axis.

In general, the burn efficiency data shows that:

- All the experiments produced a high oil removal efficiency (> 88%).
- Calm conditions result in higher burn efficiency than burning in waves. Waves cause gentle mixing of the slick, which likely increases heat transfer from the burning oil to the water which in turn causes earlier extinction.
- In calm conditions (no waves), the burn efficiency increases with the increase in aspect ratio.
- The highest burn efficiency recorded (99.6 mass % removed) was with a 9:1 aspect ratio in calm conditions with no air injection (due to the additional aeration from the long, narrow fire, but no turbulence induced by compressed air nozzles).
- The lowest measured burn efficiency (88.8 mass % removed) was measured with the 4:1 aspect ratio, in waves with the nozzles pointed at 135° (45° down towards the slick). This was due to turbulent mixing of the burning oil layer by the jets of compressed air causing earlier onset of the vigorous burn phase and extinction than in the case of a quiescent burning oil layer.
- Increases in burn efficiency due to air injection may be realized with larger fires, as it becomes more difficult to naturally supply enough air to the combustion zone.

4.2.2 Burn Rate

Figure 25 shows the effects of the experimental variables on burn rate (oil removal rate – mm/min). Note that the Y-axis extends only from 1 to 3 mm/min burn rate. The burn rates measured in calm conditions are shown with blue-filled diamond markers and lines; those measured in waves are shown with of red-filled square markers and lines. Data points for runs with no additional compressed air are shown with the solid fill; those with compressed air added are hashed – horizontal hash marks indicate 90° air nozzles; hash marks angled up to the right indicate 45° air nozzles and one data point (Test 14 = 4:1, waves and air, 45° down) has hash marks down to the right indicating a 135° nozzle angle. Data points from experiments with the air nozzles at 45° are connected with single dashed lines.

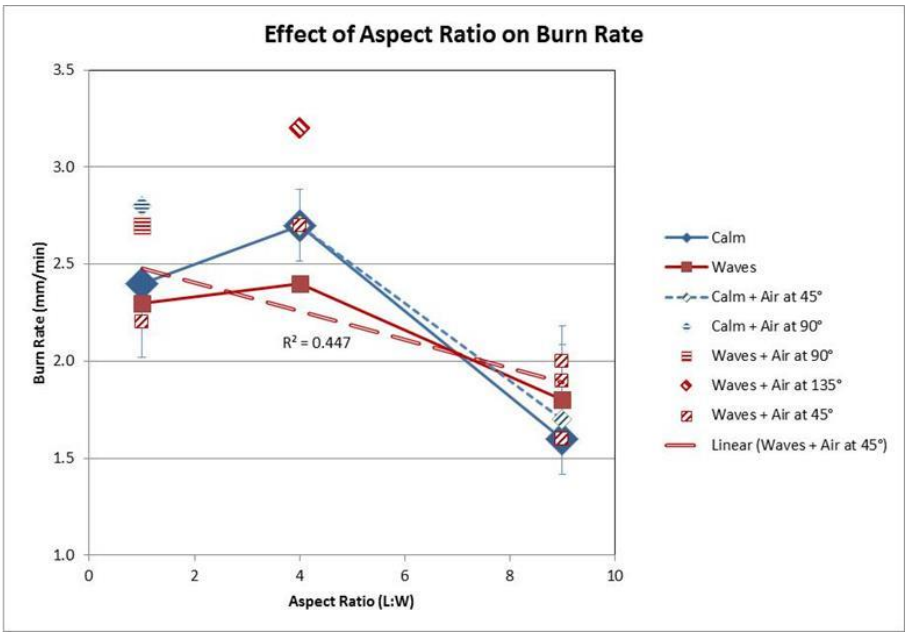

Figure 25: Effect of Aspect Ratio on Burn Rate in CRREL Wave Tank Experiments.

The r^2 of the least squares linear fit to the data for the experimental results for burn rate as a function of aspect ratio in waves with air added at 45° is not very good, at only 0.447. The boom configuration 9:1, air added at 45°, in waves was repeated three times in burns 9, 15, and 16. The results showed a burn rate average of 1.8 mm/min and standard deviation (RSD) of 0.18 mm/min.

For a circular crude oil burn with an area of approximately 3.4 m^2 (an equivalent diameter of approximately 210 cm) and an initial thickness of 10 mm (35 L of crude oil over an area of approximately 3.4 m^2) the normal burn rate would be approximately 2.2 mm/min (Buist *et al*. 2013).

In general, the oil removal rate data shows that:

- The estimated burn rate at an aspect ratio of 9:1 is lower than at an aspect ratio of 1:1 or 4:1 (probably because the longer narrower burn shape reduces the unit heat radiation back to the surface of the slick);
- Waves appear to reduce burn rate slightly;

- There appears to be a slight increase in burn rate with air injection;
- The lowest measured burn rate (1.6 mm/min) was measured with the 9:1 aspect ratio, in calm conditions with no air injection (again, as noted above, probably due to reduced radiant heat transfer to the slick); and.
- The highest burn rate estimated (3.2 mm/min) was with a 4:1aspect ratio in waves with air injected at 135° from vertical up (i.e., 45° downward toward the burning slick). This is probably because the turbulent mixing energy of the compressed air impinging on the burning slick increases the convective heat transfer to the slick and thus increases the vaporization rate of the hot oil).

4.2.3 Smoke Density

The Ringlemann smoke density, or opacity, factors estimated by visual observation from the side of the wave tank during a burn, and those estimated from reviewing videos of the burn taken from nearby, are shown in Table 5. Unfortunately, these visual methods do not yield reliable quantitative data; just the observer's impressions at the moment. An application written for Android-based cell phone cameras was also employed to obtain spot measurements of the smoke density during each experiment; however, the size of the area of the camera view sampled was very small compared to the diameter of the smoke plume, so it did not provide an average reading for the entire plume. The best visual comparisons of the amount of soot being emitted by an individual experiment is the web images obtained from a camera mounted on a CRREL building some distance from the wave tank. For example, Figures 26 and 27 compare the smoke plume from Run 3 (1:1 aspect ratio; waves; no air) with the plume from Run 15 (9:1 aspect ratio; waves; 205 scfm of air from 12 nozzles aimed up at 45°). The reader is encouraged to view the photo montages for each run by following the hyperlinks given in Table 6.

Figure 26: Run 3, 1:1 aspect ratio; waves; no air.

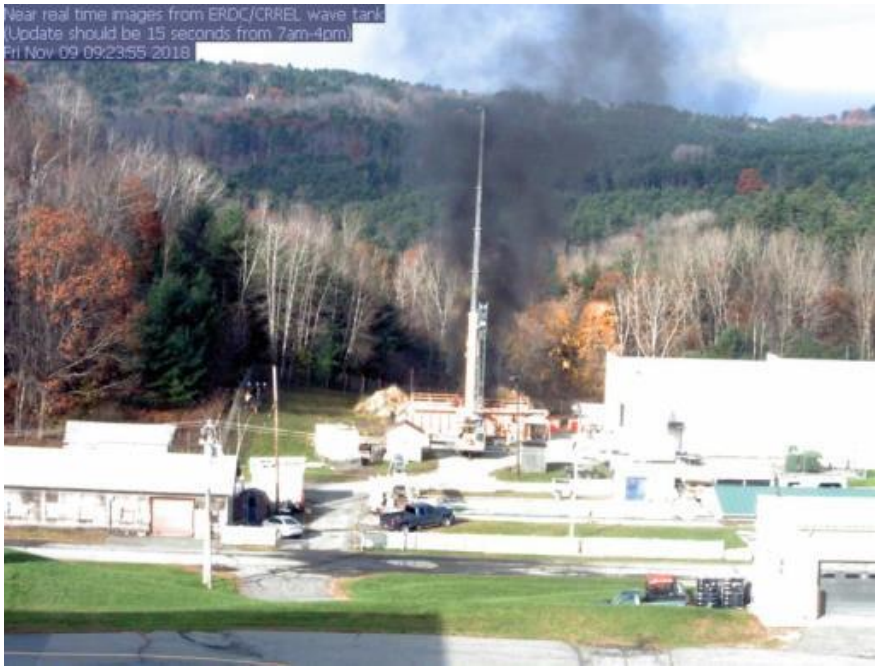

Figure 27: Run 15:1 aspect ratio; waves; 205 scfm of air from 12 nozzles aimed up at 45 .

4.2.4 $PM_{2.5}$ Soot Emission Factor

The results from the U.S. EPA plume sampling program are summarized in Figure 28. The full report is presented in Appendix E. Marker colors indicate boom configuration aspect ratio; Grey 1:1, Red 9:1, and Green 4:1. $PM_{2.5}$ emission factor are given as the average of two samples.

In Figure 28, the ordinate is expressed in terms of the oil consumed. The narrow boom configuration (9:1, red points) has the lowest $PM_{2.5}$ emission factors and the highest combustion efficiency but not necessarily the greatest amount of oil consumed. The highest $PM_{2.5}$ emission factor is 160 g/kg oil consumed for the 1:1 aspect ratio control burn (no waves, no compressed air). This emission factor is in the same range as reported by NIST for ANS crude oil (McGrattan et al., 1997).

The lowest emission factor is 60 g/kg for the case of the 9:1 aspect ratio fire boom, in waves, with air injected by 12 nozzles pointed up at 45°. The three repeats (Runs 9, 15 and 16) produced a mass loss average of 90.82%±1.39 and relative standard deviation (RSD) of 1.5%, revealing a good repeatability in the oil residue collection. The smoke sampling for these three runs produced measurements of 74, 72 and 62 g/kg of $PM_{2.5}$ respectively, with an average of 69, a Standard Deviation of 6.6 and a RSD of 9.5%.

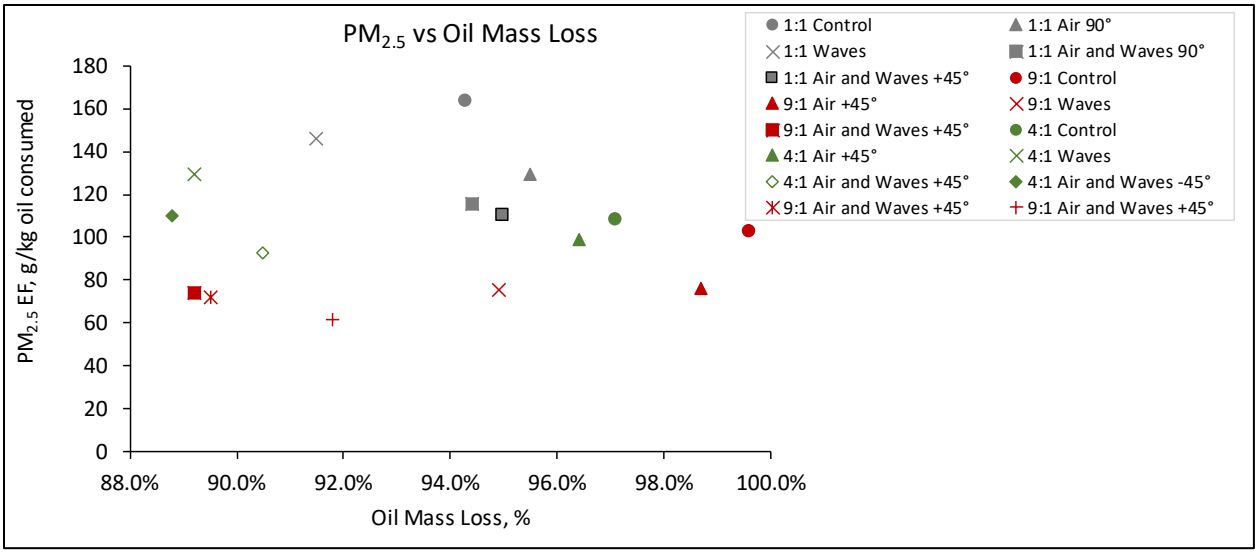

Figure 28: $PM_{2.5}$ emission factor (g $PM_{2.5}$ produced per kg oil consumed). Grey 1:1, Red 9:1, and Green 4:1. $PM_{2.5}$ emission factor average of two samples per test.

The mean Ringlemann values were compared to the $PM_{2.5}$ emission values for each burn to determine if there was a relationship between the conventional qualitative method and the analytical approach used in this study. Although there is a slight positive correlation between values (slope = 25.92°) is does not appear to be significant (R^2=0.57; Figure 29). As the EPA method is refined it will become more cost effective, given that is it more robust it should be included whenever possible in future *in situ* burn experiments. However, the method selection for future studies will depend on funding and equipment availability.

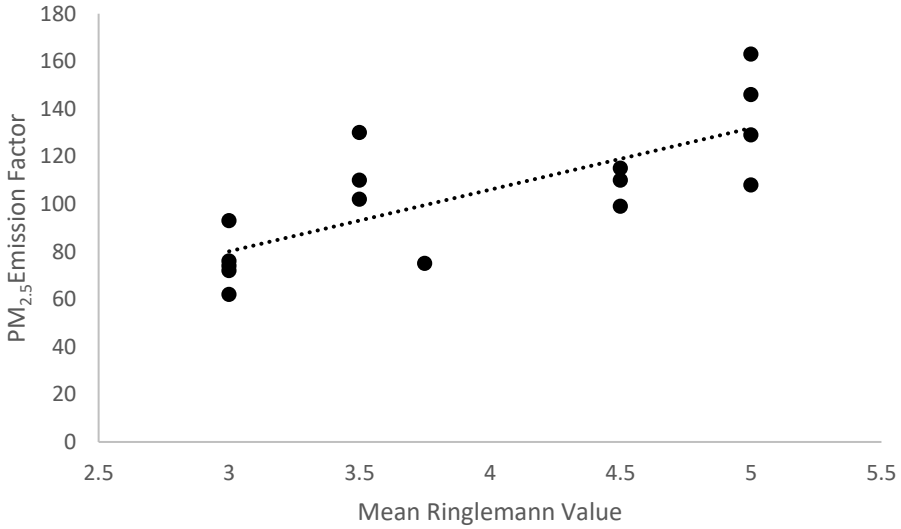

Figure 29: Graph of the linear relationship between the observed Ringlemann value for each burn base on the video footage and the $PM_{2.5}$ Emission value.

4.2.5 Combustion Efficiency

The combustion efficiency for each burn was determined using the amounts of CO_2, CO and total carbon form $PM_{2.5}$ analyses (see Appendix E). The modified combustion efficiencies were calculated to determine how well the oil burned (Equation 4).

$$MCE = \frac{CO_2}{CO_2 + CO + Total\ Carbon} \quad (4)$$

Where:
MCE=modified combustion efficiency (unitless)
CO_2=carbon dioxide in the plume in ppm
CO=carbon monoxide in the plume in ppm
Total carbon=total carbon in the particle (TC)

Figure 30 and Table 6 show the effects of boom ratio on the modified combustion efficiency for each major test condition. There was a clear increase in combustion efficiencies as boom ratio increased for each treatment (air, wave, air and waves). The 9:1 aspect ratio had the highest combustion efficiencies for each treatment ranging from 0.91-0.92 MCE. This same trend was observed for burn efficiencies (or mass loss) for the control and air treatments. However, wave action diminished burn efficiencies for all aspect ratios (Figure 31). During the wave tests, air injection increased burn efficiencies for the 1:1 ratio, not affected the 4:1 ratio, and decreased for the 9:1 ratio. As previously discussed, the wave action increases the heat transfer from hot oil to the cold water which in turn caused earlier extinction. This earlier extinction decreases the amount of oil burn; however, the combustion efficiency was not influenced by the wave action. Instead, increasing the boom aspect ratio had the only obvious influence on combustion efficiency. This may be attributed to more efficient atmospheric air penetration into the flame zone when the dimension of the oil slick are in a more linear configuration.

Table 6. Average oil weight loss and modified combustion efficiency for each *in situ* burn test (EPA final report; Appendix E).

Test Condition	Wt loss, %	MCE, unitless
Control*	97.00	0.88
Waves*	91.87	0.88
Air and Waves*	91.31	0.90
Air*	96.87	0.89
All 1:1 Boom Ratio	94.14	0.86
All 4:1 Boom Ratio	92.40	0.89
All 9:1 Boom Ratio	93.95	0.92
Control, 1:1	94.30	0.85
Control, 4:1	97.10	0.88
Control, 9:1	99.60	0.91
Air, 1:1	95.50	0.86
Air, 4:1	96.40	0.89
Air, 9:1	98.70	0.91
Waves, 1:1	91.50	0.85
Waves, 4:1	89.20	0.88
Waves, 9:1	94.90	0.92
Air and Waves, 1:1[#]	94.70	0.87
Air and Waves, 4:1[#]	89.65	0.89
Air and Waves, 9:1[#]	90.17	0.92

**All three Boom Ratios*

[#]All nozzle configurations

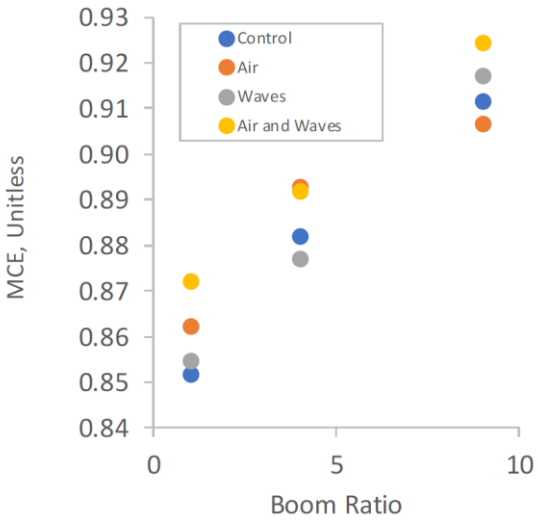

Figure 30: The effect of boom ratio on combustion efficiency for major test conditions (EPA final report; Appendix E).

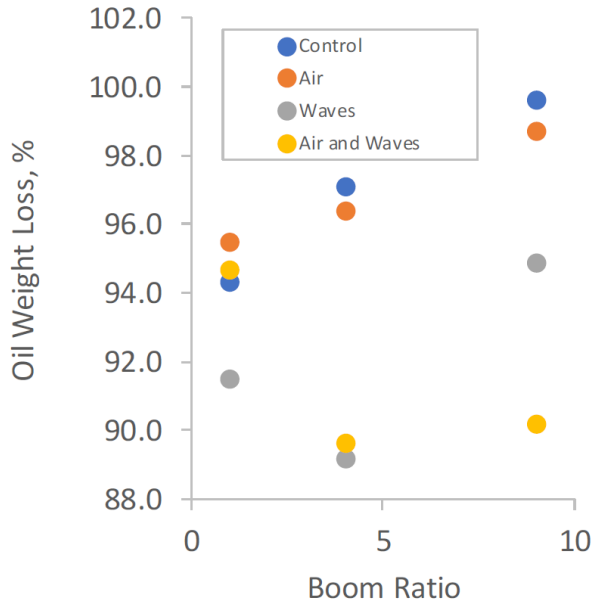

Figure 31: The effect of boom aspect ratio on burn efficiencies of crude oil (EPA final report; Appendix E).

5. Conclusions and Future Study

5.1 Small-scale Burn Experiments in the SL Ross Wave Tank

In general, the data from the small-scale experiments using a metal fire boom model in the SL Ross wave tank shows that:

1. There appears to be little or no appreciable change in burn efficiency with increasing aspect ratio (the ratio of length to width of the model fire boom) at this scale;
2. Calm conditions generally result in higher burn efficiency at this scale;
3. Increased air injection increases burn efficiency at this scale;
4. 90° nozzles generally result in higher efficiency than 45° nozzles;
5. Increasing aspect ratio (longer, narrower burns) results in declining burn rate;
6. Calm conditions generally result in higher burn rates;
7. Increased air injection increases burn rate; and,
8. 90° nozzles generally result in higher burn rate than 45° nozzles.

The weights of soot samples collected over the short burn times were very small compared to the initial weights of the filter and no significant trends could be determined in the data due to accumulated errors.

5.2 Modifications to the Fire Boom

Simple modifications were made to the PyroBoom (addition of brackets, clips) to allow its aspect ratio to be changed and additional combustion air added.

5.3 Large-scale Burn Experiments in the CRREL Wave Tank

In general, the data from the large-scale experiments in the CRREL wave tank using a modified PyroBoom® shows that:

1. All the large-scale experiments produced a high oil removal efficiency (> 88%);
2. There appears to be a slight increase in burn efficiency with increasing aspect ratio in calm conditions;
3. Calm conditions generally result in higher burn efficiency than burning in waves;
4. Increased air injection does not seem to affect burn efficiency appreciably at this scale (the scatter in the data masks any effects);
5. The lowest measured burn efficiency (88.8 mass %) was measured with the 4:1 aspect ratio, in waves with the nozzles pointed at 135° (45° down towards the slick) with the compressed; and.
6. The highest burn efficiency recorded (99.6 %) was with a 9:1aspect ratio in calm conditions with no air injection.
7. The estimated burn rate with an aspect ratio of 9:1 is lower than with an aspect ratio of 1:1 or 4:1;
8. Waves appear to reduce burn rates slightly;
9. There appears to be a slight increase in burn rate with air injection;
10. The lowest measured burn rate (1.6 mm/min) was measured with the 9:1 aspect ratio, in calm conditions with no air injection;
11. The highest burn rate estimated (3.2 mm/min) was with a 4:1aspect ratio in waves with air injected at 135° from vertical up (i.e., 45° downward toward the burning slick).
12. The narrow boom configuration (9:1, red points) has the lowest $PM_{2.5}$ emission factors and the highest combustion efficiency, but not necessarily the greatest amount of oil consumed,
13. The highest $PM_{2.5}$ emission factor is 160 g/kg oil consumed for the 1:1 aspect ratio control burn (no waves, no compressed air). The lowest emission factor is 60 g/kg for the case of the 9:1 aspect ratio fire boom, in waves, with air injected by 12 nozzles pointed up at 45°.
14. Combustion efficiencies increased at the boom aspect ratio increased (making the oil slick more linear), independent of air and wave treatments.
15. The 9:1 aspect ratio showed the best combustion efficiencies across all treatment, even though burn efficiencies were decrease with wave action.

The 9:1 aspect ratio had the highest burn and combustion efficiencies for all treatments, except in wave plus air. This configuration should be further assessed for application in active oil spill response scenarios at a larger scale than the one used in this study.

5.4 Recommendations

Based on the results of the experiments, the following recommendations are made:

1. Further testing at CRREL is warranted to assess whether additional compressed air would reduce

soot emission factors.

2. The system as tested, with a 185 scfm compressor, supplies about 100 g/s of compressed air to a fire burning about 100 g/s of crude oil. Stoichiometric air requirement is about 15 g air/g crude oil. Additional tests to determine how much more compressed air would be required to virtually eliminate soot would be useful.
3. Redesign compressed air system with field use in mind (i.e., use common air header built into boom floatation or skirt, like Hydro Fire Boom concept) and tow test at Ohmsett.
4. Consider use of central compressed air nozzles placed just above the fuel surface to allow wider aspect ratios (i.e., feed combustion air into central area of fire that is usually starved of combustion air).
5. Consider using multiple spouts with the optimum aspect ratio obtained from this study (9:1). A recent study (Wan et al., 2019) demonstrated that the interaction of multiple pool fires might lead to higher burning rate and flame height than single pool fire. The flame of the optimally spaced multiple spouts will couple and result a higher heat feedback to the pool surface. The spacing between the spouts will drag air into flame and reduce the soot production. By changing the length of the adjacent spouts (one short, one long spout) a fire whirl can be created to further enhance the burn efficiency.

References

Alaska Clean Seas. 1991. Long duration test burn: 3M 8-inch fire containment boom. ACS Newsletter. Vol (1), No.1, March 31, 1991. Anchorage.

Buist, I.A., S.G. Potter, B.K. Trudel, S.R. Shelnutt, A.H. Walker, D.K. Scholz, P.J. Brandvik, J. Fritt-Rasmussen, A.A. Allen. 2013. In Situ Burning in Ice-Affected Waters: State of Knowledge Report. Joint Industry Programme Final Report 7.1.1. http://www.arcticresponsetechnology.org/wp-content/uploads/2013/10/Report-7.1.1-OGP_State_of_Knowledge_ISB_Ice_Oct_14_2013.pdf

Franken, P., D. Perry, R Randt, R Petersen, and C. Thorpe. 1992. Combustive management of oil spills -Final report. University of Arizona.

Koseki, H., 2000. Large Scale Pool Fires : Results Of Recent Experiments. Fire Safety Science 6: 115-132.

Kupersmith, J.A. 1995. Trip Report: MSRC Mesoscale Fuel Burn Experiments at SwRI. MSRC R&D Division, Washington, D.C.

McGrattan, K., H. Baum, W. Walton, and J. Trelles. 1997. Smoke Plume Trajectory from In Situ Burning of Crude Oil in Alaska ---Field Experiments and Modeling of Complex Terrain. National Institute of Standards and Technology (NIST), Gaithersburg, MD, U.S., 127 p.

Nordvik, A., J. Simmons, J. Burkes, I. Buist, D. Blersch and M. Reed. 1995. Mesoscale In Situ Burn Aeration Tests. MSRC Technical Report 95-017, Washington, DC.

NRT Science and Technology Committee. 1995. Aeration Techniques for In Situ Burning of Oil: Enhancing an Alternative Spill Response Method. https://www.nrt.org/sites/2/files/aeration.pdf

Panetta, P.D., and S. Potter. 2016. TRL Definitions for Oil Spill Response Technologies and Equipment. Final Report on Project 1042, U.S. Department of the Interior, Bureau of Safety and Environmental Enforcement (BSEE), Sterling, VA

Wan H., Z. Gao, J. Ji, Y. Zhang, K. Li, L. 2019.Wang. Effects of pool size and spacing on burning rate and flame height of two square heptane pool fires. Journal of Hazardous Materials, Volume 369, pp. 116-124.

Zhang, C., T. Nedwed, A. Tidwell, N. Urbanski, D. Cooper, I. Buist and R. Belore. 2014. One-Step Offshore Oil Skim And Burn System For Use With Vessels Of Opportunity.IOSC Proc: Vol. 2014, No. 1, pp. 1834-1845.

Appendix A – Small-scale Test Protocol

The test protocol (the same for all of the boom configurations) was as follows:

1. Fill tank to the 86 cm mark with fresh water.
2. Install the correct nozzle to the boom (45° or 90°).
3. Attach air hoses to the boom and place the boom in the tank, centered under the fume hood.
4. Verify air sampler flowrate with filter in place. After verifying the air flow, replace filter with a tared filter.
5. Verify air flow through nozzles (0, 2, or 3 SCFM).
6. Configure wave generator to produce a sinusoidal 3 cm wave every 0.8 seconds.
7. Weigh out 6 clean sorbent sheets.
8. Measure out 1 L of the oil to be tested and weigh. (Weigh the oil plus container plus spatula)
9. Transfer the oil to the boom using a spatula as a spill plate to prevent the oil from penetrating the water too deeply.
10. Weigh the empty container and spatula.
11. Turn on the wave generator if required.
12. Verify that all safety equipment is in place.
13. Start the video recording.
14. Ignite oil using a propane torch while starting the stopwatch.
15. Start the fume hood extraction fan once the oil is lit.
16. Start the air sampler and record the time.
17. If required, start the air injection and note the time.
18. Observe the progression of the burn and record the observations and time.
19. Once the flame is out, wait 10 seconds and turn off the air sample while recording the time.
20. Let the boom and residue cool to a safe handling temperature.
21. Weigh the air sampler filter paper and record.
22. Once the boom has cooled, turn off the extractor fan.
23. Use the tared sorbent pads to recover the oil remaining inside and outside the boom.
24. Hang up the sorbent pads to dry overnight. Weigh the pads the next morning.

Appendix B – Test Plan and Data Sheets for Small-scale In-situ Burn Experiments

Test Plan

for

Small-Scale In Situ Burn Tests

Task 1

of

RESEARCH AND DEVELOP A LINEAR AUGMENTED FIRE BOOM CONFIGURATION TO INCREASE BURN EFFICIENCY AND REDUCE SOOT EMISSIONS

Contract No. E17PG00034

For

BSEE Oil Spill Preparedness Division

45600 Woodward Road, VAE-OSRD

Sterling, VA 20166-9216

By

U.S. Army Engineer Research and Development Center

Cold Regions Research and Engineering Laboratory

Hanover, NH

And

S.L. Ross Environmental Research Ltd.

Ottawa, ON

February 26, 2018

Introduction

In situ burning is an effective response option for oil spills; however, the smoke plume, burn residues and black carbon soot from unburned oil and incomplete combustion are significant drawbacks. The dramatic appearance of a large column of dark smoke rising from a burning slick can lead to significant public criticism. In situ burning has been discounted or curtailed due to concerns over the appearance of a smoke plume, despite the scientifically proven net environmental benefits of removing oil from the water surface. Improvements in technology to achieve a cleaner in situ burn would allow On-Scene Commanders to use the technique in more situations, with less worry about negative environmental effects and potential public reaction.

Background

It is known that the rates of oil consumption and soot production are functions of the surface area of the burning slick. The generally accepted burn rate correlation with size for circular in situ crude oil fires (Equation 1) is:

$$\dot{r}''=3.5(1-e^{-D}) \quad (1)$$

Where:

$\dot{r}''$ is the burning oil slick regression rate (mm/min)

D is the pool diameter (m)

The crude oil burn rate increases with pool diameter until it reaches about 3 m, at which point oil consumption levels off at around 3.5 mm/min. The oil consumption rate is limited by the radiant heat transfer back to the burning slick.

Smoke is produced by the incomplete combustion of crude oil, which is largely because of a lack of oxygen, or the inability to supply sufficient air to the center of the fire. Large in situ oil fires draw in considerable amounts of air and most of this entrained air is drawn upwards by the rising column of hot combustion gases. These gases do not penetrate to the middle of the burning slick. Smoke yield is defined as the ratio of the smoke emission rate (mass/time) to the oil consumption rate (mass/time). Figure 1 shows the measured smoke yield for in situ

burns of crude oil over a range of pool sizes (Koseki, 2000). The smoke yield increases with the pan diameter until about 3 m (e.g., from 0.055 kg smoke/kg oil burned in a 0.09-m pan to about 0.2 kg smoke/kg oil burned in a 3-m pan), but does not increase with further increases in diameter. Large-scale in situ burns of crude oil in fire booms at sea have diameters on the order of 40 m, will burn at about 3.5 mm/min and produce a yield of approximately 0.2 kg smoke/kg oil burned.

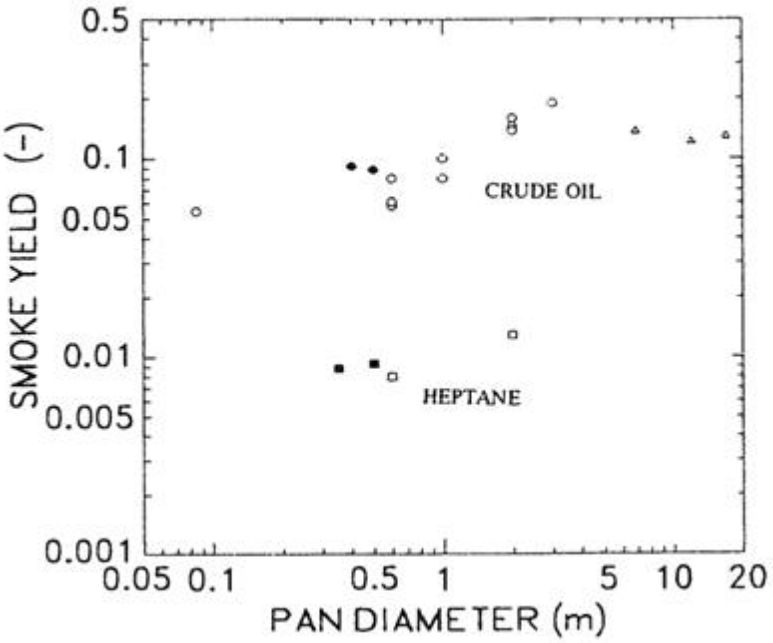

Figure 32. Smoke yield vs. in situ fire diameter (Koseki, 2000)

A considerable amount of research has gone into ways to supplement the natural aeration of in situ burns to increase burn efficiency and rate and reduce soot emissions. A summary of the earlier research was provided by the NRT Science and Technology Committee (NRT 1995). An update on recent studies is also available (Buist et al., 2013). A summary of the most relevant research is as follows:

2.1.1 University of Arizona Burners

In the early 1990s, research was undertaken on methods to enhance in-situ combustion of oil on water (Franken *et al.* 1992) by mechanically enhancing air entrainment into the combustion zone. Any buoyant column of heated rising air or hot combustion gases tends to have a swirl component, commonly referred to as the "Fire

Whirl". This is a desirable effect as it encourages the entrainment of surrounding air and thereby increases aeration at the center of the flames. Several approaches to augmenting this fire whirl have been studied.

One method involved deploying sheet metal vanes around the perimeter of a burning pool to guide the in-flowing air into a cyclonic pattern (see Figure 2). Experiments performed in pools up to 2.4 m in diameter indicated that the addition of vanes increased the flame height by 200%, produced 50% less smoke, and burned faster and more efficiently than control experiments performed without the vanes (Franken *et al.* 1992). Tests were also carried out with different vane configurations. No significant differences in burn rate or smoke production were found between semi-circular and straight vane configurations. It was determined that the vanes augmented the combustion by directing additional air to the center of the blaze, but the configuration or shape of the vanes seemed to have little impact on the combustion rate.

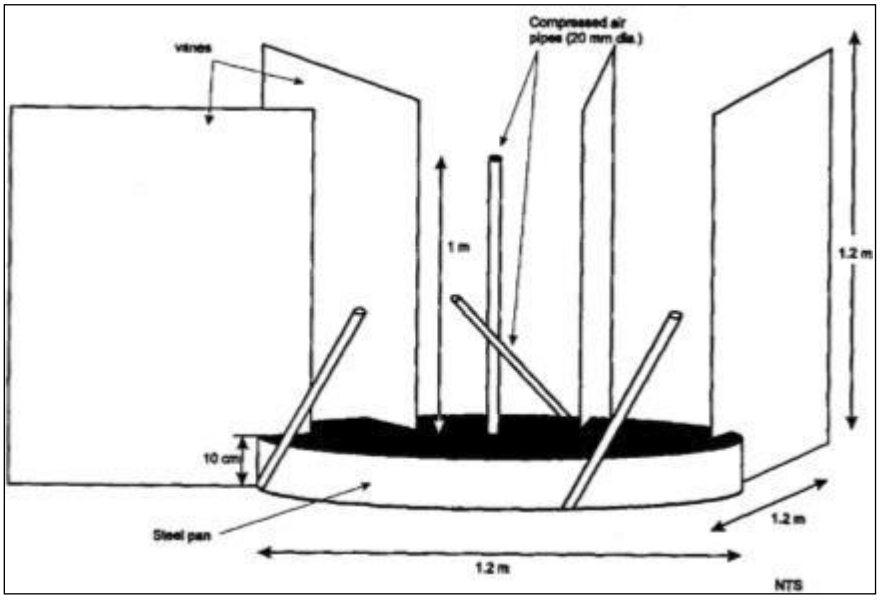

Figure 33. Burn pool showing vanes and compressed air jets

Alaska Clean Seas tested the use of vanes around a larger-scale burn test of fire resistant boom in a large tank (ACS 1991) and found no induced vortex and no reduction in smoke. The increase in the size of the fire reduced the relative effectiveness of the vanes, and it was concluded that vanes alone may not be sufficient to significantly affect the flow of air into the combustion zone when ambient wind effects were present.

Subsequent experiments were designed to research an effective method of augmenting the vane ducting effect described above by supplying more air to the combustion zone. It was concluded that it was not effective in practice to supply the total stoichiometric air needed for combustion using low velocity, high volume air blowers; rather, "the addition of a few hundred cfm of compressed air is more utilitarian than the addition of more than 50,000 cfm of low velocity streams" (Franken et al. 1992).

An effective arrangement for the 1.2 m diameter pool with the vane structure, as described above, was to employ four high pressure air jets, with one placed about 1 m above the liquid surface, aimed straight up the axis of the flames, and the remaining three each placed about 0.6 m from the central axis, a few feet above the liquid and canted by some 30° from vertical (Figure 2). These jets produced a "cyclonic" or "whirling" action within the flame in the same rotational sense as produced by the external vanes. The addition of the high velocity air increased the burning rate by about three and one half times, over that of the vanes alone.

2.1.2 MSRC Testing of Augmented In-situ Combustion

In June 1995, MSRC conducted a series of large-scale pan burn tests to evaluate the effectiveness of several air injection techniques at reducing smoke emissions from in situ burning (Nordvik *et al.* 1995):

High Volume/Low Velocity Diffusers: Heavy industrial blowers were used to provide up to 150% of the stoichiometric air requirement (which for liquid petroleum oils is approximately 16 pounds of air per pound of oil). The air was delivered to the test pool via four ducts positioned outside the burn perimeter, aimed across the surface of the oil. This arrangement reduced smoke production, doubled the natural free burn rate and increased flame temperatures. However, much of the supplemental air was carried away by the rising hot air at the perimeter of the flames, preventing the necessary aeration at the center of the burn. Additionally, the duct equipment was cumbersome and prone to failure in the high-temperature environment (Kupersmith, 1995).

Subsurface Air Bubblers*:* Adding air from underneath the burning zone was attempted. The use of a submerged bubbler did reduce smoke emissions; however, it also greatly reduced the burn rate and increased residue mass

because the mixing and turbulence from the rising air bubbles disrupted the oil surface and reduced the temperature and volatilization of the slick.

Compressed Air Injection*:* The most successful was a compressed air injection system. Figure 3 shows a pan burn with no air injected on the left, and with 66 m3/min of compressed air injected into the fire from five 4-cm diameter nozzles (four canted 45° in a clockwise direction and one straight up in the center of the burn) on the right. The burn rate was increased from 3.5 to almost 5 mm/min using this technique; however, the system was very susceptible to wind. Even a slight breeze would move the fire away from the influence of the compressed air nozzles and cause an increase in smoke and decrease in burn rate.

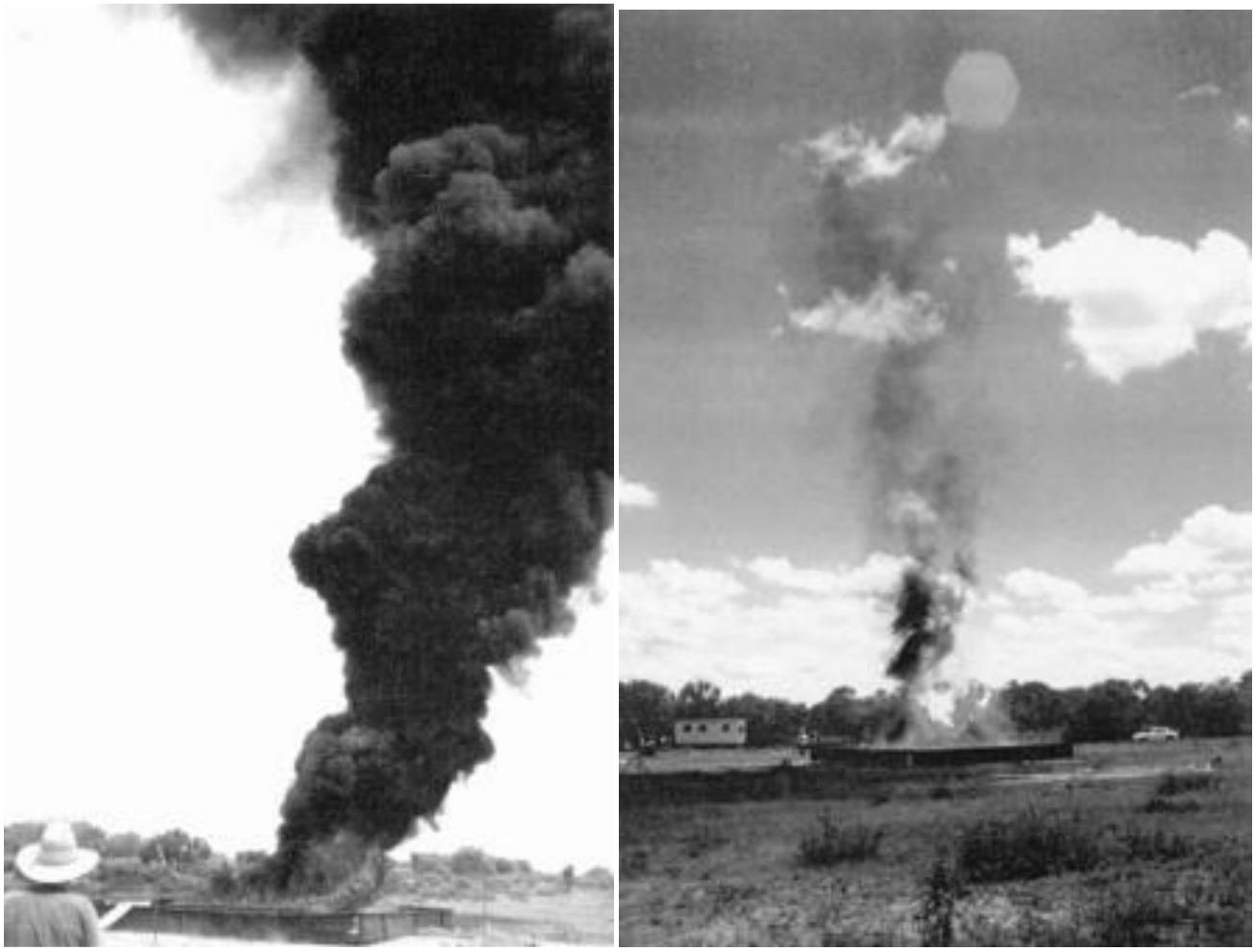

Figure 34. MSRC burn tests without and with aeration

2.1.3 Floating Burner

A recently-developed floating burner designed to combust crude oil recovered by skimmers on smaller recovery vessels was based on the canted compressed air injection concept as well as other enhancement techniques (Zhang et al, 2014). Figure 4 shows a test of the prototype burner at CRREL burning oil from a pan at a rate equivalent to about 15 mm/min.

Figure 35. Floating burner tests at CRREL

Summary

To achieve a cleaner in situ burn, more air must reach the burning oil. The research completed to date suggests that there is significant potential for increased burn rate and efficiency, and reduced smoke emissions, by altering the burn geometry and layout, and supplementing the air supply during in situ burning. There is sufficient past research to conclude that the concept is at Technology Readiness Level 2 (i.e., technology concept and speculative application formulated).

We propose to build on the existing research and investigate techniques to change the shape of the burning slick and supplement the air to the burn using simple, practical enhancements to existing spill response equipment. We propose to develop the design for such a system through a work plan consisting of scaled tests in two wave tanks using crude oil and varying burn geometries, culminating in the burn testing of a near-full-scale prototype in relevant conditions at CRREL in the newly-refurbished wind/wave tank.

The first technology advancement we propose to investigate is in situ burns in long, narrow, parallel fire boom configurations (denoted as linear fires). This arrangement would allow better natural penetration of air into the burn zone to both reduce soot yields and increase radiant heat feedback to the burning slick to increase oil removal efficiency. The existing research suggests that using linear burn geometry with a width of 2 m instead of semi-circular or semi-ellipsoidal burns could reduce soot yields by half (from 0.2 to 0.1). Concomitantly, the overall burn rate will naturally reduce slightly, to approximately 3 mm/min, due to the reduction in heat transfer back to the narrower burn area. The second technology advancement proposed is to augment the linear burns using compressed air to promote better mixing of fuel and naturally entrained air, multiply burning rates, and further reduce smoke yield.

Project Objective

The objective of the project is to develop and test prototype technology and operational methods to significantly enhance in situ burning and improve burn efficiencies by decreasing both the residue remaining and soot emissions.

Small Scale Test Goals

The goals of these initial laboratory-scale experiments are to:

- Design and assemble lab-scale prototype augmented linear burn concepts for testing in the SL Ross wind/wave tank.
- Conduct small-scale in-situ burn experiments with crude oil in the SL Ross laboratory wind/wave tank to determine the efficacy of each of the augmented linear burn concepts in reducing burn residue.
- Conduct small-scale in-situ burn experiments with crude oil in the SL Ross laboratory wind/wave tank to determine the efficacy of each of the augmented linear burn concepts in reducing soot emissions.
- Analyze the data from the small-scale experiments, and prepare and submit a summary data report.
- Select the most promising fire boom layouts for larger scale tests at CRREL.

Targets

The targets for these initial laboratory-scale experiments are:

- Circulate the detailed test plan for the small-scale laboratory experiments by March 15, 2018.
- Complete the small-scale laboratory experiments by May 15, 2018.
- Submit the summary data report on the small-scale experiments by May 31, 2018.

Work Plan

Equipment

Small-scale (i.e., approximate burn area of 2,000 cm^2 or 0.2 m^2) in situ burn tests with different aspect ratios (length of burn pocket to width), and air injection configurations will be conducted in the SL Ross wind/wave tank (Figure 5). The intention of the experiments will be to measure the effects of the various configurations and air enhancements on the burn characteristics under controlled conditions, and identify the most promising combinations of burn layout and air injection settings.

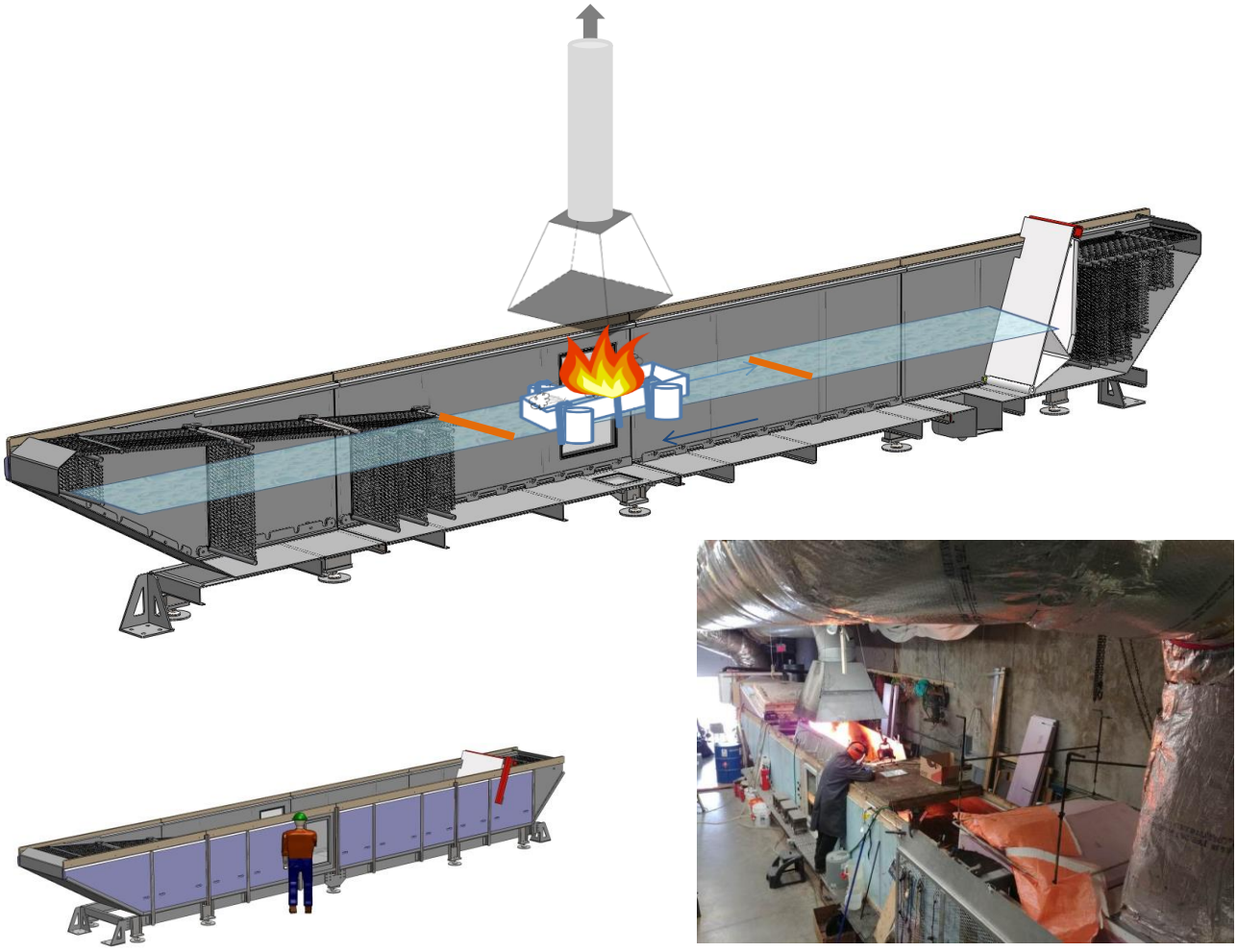

Figure 36 - CAD cutaway drawing of SL Ross wind/wave tank showing fume hood and model fire boom c/w air injection nozzles. Photo in bottom right shows experimental burns with interface insulation concepts from a related BSEE project.

The wind/wave tank measures 1.2 m wide by 11 m long; water depth can be up to 1.2 m, but is normally kept at 85 cm. For *in situ* burn tests, metal heat shields are installed along the sides of the tank and a metal fume hood is positioned over the burn area. Smoke from the burns is removed with a 200-m^3/min fan, through a 60-cm metal duct that is connected to the fume hood.

Floating sheet metal forms (Figure 6) will be fabricated and placed in the tank to simulate fire booms to contain the experimental burns. The aspect ratio of the burn area in the simulated fire booms will be varied from 1.5:1 to 6:1 (6:1 being the longest that will fit completely under the fume hood). Canted nozzles that can be

repositioned to direct air into the burn at different angles will be mounted in various positions along the top of the fire boom to enhance the combustion.

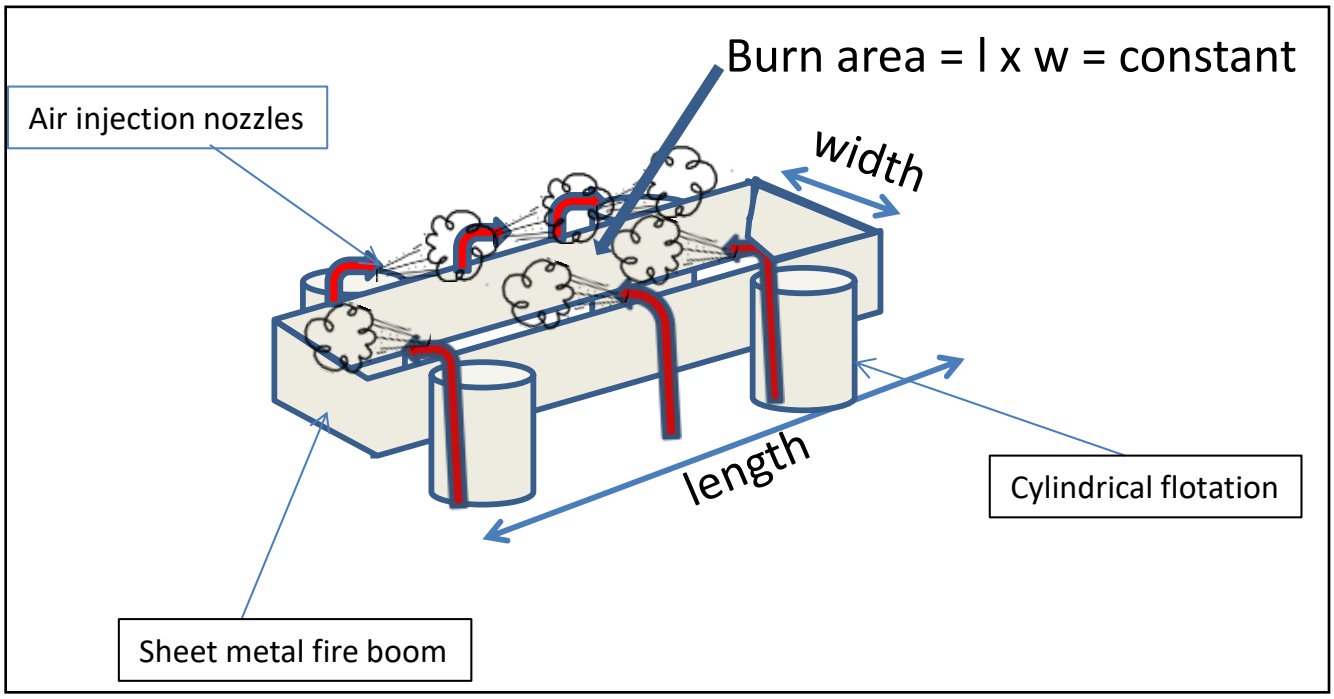

Figure 6. Schematic layout of sheet metal fire boom

Materials and Methods

The burns will be conducted with ANS crude oil. There is a stockpile of ANS crude at CRREL that will be used in the Task 4 full-scale prototype test there, to ensure consistency with the small-scale tests. The use of a crude oil (as opposed to a refined product) is necessary to simulate conditions at a spill, and for the residue characteristics to be relevant to field situations. The mass of oil added and residue recovered will be measured to allow burn removal efficiency (2) to be calculated: the burns will be videotaped and timed to permit estimates of burn rate (3). Soot yield will be measured by simple stack sampling. A test program consisting of 30 individual burns on water varying burn geometry (aspect ratio), air injection and waves (Figure 7) will be conducted.

Burn efficiency is the ratio of the volume of oil burned to the initial oil volume:

$$Burn\ Efficiency\ (vol\%) = \left[\frac{(Initial\ Oil\ Mass)\rho_{oil} - Residue\ Mass}{(Initial\ Oil\ Mass)\rho_{oil}}\right] \times 100 \quad (2)$$

The burn rate is calculated by dividing the volume of oil burned by the area of the fire as a function of time, as given below.

$$Burn\ Rate\ (mm/min) = \left[\frac{Initial\ Oil\ Mass - Residue\ Mass}{(Burn\ Time)(Burn\ Area)\rho_{oil}}\right] \quad (3)$$

A preliminary test matrix is provided in Table 7. Three duplicate experiments will be performed with each of the best combination of aspect ratio and compressed air to permit statistical analysis of the enhancements to the burn (i.e., soot and residue reduction) compared to three duplicates of the Base Case (Aspect Ratio 1.5:1 with no air injection in waves). A total of 36 experiments will be conducted.

Table 7: Test Matrix

Fire Boom Aspect Ratio	Air Injection Configuration	Air Flow Rate	Waves
1.5:1	Base Case (No air)	0	Calm
			Waves x 3
	Nozzle Configuration 1	2 scfm	Calm
			Waves
		4 scfm	Calm
			Waves
	Nozzle Configuration 2	2 scfm	Calm
			Waves
		4 scfm	Calm
			Waves
3:1	Base Case (No air)	0	Calm

			Waves
	Nozzle Configuration 1	2 scfm	Calm
			Waves
		4 scfm	Calm
			Waves
	Nozzle Configuration 2	2 scfm	Calm
			Waves
		4 scfm	Calm
			Waves
6:1	Base Case (No air)	0	Calm
			Waves
	Nozzle Configuration 1	2 scfm	Calm
			Waves
		4 scfm	Calm
			Waves
	Nozzle Configuration 2	2 scfm	Calm
			Waves
		4 scfm	Calm
			Waves

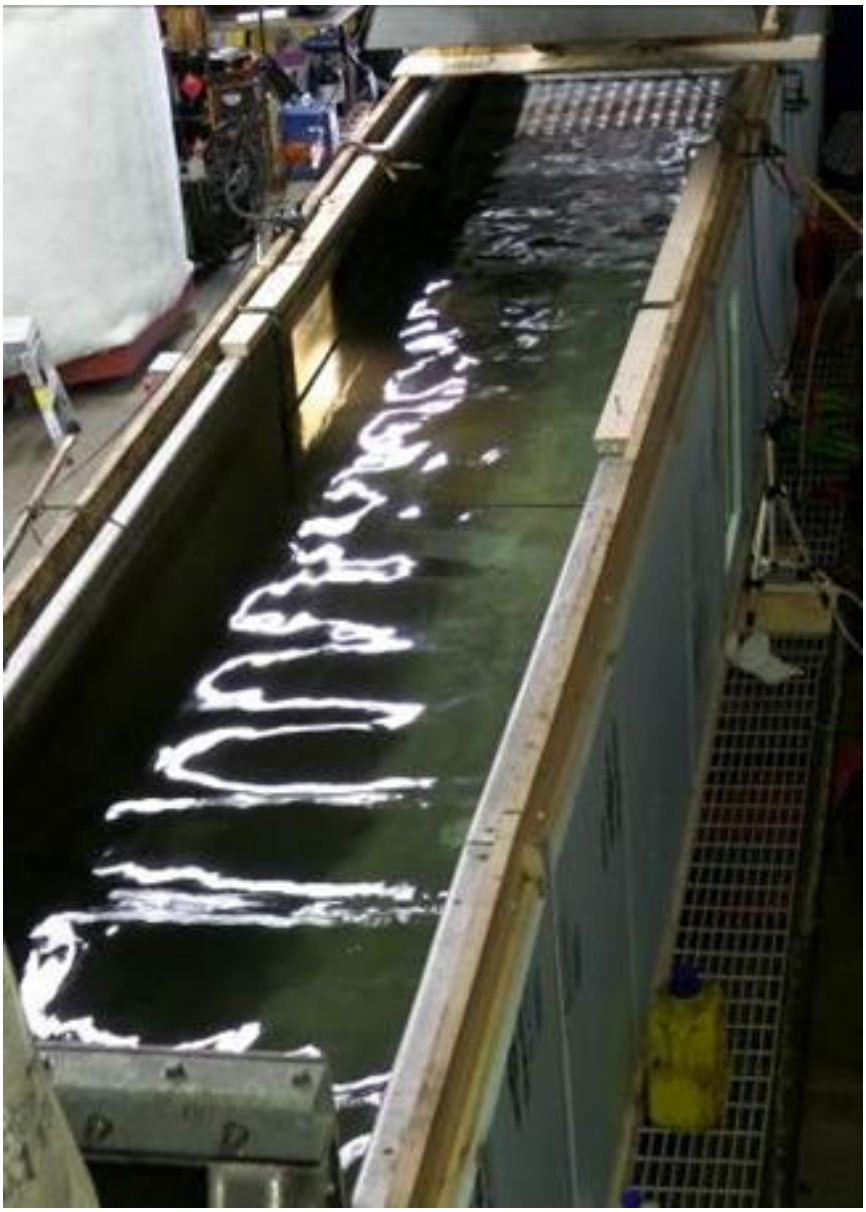

Figure 7 - Example of waves in the SL Ross wave tank.

Test Procedure

The test procedure for a Linear Augmented Burn experiment in the wind/wave tank is as follows:

1. Raise the floating barriers at either end of the test section and thoroughly clean the water surface with sorbent pads to remove any oil or residue traces.
2. Measure and record the air and water temperatures with a digital thermometer.

3. Place fire boom mock-up with specified aspect ratio and air nozzles in test area and attach with steel cables.
4. Measure 1000 mL of fresh crude oil (to form an approximately 5-mm thick slick in the fire boom mock-up) into a graduated cylinder; record mass of cylinder and oil.
5. Place a sign at the edge of the tank that will be visible in the video denoting test number, conditions and approximate test time of day.
6. Carefully pour the oil onto the water surface of the tank at the open end of the fire boom mock-up.
7. Measure and record mass of empty graduated cylinder.
8. Allow the oil to spread over the enclosed area of the fire boom mock-up and stabilize.
9. If required for the test, start wave generator and allow waves to stabilize.
10. Ignite slick with a propane soldering torch. If this fails, attempt ignition with a diesel-soaked sorbent pad. If this also fails, employ a small amount (~ 50 g) of gelled gasoline.
11. Once ignition is achieved and the flame stabilized, start the exhaust fan.
12. Measure and record the following times: initial ignition time, time to full ignition (100% flame coverage); time to the vigorous (or intense) burn phase; time to 50% flame coverage; and, time to extinction.
13. If specified, once the flame is fully established over the entire enclosed area of the fire boom mock-up, start the compressed air flow to the nozzles.
14. Once the flame is fully established, start soot sampling apparatus
15. Record any notable observations during the burn.
16. Once the burn extinguishes turn off the soot sampling, compressed ait, exhaust fan and wave generator.
17. After extinction of the flame, collect the residue with pre-weighed rectangles of sorbent pad. Shake each pas to remove as much water as possible, then hang to dry overnight. Measure and record mass after drying (it is assumed that very little of the burn residue evaporates over this period).

Small-scale Data Analysis and Summary Report

Task 1 of the project also involves analyzing and summarizing the data from the small-scale experiments. The data collected from the small-scale burn experiments will be entered into an Excel spreadsheet, analyzed and summarized. A summary data report will be produced and circulated that presents the data and makes recommendations for which linear burn augmentation systems should be pursued for the full-scale prototype design and CRREL experiment program.

Data Management Plan

The data inputs for the small-scale test program are shown in Table 8. Data inputs for the small-scale tests include existing information on the properties of the fresh oils, and data generated by the tests. The fresh oil properties are available in an Excel spreadsheet that is stored at the SL Ross office in Ottawa.

The data processing that will occur during this Task is presented in Table 9.

Table 8: Data inputs for small-scale experimental program

Dataset	Format	Source	Use Restrictions
Fresh Oil Properties (e.g., density, viscosity, pour point, interfacial tension)	Excel	SL Ross	No restrictions.

Small-scale Experiment Data
• Test Conditions
  ○ Date and time of test
  ○ Air and water temperature
  ○ Wave height and period
  ○ Current speed
• Test Results
  ○ Oil and residue mass
  ○ Burn duration
  ○ Visual observations
	This data will be recorded manually, in ink, on prepared test sheets during the experiments.	This data will be generated by the experiments.	The data from the experiments is the property of CRREL and BSEE.

Small-scale Experiment Video	mp4	This data will be generated by the experiments.	The video of the experiments is the property of CRREL and BSEE.

Table 9: Data processing summary for small-scale experiments

Access and Sharing	Access to data generated by the small-scale tests will be restricted to the project participants, SL Ross, CRREL and BSEE, and to the EPA. The metadata resulting from the tests will be presented to the BSEE in a summary report.
Data Storage	Test sheets with the manually recorded experimental data will be collected in a binder, which will be stored at the SL Ross laboratory facility for the duration of the testing. Upon completion of the small-scale experimental program, the test sheets will be scanned into a pdf format, and stored electronically at the SL Ross office. Video recordings of the tests will be stored electronically at the SL Ross laboratory.
Data Processing	Information from the test sheets will be periodically transcribed into an Excel spreadsheet. Data transcription will be audited by a second key project member.

	Calculation of burn efficiency will be done for each test. The results will be organized in tables to allow comparisons of burn efficiency against the different test conditions.

Data gathered during the experiments will be transferred to an Excel spreadsheet for processing and analysis. The data will be organized into tables to analyse the results for the effects of the test conditions on burn efficiency and soot production. Charts will be prepared to highlight the effects of particular test parameters. Visual observations of the tests will be used, as needed, to provide further insight into the effectiveness of the augmented linear burn concepts.

The proposed data publishing arrangement is summarised in Table 10.

Table 10: Proposed project metadata publishing arrangements

Title	Summary Data Report on Small-scale Burn Tests
Description	A report summarising the results and conclusions from the small-scale experiments will be prepared.
Formats	Word, pdf, Excel
Data Storage	Word and pdf versions of the summary report will be provided to CRREL and BSEE by email. Copies of the report and the Excel spreadsheet containing the test data will be stored at the SL Ross office in Ottawa.
Metadata Point of Contact	The point of contact for the project metadata will be the Project Manager, James McCourt.
Restrictions	The summary report is the property of CRREL and BSEE and will not be shared outside of the project personnel.

Quality Control Plan

The following quality control measures will be employed for these experiments.

Initial Calibration Data. A check is made to ensure that data is available to show the initial source of calibration data for each piece of instrumentation used in the project. This includes any calibration information necessary to assure that the calibration data is current for the project.

Pre- and Post-Daily Checks. These are checks that are performed on the instrumentation each morning before testing starts and at the end of the day when testing stops. This is done on all days that testing occurs. Note is made of any unusual conditions that occur

Test Checks and Conditions. These checks ensure that the test plan's instructions on how the experiment is to be done are followed and that the records that are to be made during the experiment are completed accurately.

Significant Occurrences/Variations. This part of the quality checks will be concerned with recording any significant occurrences/variations that might occur during the experiments. These will be immediately reported to the SL Ross Project Manager.

Data Reduction and Validation. All data reduction and validation will be performed in accordance with approved and accepted methods. When non-standard methods are utilized, they shall be included in the Draft Technical Report and sufficiently described so that they can be used by independent sources to duplicate the results. With respect to written material, all draft material will be reviewed by at least one other SL Ross senior staff Professional Engineer before submission to CRREL and BSEE.

Safety and Environmental Plan

SL Ross staff has been conducting such experiments at the SL Ross facility for more than thirty years without a lost-time incident. Only minor safety hazards are involved, and these are mitigated by proper lab procedures, appropriate PPE, solvent storage systems, fume hoods, fire extinguishers, eyewash stations and an emergency shower. The 2012 SL Ross EH&S plan for the laboratory will be employed. Copies of the plan are available on request. The oily waste and spent solvents are disposed of using an approved waste handler in accordance with the regulations of the Province of Ontario.

References

Alaska Clean Seas. 1991. Long duration test burn: 3M 8-inch fire containment boom. ACS Newsletter. Vol (1), No.1, March 31, 1991. Anchorage.

Buist, I.A., S.G. Potter, B.K. Trudel, S.R. Shelnutt, A.H. Walker, D.K. Scholz, P.J. Brandvik, J. Fritt-Rasmussen, A.A. Allen. 2013. In Situ Burning in Ice-Affected Waters: State of Knowledge Report. Joint Industry Programme Final Report 7.1.1. http://www.arcticresponsetechnology.org/wp-content/uploads/2013/10/Report-7.1.1-OGP_State_of_Knowledge_ISB_Ice_Oct_14_2013.pdf

Franken, P., D. Perry, R Randt, R Petersen, and C. Thorpe. 1992. Combustive management of oil spills -Final report. University of Arizona.

Koseki, H., 2000. Large Scale Pool Fires: Results Of Recent Experiments. Fire Safety Science 6: 115-132.

Kupersmith, J.A. 1995. Trip Report: MSRC Mesoscale Fuel Burn Experiments at SwRI. MSRC R&D Division, Washington, D.C.

Nordvik, A., J. Simmons, J. Burkes, I. Buist, D. Blersch and M. Reed. 1995. Mesoscale In Situ Burn Aeration Tests. MSRC Technical Report 95-017, Washington, DC.

NRT Science and Technology Committee. 1995. Aeration Techniques for In Situ Burning of Oil: Enhancing an Alternative Spill Response Method. https://www.nrt.org/sites/2/files/aeration.pdf

Zhang, C., T. Nedwed, A. Tidwell, N. Urbanski, D. Cooper, I. Buist and R. Belore. 2014. One-Step Offshore Oil Skim And Burn System For Use With Vessels Of Opportunity.IOSC Proc: Vol. 2014, No. 1, pp. 1834-1845.

Data sheet

Linear Augmented Burn – Small-scale Burn Tests in SL Ross Wave Tank: Preliminary Indications from Experimental Results

- See attached spreadsheet graphs and summary table
- 38 experiments conducted varying boom aspect ratio (Appendix 1), wave height (calm and 3 cm with 0.8 s period), air injection nozzle angle (45° and 90° from vertical) and air flow rate (0, 2 and 3 scfm)
- Key runs repeated three times (see coloured highlighted rows in Table 1)
- Table 1 summarizes data
- Figure 1 shows effects of variables on burn efficiency
    - Little or no change in efficiency with increasing aspect ratio
    - Calm conditions generally result in higher burn efficiency
    - Increased air injection increases burn efficiency
    - 90° nozzles generally result in higher efficiency than 45° nozzles

- Figure 2 shows effects of variables on burn rate
    - Increasing aspect ratio results in declining burn rate
    - Calm conditions generally result in higher burn rates
    - Increased air injection increases burn rate
    - 90° nozzles generally result in higher burn rate than 45° nozzles

Run	Date	Air Flow (SCFM)	Wave (h=3 cm; P= 0.8 s)	Nozzle config.	Boom Aspect Ratio (L:W)	Air Temp (C)	Water Temp (C)	Burn Area (cm^2)	Mass of soot (g/hr)	Average Burn Rate (mm/min)	Burn Efficiency (mass %)
1	27-Jun-18	No	No	NA	1.5:1	24.9	21	1665	0.01	1.31	83.7
2	27-Jun-18	2	No	45	1.5:1	25.1	21	1665	0.01	1.23	82.6
3	27-Jun-18	2	Yes	45	1.5:1	25.3	21	1665	-0.24	1.00	64.0
4	27-Jun-18	No	Yes	NA	1.5:1	25.9	21	1665	0.00	1.03	59.6
5	27-Jun-18	3	No	45	1.5:1	26	21	1665	0.01	1.24	79.7
6	27-Jun-18	No	Yes	NA	1.5:1	26.6	21	1665	0.00	0.93	62.9
7	28-Jun-18	3	Yes	45	1.5:1	25.1	22	1665	0.01	0.84	61.6
8	28-Jun-18	No	Yes	NA	1.5:1	25.5	22	1665	0.01	0.99	64.8
9	29-Jun-18	2	No	90	1.5:1	26.3	22	1665	0.00	1.60	92.0
10	29-Jun-18	3	No	90	1.5:1	26.5	22	1665	0.01	2.75	93.6
11	29-Jun-18	3	Yes	90	1.5:1	26.9	22	1665	0.01	2.76	88.9
12	29-Jun-18	2	Yes	90	1.5:1	27.1	22	1665	0.00	1.25	79.3
13	03-Jul-18	No	No	NA	3.0:1	29.9	25	1631	0.01	1.09	79.1
14	03-Jul-18	2	No	90	3.0:1	29.6	25	1631	0.01	1.58	87.8
15	03-Jul-18	3	No	90	3.0:1	29.7	26	1631	0.01	2.44	92.2
16	03-Jul-18	2	Yes	90	3.0:1	29.8	26	1631	0.00	1.34	78.3
17	03-Jul-18	3	Yes	90	3.0:1	29.9	26	1631	0.00	1.94	87.0
18	03-Jul-18	No	Yes	NA	3.0:1	30.1	26	1631	0.00	1.12	66.9
19	04-Jul-18	2	Yes	45	3.0:1	30	26	1631	0.00	0.95	73.9
20	04-Jul-18	3	No	45	3.0:1	30.5	26	1631	0.00	1.01	76.4
21	04-Jul-18	3	Yes	45	3.0:1	31	26	1631	0.00	1.01	69.9
22	04-Jul-18	2	No	45	3.0:1	31.5	26	1631	0.00	1.13	79.1
23	05-Jul-18	2	No	45	6.0:1	30.1	26	1670	0.00	0.86	76.6
24	05-Jul-18	2	Yes	45	6.0:1	31	26	1670	0.00	0.56	62.5
25	05-Jul-18	3	No	45	6.0:1	31.5	26	1670	0.00	0.88	76.0
26	05-Jul-18	3	Yes	45	6.0:1	31.7	26	1670	0.00	0.66	67.2
27	06-Jul-18	No	No	NA	6.0:1	28	27	1670	0.01	0.83	77.5

28	06-Jul-18	No	Yes	NA	6.0:1	27.4	26	1670	0.00	0.71	68.8
29	06-Jul-18	2	No	90	6.0:1	27.2	26	1670	0.01	1.35	84.6
30	06-Jul-18	2	Yes	90	6.0:1	27.1	26	1670	0.00	0.88	72.7
31	06-Jul-18	3	No	90	6.0:1	27.1	26	1670	0.00	1.57	91.2
32	06-Jul-18	3	Yes	90	6.0:1	27	26	1670	0.00	1.22	82.1
33	12-Jul-18	3	Yes	90	6.0:1	27.6	24	1670	-0.01	1.35	84.3
34	12-Jul-18	3	Yes	90	6.0:1	27.9	24	1670	0.00	1.41	84.4
35	13-Jul-18	3	Yes	90	3.0:1	27.9	24	1631	0.01	1.97	86.5
36	13-Jul-18	3	Yes	90	3.0:1	27.9	24	1631	-0.01	1.92	87.1
37	13-Jul-18	3	Yes	90	1.5:1	28.7	24	1665	0.00	2.15	85.7
38	13-Jul-18	3	Yes	90	1.5:1	29.1	24	1665	0.00	2.16	86.1

Table 11. Experimental Results Summary

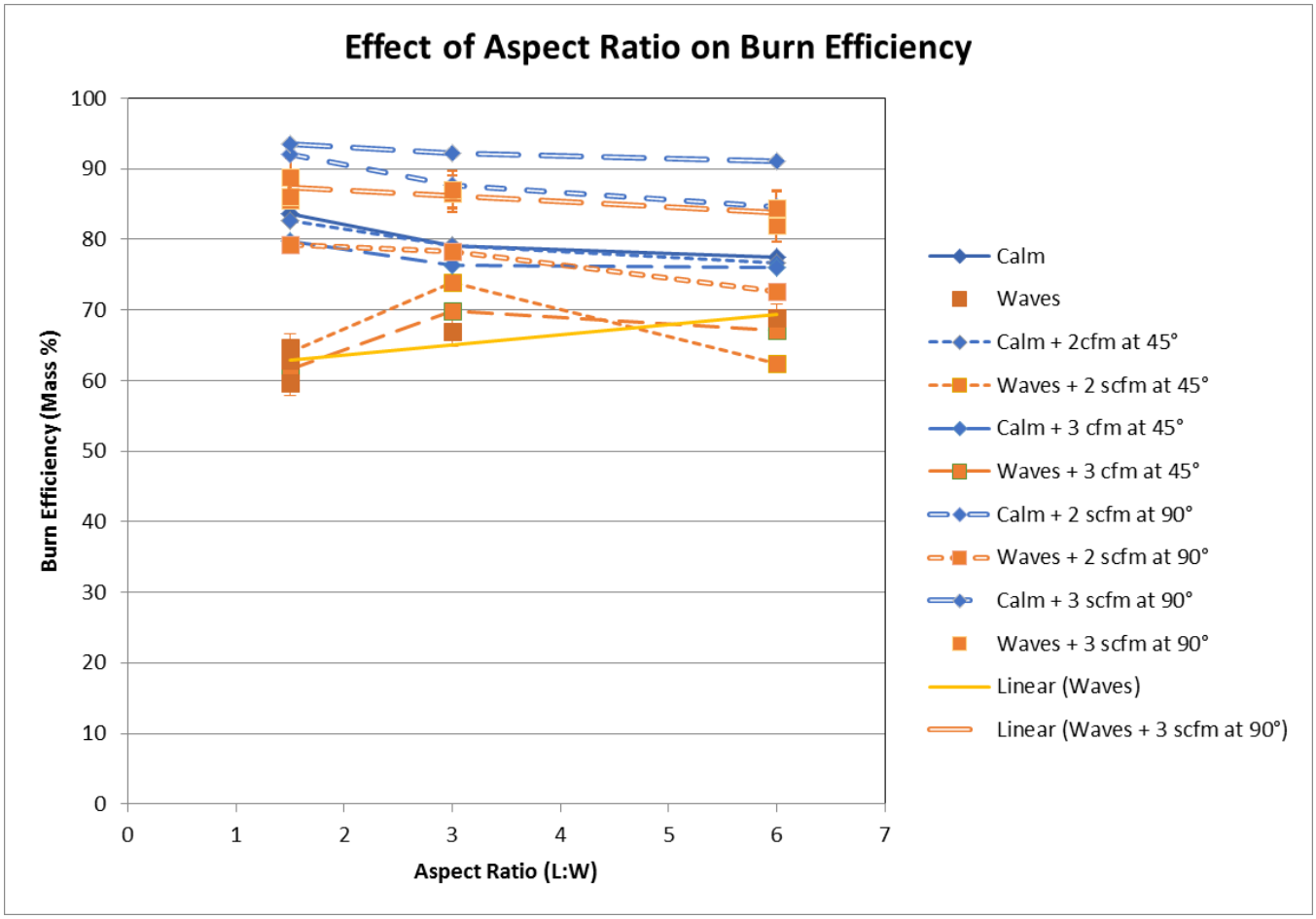

Figure 37: Burn Efficiency

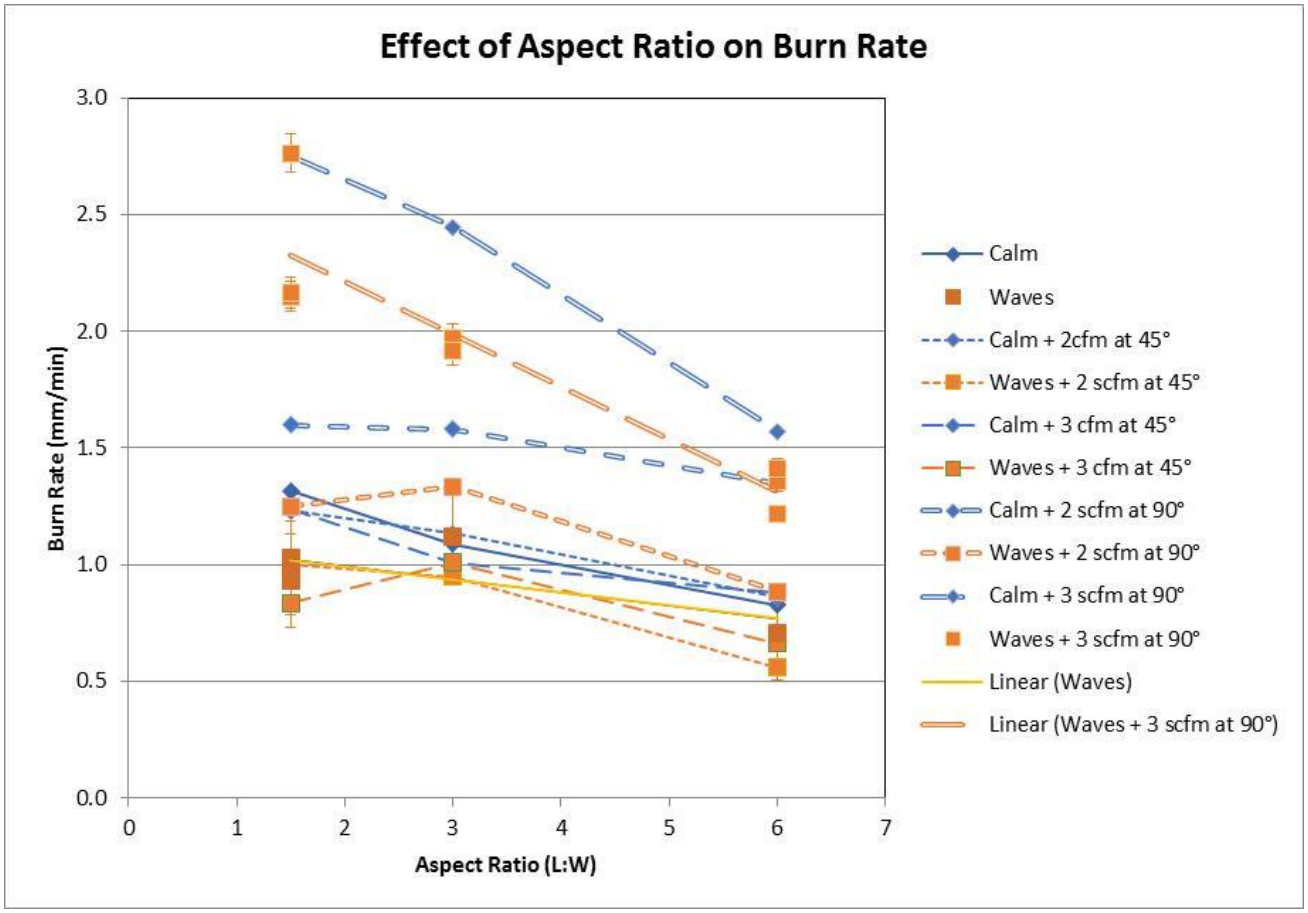

Figure 38. Burn rate

Appendix 1

Augmented Burn Test Procedure:

Boom Design:

Three rectangular booms were constructed. Each had an area of 0.16 m^2, but with different aspect ratios of 1.5:1, 3:1 and, 6:1. The actual dimensions are in **Table 12**.

Table 12: Boom Dimensions

Ratio	Width (cm)	Length (cm)	Area (cm^2)	Height
1.5:1	33.3	50	1665	20.3
3:1	23.3	70	1631	20.3
6:1	16.7	100	1670	20.3

The booms were constructed of 18 Gauge galvanized steel. Sheets were purchased and formed in-house. Each boom was constructed with two cross braces placed under the water line (three cross braces for the 6:1 boom). Floats were constructed from 3.75L paint cans. The air injection nozzles were assembled using ½" pipe and were attached to a 6-place manifold.

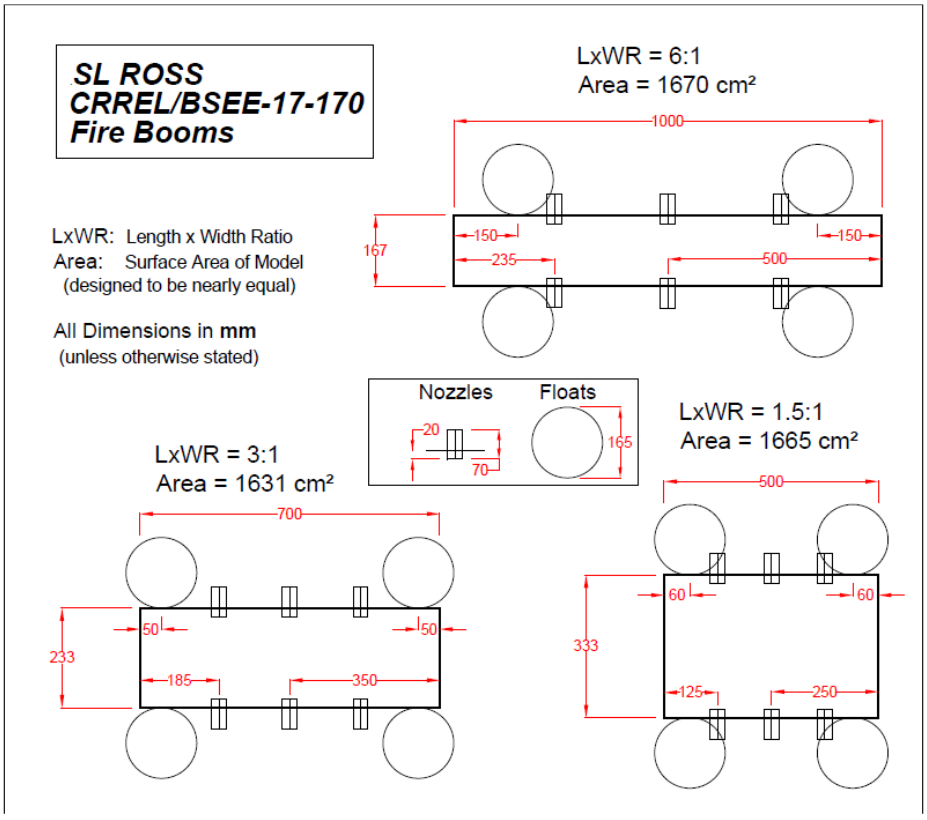

Figure 39: Schematic of booms

Procedure:

The procedure was the same for all of the boom configurations.

1. Fill tank to the 86 cm mark with fresh water.
2. Install the correct nozzle to the boom (45^0 of 90^0).
3. Attach air hoses to the boom and place the boom in the tank, centered under the extraction vent.
4. Verify air sampler volume with filter in place. After verifying the air flow, replace filter with a tared filter.
5. Verify air flow through nozzles (0, 2, or 3 SCFM).
6. Configure wave generator to produce a 3cm wave every 0.8 seconds.
7. Weigh out 6 clean sorbent sheets.
8. Weigh out 1 L of the oil to be tested. (Weigh the oil plus container plus spatula)
9. Transfer the oil to the boom using a spatula as an impact surface to prevent the oil from subsiding.
10. Weigh the empty container and spatula.
11. Turn on the wave generator if required. A time of 600 seconds is sufficient for these runs.
12. Verify that all safety protocols are in place. Read aloud the safety protocol list to ensure that all items are in place.
13. Ignite oil using a propane torch while starting the stopwatch.
14. Start the extractor fan once the oil is lit.
15. Start the air sampler and record the time.
16. If required, start the air injection and note the time.
17. Observe the progression of the burn and record the observations and time.
18. Once the flame is out, wait 10 seconds and turn off the air sample while recording the time.
19. Let the boom cool.
20. Weigh the air sampler filter paper and record.
21. Once the boom has cooled, turn off the extractor fan.
22. Use the tared sorbent pads to recover the oil remaining (inside and outside the boom.
23. Hang up the sorbent pads to dry overnight. Weigh the pads the next morning.

Appendix C – Test Plan and Safety Datasheets for CRREL Wave Tank In-situ Burn Experiments

Test Plan

for

Large-Scale Linear Augmented Fire Boom In Situ Burn Experiments

Task 4

of

RESEARCH AND DEVELOP A LINEAR AUGMENTED FIRE BOOM CONFIGURATION TO INCREASE BURN EFFICIENCY AND REDUCE SOOT EMISSIONS

Contract No. E17PG00034

For

BSEE Oil Spill Preparedness Division

45600 Woodward Road, VAE-OSRD

Sterling, VA 20166-9216

By

U.S. Army Engineer Research and Development Center

Cold Regions Research and Engineering Laboratory

Hanover, NH

And

S.L. Ross Environmental Research Ltd.

Ottawa, ON

August 31, 2018

Table of Contents

List of Tables

List of Figures

Participating Organizations

Sponsor: Bureau of Safety and Environmental Enforcement, U.S. Department of the Interior
Contact: Mr. Joe Mullin

Karen Stone, Contracting Officer's Representative 703-787-1810

Karen.stone@bsee.gov

Facility: USACE Engineer Research and Development Center

Cold Regions Research and Engineering Laboratory

Research Area

Hanover, NH

Contact: Nathan Lamie

(603) 646-4598

Nathan.J.Lamie@usace.army.mil

CRREL Contractor: S.L. Ross Environmental Research Ltd

Contact: Ian Buist, Test Director

(613) 232-1564 ext. 22

Ian@slross.com

Air Emissions Sampling:

Air and Energy Management Division, Environmental Protection Agency

Contact: Brian Gullet

919-541-2821

gullett.brian@epa.gov

Time Frame: November 2016

Introduction

In situ burning is an effective response option for oil spills; however, the smoke plume, burn residues and black carbon soot from unburned oil and incomplete combustion are significant drawbacks. The dramatic appearance of a large column of dark smoke rising from a burning slick can lead to significant public criticism. In situ burning has been discounted or curtailed due to concerns over the appearance of a smoke plume, despite the scientifically proven net environmental benefits of removing oil from the water surface. Improvements in technology to achieve a cleaner in situ burn would allow On-Scene Commanders to use the technique in more situations, with less worry about negative environmental effects and potential public reaction.

Background

It is known that the rates of oil consumption and soot production are functions of the surface area of the burning slick. The generally accepted burn rate correlation with size for circular in situ crude oil fires (Equation 1) is:

$$\dot{r}''=3.5(1-e^{-D}) \quad (1)$$

Where:

$\dot{r}''$ is the burning oil slick regression rate (mm/min)

D is the pool diameter (m)

The crude oil burn rate increases with pool diameter until it reaches about 3 m, at which point oil consumption levels off at around 3.5 mm/min. The oil consumption rate is limited by the radiant heat transfer back to the burning slick.

Smoke is produced by the incomplete combustion of crude oil, which is largely because of a lack of oxygen, or the inability to supply sufficient air to the center of the fire. Large in situ oil fires draw in considerable amounts of air and most of this entrained air is drawn upwards by the rising column of hot combustion gases. These gases do not penetrate to the middle of the burning slick. Smoke yield is defined as the ratio of the smoke emission rate (mass/time) to the oil consumption rate (mass/time). Figure 1 shows the measured smoke yield for in situ burns of crude oil over a range of pool sizes (Koseki, 2000). The smoke yield increases with the pan diameter

until about 3 m (e.g., from 0.055 kg smoke/kg oil burned in a 0.09-m pan to about 0.2 kg smoke/kg oil burned in a 3-m pan), but does not increase with further increases in diameter. Large-scale in situ burns of crude oil in fire booms at sea have diameters on the order of 40 m, will burn at about 3.5 mm/min and produce a yield of approximately 0.2 kg smoke/kg oil burned.

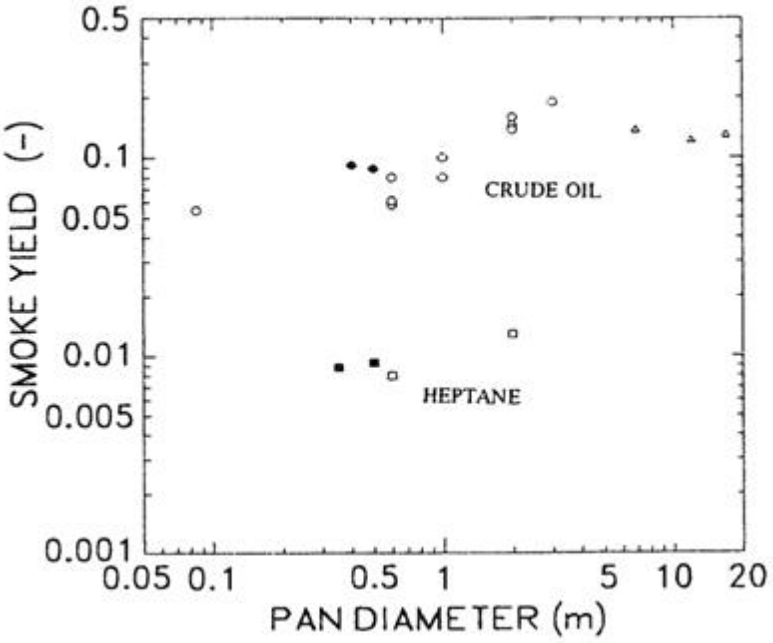

Figure 40. Smoke yield vs. in situ fire diameter (Koseki, 2000)

A considerable amount of research has gone into ways to supplement the natural aeration of in situ burns to increase burn efficiency and rate and reduce soot emissions. A summary of the earlier research was provided by the NRT Science and Technology Committee (NRT 1995). An update on recent studies is also available (Buist et al., 2013). A summary of the most relevant research is as follows:

University of Arizona Burners

In the early 1990s, research was undertaken on methods to enhance in-situ combustion of oil on water (Franken *et al.* 1992) by mechanically enhancing air entrainment into the combustion zone. Any buoyant column of heated rising air or hot combustion gases tends to have a swirl component, commonly referred to as the "Fire

Whirl". This is a desirable effect as it encourages the entrainment of surrounding air and thereby increases aeration at the center of the flames. Several approaches to augmenting this fire whirl have been studied.

One method involved deploying sheet metal vanes around the perimeter of a burning pool to guide the in-flowing air into a cyclonic pattern (see Figure 2). Experiments performed in pools up to 2.4 m in diameter indicated that the addition of vanes increased the flame height by 200%, produced 50% less smoke, and burned faster and more efficiently than control experiments performed without the vanes (Franken *et al.* 1992). Tests were also carried out with different vane configurations. No significant differences in burn rate or smoke production were found between semi-circular and straight vane configurations. It was determined that the vanes augmented the combustion by directing additional air to the center of the blaze, but the configuration or shape of the vanes seemed to have little impact on the combustion rate.

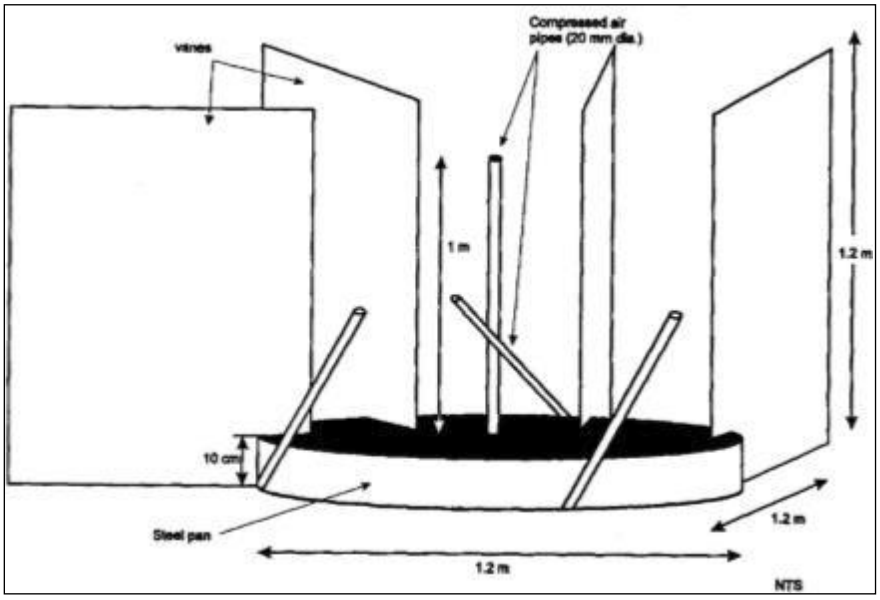

Figure 41. Burn pool showing vanes and compressed air jets

Alaska Clean Seas tested the use of vanes around a larger-scale burn test of fire resistant boom in a large tank (ACS 1991) and found no induced vortex and no reduction in smoke. The increase in the size of the fire reduced the relative effectiveness of the vanes, and it was concluded that vanes alone may not be sufficient to significantly affect the flow of air into the combustion zone when ambient wind effects were present.

Subsequent experiments were designed to research an effective method of augmenting the vane ducting effect described above by supplying more air to the combustion zone. It was concluded that it was not effective in practice to supply the total stoichiometric air needed for combustion using low velocity, high volume air blowers; rather, "the addition of a few hundred cfm of compressed air is more utilitarian than the addition of more than 50,000 cfm of low velocity streams" (Franken et al. 1992).

An effective arrangement for the 1.2 m diameter pool with the vane structure, as described above, was to employ four high pressure air jets, with one placed about 1 m above the liquid surface, aimed straight up the axis of the flames, and the remaining three each placed about 0.6 m from the central axis, a few feet above the liquid and canted by some 30° from vertical (Figure 2). These jets produced a "cyclonic" or "whirling" action within the flame in the same rotational sense as produced by the external vanes. The addition of the high velocity air increased the burning rate by about three and one half times, over that of the vanes alone.

MSRC Testing of Augmented In-situ Combustion

In June 1995, MSRC conducted a series of large-scale pan burn tests to evaluate the effectiveness of several air injection techniques at reducing smoke emissions from in situ burning (Nordvik *et al.* 1995):

High Volume/Low Velocity Diffusers: Heavy industrial blowers were used to provide up to 150% of the stoichiometric air requirement (which for liquid petroleum oils is approximately 16 pounds of air per pound of oil). The air was delivered to the test pool via four ducts positioned outside the burn perimeter, aimed across the surface of the oil. This arrangement reduced smoke production, doubled the natural free burn rate and increased flame temperatures. However, much of the supplemental air was carried away by the rising hot air at the perimeter of the flames, preventing the necessary aeration at the center of the burn. Additionally, the duct equipment was cumbersome and prone to failure in the high-temperature environment (Kupersmith, 1995).

Subsurface Air Bubblers*:* Adding air from underneath the burning zone was attempted. The use of a submerged bubbler did reduce smoke emissions; however, it also greatly reduced the burn rate and increased residue mass

because the mixing and turbulence from the rising air bubbles disrupted the oil surface and reduced the temperature and volatilization of the slick.

Compressed Air Injection*:* The most successful was a compressed air injection system. Figure 3 shows a pan burn with no air injected on the left, and with 66 m3/min of compressed air injected into the fire from five 4-cm diameter nozzles (four canted 45° in a clockwise direction and one straight up in the center of the burn) on the right. The burn rate was increased from 3.5 to almost 5 mm/min using this technique; however, the system was very susceptible to wind. Even a slight breeze would move the fire away from the influence of the compressed air nozzles and cause an increase in smoke and decrease in burn rate.

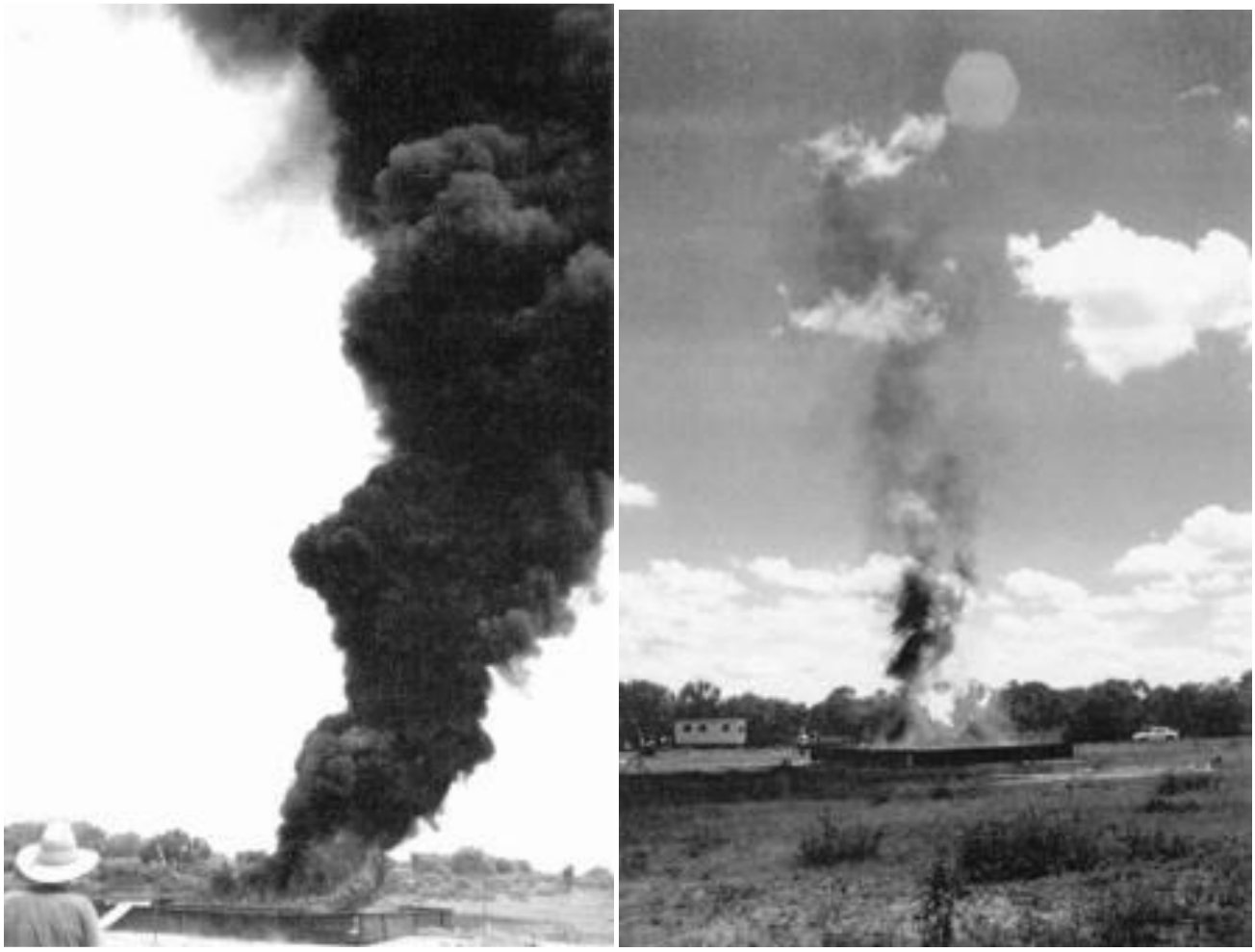

Figure 42. MSRC burn tests without and with aeration

Floating Burner

A recently-developed floating burner designed to combust crude oil recovered by skimmers on smaller recovery vessels was based on the canted compressed air injection concept as well as other enhancement techniques (Zhang et al, 2014). Figure 4 shows a test of the prototype burner at CRREL burning oil from a pan at a rate equivalent to about 15 mm/min.

Figure 43. Floating burner tests at CRREL

Summary

To achieve a cleaner in situ burn, more air must reach the burning oil. The research completed to date suggests that there is significant potential for increased burn rate and efficiency, and reduced smoke emissions, by altering the burn geometry and layout, and supplementing the air supply during in situ burning. There is sufficient past research to conclude that the concept is at Technology Readiness Level 2 (i.e., technology concept and speculative application formulated).

We propose to build on the existing research and investigate techniques to change the shape of the burning slick and supplement the air to the burn using simple, practical enhancements to existing spill response equipment. We propose to develop the design for such a system through a work plan consisting of scaled experiments in two wave tanks using crude oil and varying burn geometries, culminating in the burn testing of a near-full-scale prototype in relevant conditions at CRREL in the newly-refurbished wind/wave tank.

The first technology advancement we propose to investigate is in situ burns in long, narrow, parallel fire boom configurations (denoted as linear fires). This arrangement would allow better natural penetration of air into the burn zone to both reduce soot yields and increase radiant heat feedback to the burning slick to increase oil removal efficiency. The existing research suggests that using linear burn geometry with a width of 2 m instead of semi-circular or semi-ellipsoidal burns could reduce soot yields by half (from 0.2 to 0.1). Concomitantly, the overall burn rate will naturally reduce slightly, to approximately 3 mm/min, due to the reduction in heat transfer back to the narrower burn area. The second technology advancement proposed is to augment the linear burns using compressed air to promote better mixing of fuel and naturally entrained air, multiply burning rates, and further reduce smoke yield.

Small-scale Burn Experiments in SL Ross Wave Tank: Preliminary Indications from Experimental Results

- 38 experiments were conducted varying boom aspect ratio, wave height (calm and 3 cm with 0.8 s period), air injection nozzle angle (45° and 90° from vertical) and air flow rate (0, 2 and 3 scfm)
- Key runs repeated three times (see colored highlighted rows in Table 1)
- Table 1 summarizes key experimental data: no variable has measureable effect on soot production at this small fire scale
- Figure 5 shows effects of variables on burn efficiency
    - Little or no change in efficiency with increasing aspect ratio
    - Calm conditions generally result in higher burn efficiency
    - Increased air injection increases burn efficiency
    - 90° nozzles generally result in higher efficiency than 45° nozzles
- Figure 6 shows effects of variables on burn rate
    - Increasing aspect ratio results in declining burn rate

- Calm conditions generally result in higher burn rates
- Increased air injection increases burn rate
- 90° nozzles generally result in higher burn rate than 45° nozzles

Table 13 - Small-scale Test Burn Experimental Results Summary

Run	Date	Air Flow (SCFM)	Wave (h=3 cm; P= 0.8 s)	Nozzle config.	Boom Aspect Ratio (L:W)	Air Temp (C)	Water Temp (C)	Burn Area (cm^2)	Mass of soot (g/hr)	Average Burn Rate (mm/min)	Burn Efficiency (mass %)
1	27-Jun-18	No	No	NA	1.5:1	24.9	21	1665	0.01	1.31	83.7
2	27-Jun-18	2	No	45	1.5:1	25.1	21	1665	0.01	1.23	82.6
3	27-Jun-18	2	Yes	45	1.5:1	25.3	21	1665	-0.24	1.00	64.0
4	27-Jun-18	No	Yes	NA	1.5:1	25.9	21	1665	0.00	1.03	59.6
5	27-Jun-18	3	No	45	1.5:1	26	21	1665	0.01	1.24	79.7
6	27-Jun-18	No	Yes	NA	1.5:1	26.6	21	1665	0.00	0.93	62.9
7	28-Jun-18	3	Yes	45	1.5:1	25.1	22	1665	0.01	0.84	61.6
8	28-Jun-18	No	Yes	NA	1.5:1	25.5	22	1665	0.01	0.99	64.8
9	29-Jun-18	2	No	90	1.5:1	26.3	22	1665	0.00	1.60	92.0
10	29-Jun-18	3	No	90	1.5:1	26.5	22	1665	0.01	2.75	93.6
11	29-Jun-18	3	Yes	90	1.5:1	26.9	22	1665	0.01	2.76	88.9
12	29-Jun-18	2	Yes	90	1.5:1	27.1	22	1665	0.00	1.25	79.3
13	03-Jul-18	No	No	NA	3.0:1	29.9	25	1631	0.01	1.09	79.1
14	03-Jul-18	2	No	90	3.0:1	29.6	25	1631	0.01	1.58	87.8
15	03-Jul-18	3	No	90	3.0:1	29.7	26	1631	0.01	2.44	92.2
16	03-Jul-18	2	Yes	90	3.0:1	29.8	26	1631	0.00	1.34	78.3
17	03-Jul-18	3	Yes	90	3.0:1	29.9	26	1631	0.00	1.94	87.0
18	03-Jul-18	No	Yes	NA	3.0:1	30.1	26	1631	0.00	1.12	66.9
19	04-Jul-18	2	Yes	45	3.0:1	30	26	1631	0.00	0.95	73.9
20	04-Jul-18	3	No	45	3.0:1	30.5	26	1631	0.00	1.01	76.4
21	04-Jul-18	3	Yes	45	3.0:1	31	26	1631	0.00	1.01	69.9
22	04-Jul-18	2	No	45	3.0:1	31.5	26	1631	0.00	1.13	79.1
23	05-Jul-18	2	No	45	6.0:1	30.1	26	1670	0.00	0.86	76.6
24	05-Jul-18	2	Yes	45	6.0:1	31	26	1670	0.00	0.56	62.5
25	05-Jul-18	3	No	45	6.0:1	31.5	26	1670	0.00	0.88	76.0
26	05-Jul-18	3	Yes	45	6.0:1	31.7	26	1670	0.00	0.66	67.2
27	06-Jul-18	No	No	NA	6.0:1	28	27	1670	0.01	0.83	77.5

28	06-Jul-18	No	Yes	NA	6.0:1	27.4	26	1670	0.00	0.71	68.8
29	06-Jul-18	2	No	90	6.0:1	27.2	26	1670	0.01	1.35	84.6
30	06-Jul-18	2	Yes	90	6.0:1	27.1	26	1670	0.00	0.88	72.7
31	06-Jul-18	3	No	90	6.0:1	27.1	26	1670	0.00	1.57	91.2
32	06-Jul-18	3	Yes	90	6.0:1	27	26	1670	0.00	1.22	82.1
33	12-Jul-18	3	Yes	90	6.0:1	27.6	24	1670	-0.01	1.35	84.3
34	12-Jul-18	3	Yes	90	6.0:1	27.9	24	1670	0.00	1.41	84.4
35	13-Jul-18	3	Yes	90	3.0:1	27.9	24	1631	0.01	1.97	86.5
36	13-Jul-18	3	Yes	90	3.0:1	27.9	24	1631	-0.01	1.92	87.1
37	13-Jul-18	3	Yes	90	1.5:1	28.7	24	1665	0.00	2.15	85.7
38	13-Jul-18	3	Yes	90	1.5:1	29.1	24	1665	0.00	2.16	86.1

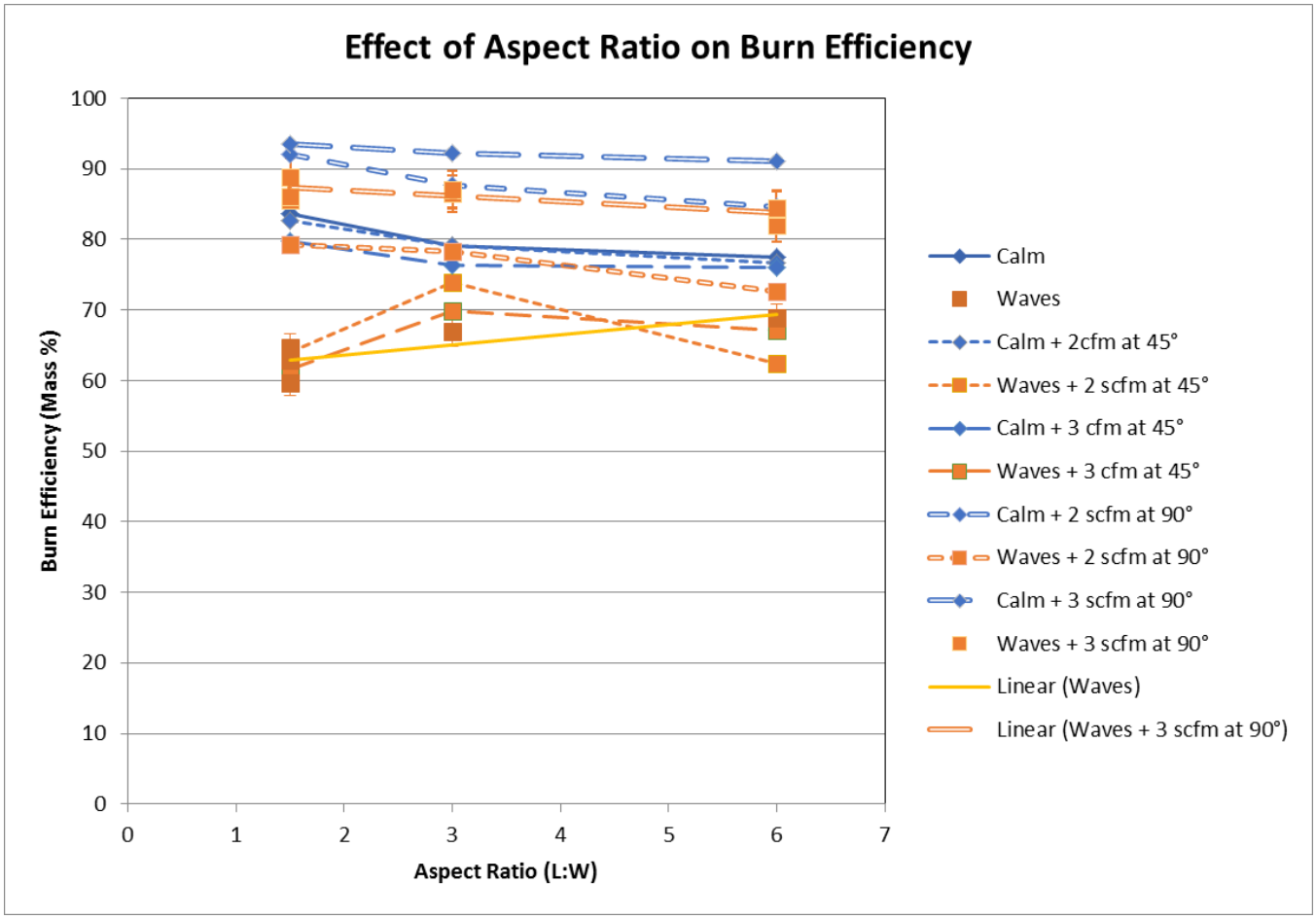

Figure 44: Small-scale Experimental Burn Efficiency

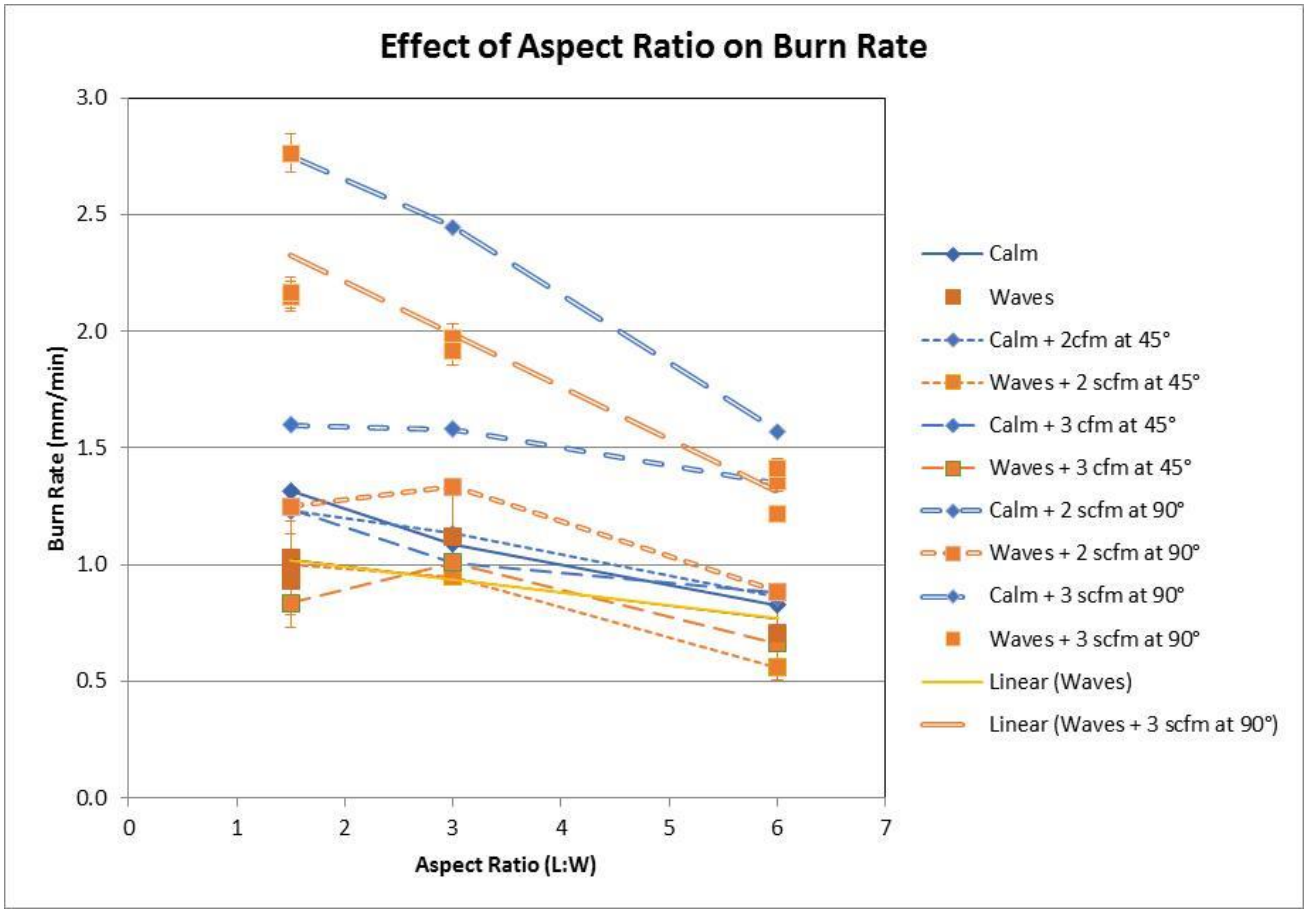

Figure 45. Small-scale Experimental Burn rate

Project Objective

The objective of the project is to develop and test prototype technology and operational methods to significantly enhance in situ burning and improve burn efficiencies by decreasing both the residue remaining and soot emissions.

Large-Scale Test Goals

The goals of these large-scale experiments at CRREL are to:

- Design and assemble large-scale prototype augmented linear burn concepts for outdoor testing in the refurbished CRREL wave tank.
- Conduct large-scale in-situ burn experiments with crude oil in the refurbished CRREL wave tank outdoors to determine the efficacy of each of the augmented linear burn concepts in reducing burn residue.
- Conduct large-scale in-situ burn experiments with crude oil in the refurbished CRREL wave tank outdoors to determine the efficacy of each of the augmented linear burn concepts in reducing soot emissions.
- Analyze the data from the large-scale experiments, and prepare and submit a summary data report.

Targets

The targets for these large-scale experiments are:

- Circulate the detailed test plan for the large-scale laboratory experiments by August 31, 2018.
- Complete the large-scale outdoor burn experiments in the refurbished CRREL wave tank by November 30, 2018.
- Submit the summary data report on the large-scale experiments by December 15, 2018.

Work Plan

Equipment

Large-scale (i.e., approximate burn area of 3.4 m^2) in situ burn experiments with different aspect ratios (length of boomed area to width), and air injection configurations will be conducted in the refurbished CRREL wave tank (Figures 7 and 8). The intention of the experiments will be to measure the effects of the various configurations and air injection enhancements on the burn characteristics under controlled conditions, and identify the most promising combinations of burn layout and air injection settings. The tank will be filled with fresh water to simplify the experiments and disposal.

Figure 46 – Photo of original ACS wave tank showing burn test being conducted in Prudhoe Bay. This tank has been obtained by CRREL and shipped to Hanover for refurbishment.

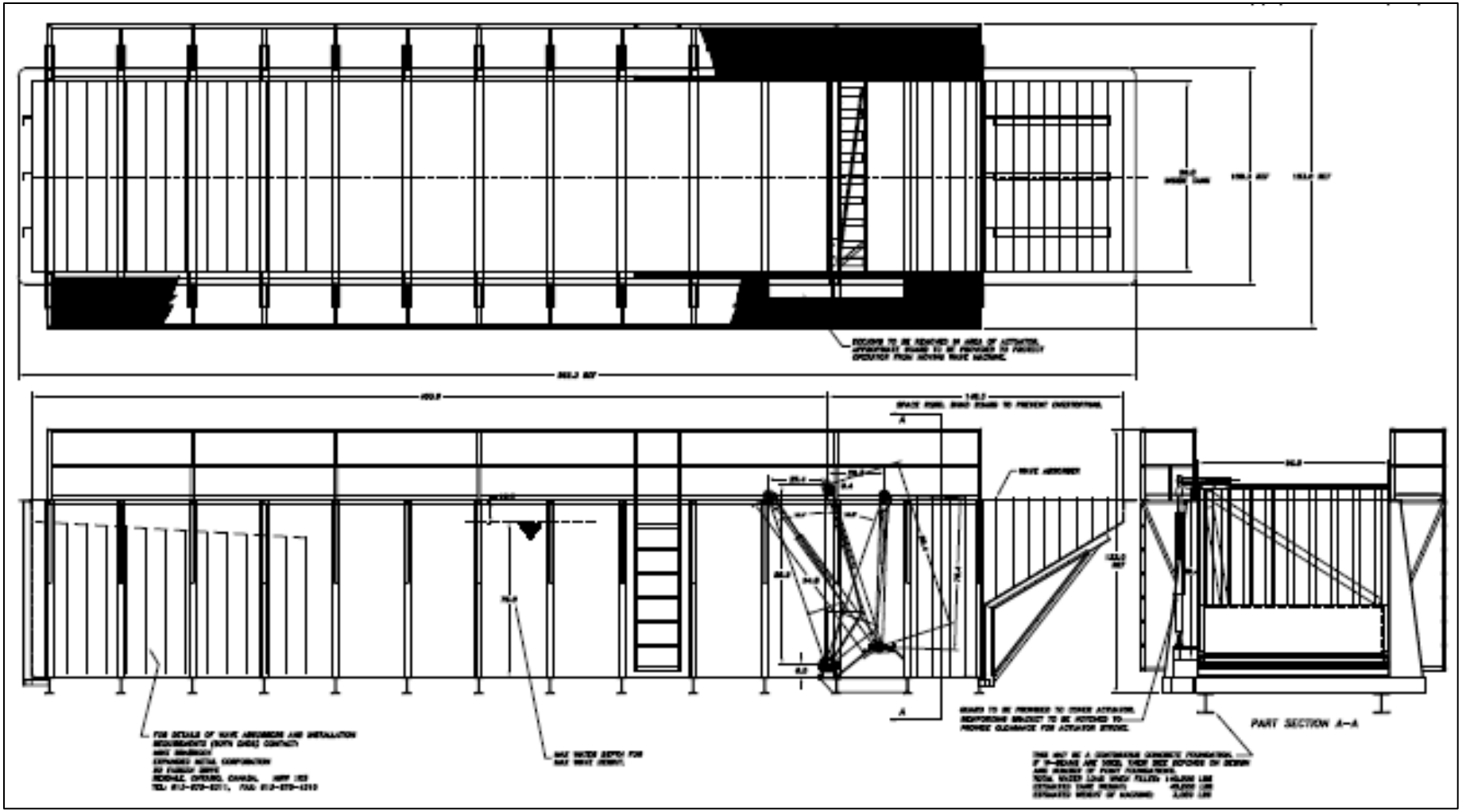

Figure 47. Design drawing for original wave tank. CRREL is refurbishing wave absorber panels and wave generator actuator and controls.

The refurbished CRREL wave tank measures 2.4 m wide by 14.3 m long (working length is 6 m); water depth can be up to 2 m. For *in situ* burn experiments, water deluge pipes are installed along the top of the inside walls of the tank to provide radiant heat and flame impingement protection.

A 50-foot section of DESMI PyroBoom will be modified and positioned in the wave tank to contain the experimental burns. The aspect ratio of the burn area in the modified fire boom will be varied from 1:1 to 9:1 (9:1 being the longest that will fit into the working length of the wave tank). Nozzles that can be repositioned to direct air into the burn at different angles will be mounted in various positions along the top of the fire boom to enhance the combustion. Figure 9 shows the general construction features of the DESMI PyroBoom and Figure 10 shows its key dimensions. Figure 11 shows how it will be modified for the testing in the confines of the CRREL wave tank..

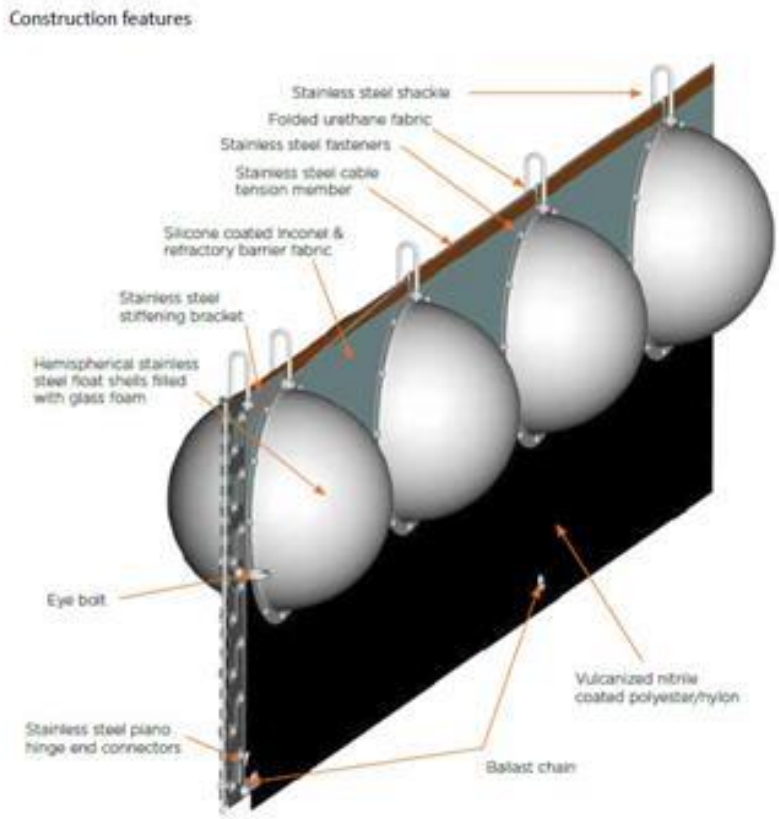

Figure 48. General construction of the DESMI PyroBoom

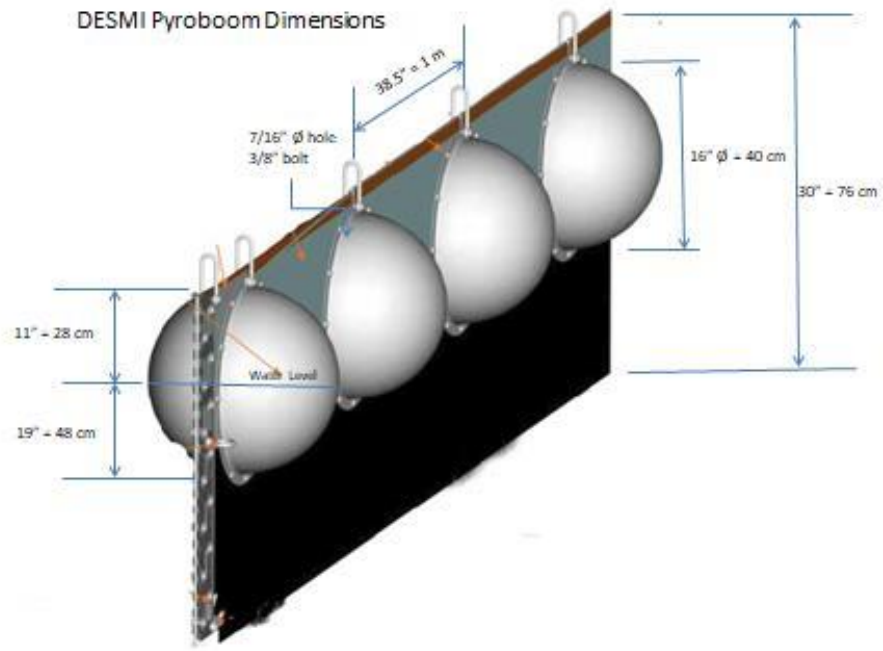

Figure 49. Dimensions of the DESMI PyroBoom

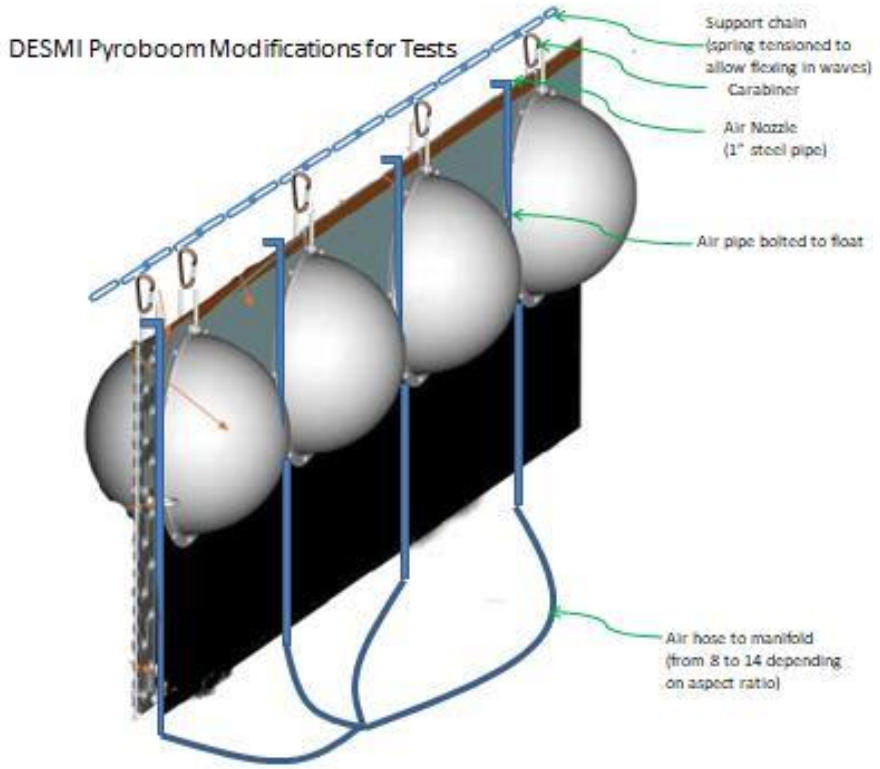

Figure 50. Proposed modifications for testing in CRREL wave tank.

Figure 12 shows the proposed configurations of the PyroBoom to achieve the aspect ratios (L:W) for the testing in the CRREL wave tank while maintaining a relatively constant burn area.

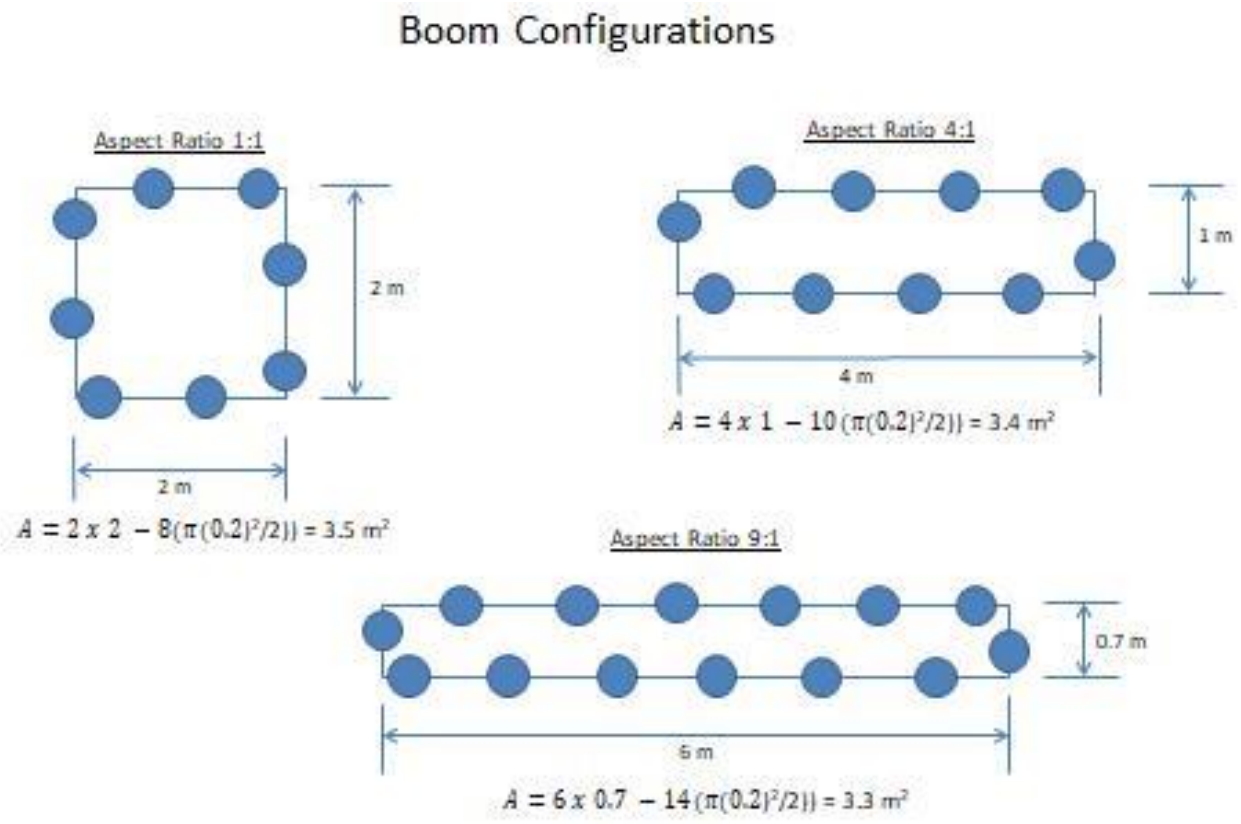

Figure 51. Configurations of the PyroBoom in the CRREL wave tank to achieve the desired aspect ratios.

As an example, Figure 13 shows how the 4:1 aspect ratio PyroBoom configuration will be held in the working area of the CRREL wave tank. First, the desired length of PyroBoom (in this case 33 ft. = 10 m) will be created by clamping the end connector to a point 10 m along the boom using two pieces of angle iron hinged at the top and clamped with bolt and wing nut below the water line. A tight seal between the two boom skirts will be ensured. The free end of extra boom will float freely, but be lightly secured to a wall to prevent it interfering with the experiments.

The rectangle of boom for an experiment will be attached to chains (i.e., Grade 30, 3/8" unfinished steel chain) stretched longitudinally and across the tank at suitable locations. The longitudinal chains will be attached to a piece of structural steel (I-beam, angle, box beam, etc.) attached across the

tank just beyond the maximum reach of the wave board at one end, and to the end of the tank at the other end.

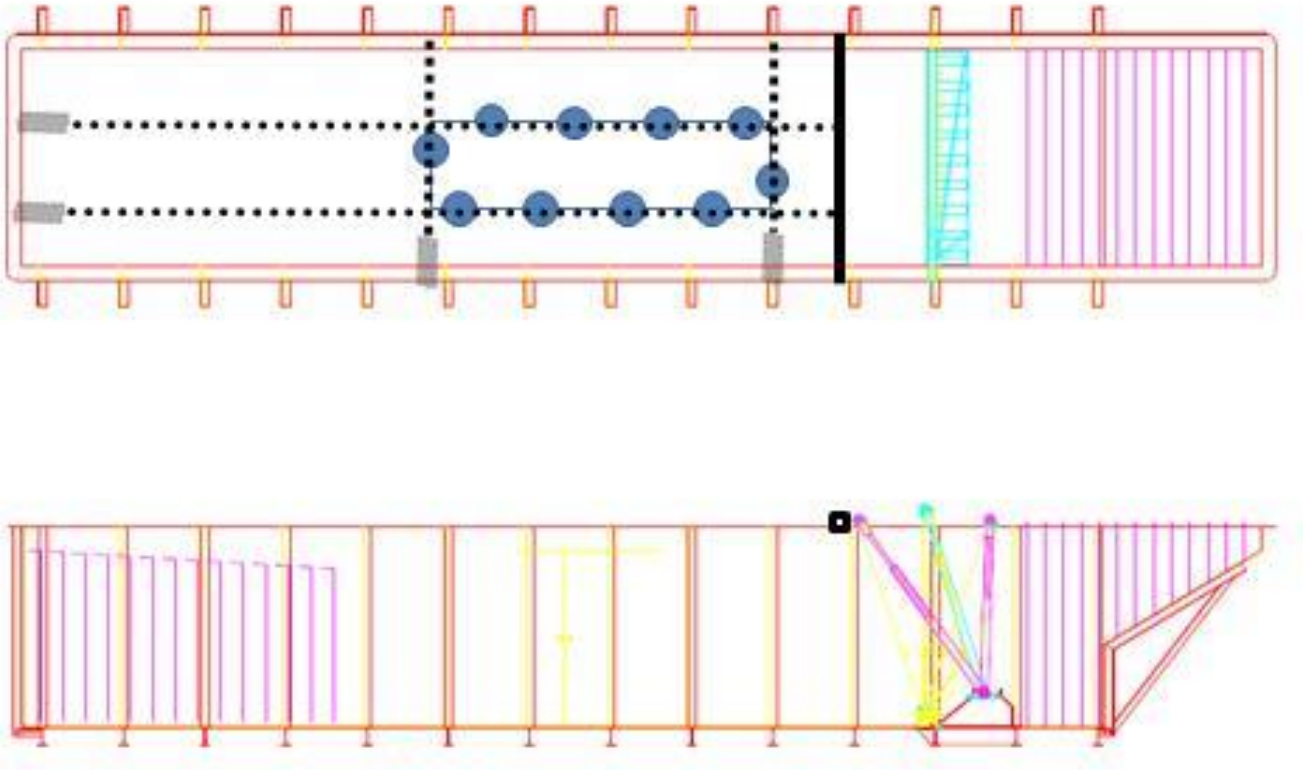

Figure 52. Positioning and securing of the 4:1 aspect ratio PyroBoom configuration in the CRREL wave tank.

Clamps will be used to attach the chains so they can be easily repositioned. Springs (e.g., extension springs with hook ends) will be used to hold the chains at a constant tension, so that the boom can follow the waves. The shackles at the top of the PyroBoom floats will be attached to the chain using stainless steel carabiners (see Figure 12).

One ½" compressed air injection nozzle with a 90° elbow will be attached to each float using its 7/16" bolt holes; the nozzle will be positioned above the top of the boom material at a variable height. The weighted air supply hoses for each nozzle will be connected underwater to a manifold fed by a 50 scfm air compressor. Each nozzle will be individually valved at the manifold. Details of the manifold size and layout will follow.

Materials and Methods

The burns will be conducted with ANS crude oil. There is a stockpile of ANS crude at CRREL that will be used to ensure consistency with the small-scale experiments. Each burn will require 35 L (9.25 gallons) of fresh crude, with the total requirement being 1,260 L (333 gallons) to complete 36 experiments. The use of a crude oil (as opposed to a refined product) is necessary to simulate conditions at a spill, and for the residue characteristics to be relevant to field situations. The mass of oil added and residue recovered will be measured to allow burn removal efficiency (2) to be calculated: the burns will be videotaped and timed to permit estimates of burn rate (3). Soot emissions will be measured by the US EPA. A test program consisting of 36 individual burns on water varying burn geometry (aspect ratio), air injection and waves will be conducted.

Burn efficiency is the ratio of the volume of oil burned to the initial oil volume:

$$Burn\ Efficiency\ (vol\%) = \left[\frac{(Initial\ Oil\ Mass)\rho_{oil} - Residue\ Mass}{(Initial\ Oil\ Mass)\rho_{oil}}\right] \times 100 \qquad (2)$$

The burn rate is calculated by dividing the volume of oil burned by the area of the fire as a function of time, as given below.

$$Burn\ Rate\ (mm/min) = \left[\frac{Initial\ Oil\ Mass - Residue\ Mass}{(Burn\ Time)(Burn\ Area)\rho_{oil}}\right] \qquad (3)$$

An example of a burn with an approximate diameter of 2 m conducted in 1997 in the wave tank is shown in Figure 14.

Figure 53. Burn in 1997 in wave tank.

A preliminary test matrix is provided in Table 3. Four duplicate experiments will be performed with each of the best combination of aspect ratio and compressed air to permit statistical analysis of the enhancements to the burn (i.e., soot and residue reduction) compared to three duplicates of the Base Case (Aspect Ratio 1:1 with no air injection in waves and calm). A total of 36 experiments will be conducted.

Table 14 Test Matrix

Aspect Ratio	Air Injection [scfm]	Waves
1:1	0	No Waves
		Waves On
		No Waves
		Waves On
		No Waves
		Waves On
	15	No Waves
		Waves On
	30	No Waves
		Waves On
	50	No Waves
		Waves On
4:1	0	No Waves
		Waves On
	15	No Waves

		Waves On
	30	No Waves
		Waves On
	50	No Waves
		Waves On
9:1	0	No Waves
		Waves On
	15	No Waves
		Waves On
	30	No Waves
		Waves On
	50	No Waves
		Waves On
Best Aspect Ratio	Best Air Injection	Waves On
		Waves On
		Waves Off
		Waves Off
Repeats to measure repeatability, error, etc.		Four

Test Procedure

The proposed general test procedure for a Linear Augmented Burn experiment in the CRREL wave tank is as follows:

1. The specified volume of oil is measured out and the weight of oil recorded.
2. The oil is transferred into the linear boom containment area using a spill plate.
3. The ambient wind speed is recorded using a hand-held anemometer at a height of about 25 cm above the surface of the oil in the containment area; a portable weather station will be operated throughout the experiments to record general conditions at the test site. The temperature of the air and water is also recorded. Following the experiments, detailed weather records for the test period will be obtained from nearby weather stations.
4. The oil is ignited by hand with a propane torch mounted on a pole.
5. Once the flame had spread to cover the entire surface of the slick, the compressed air augmentation system will be started (if required for the test) and the waves turned on at the desired setting (if required for the test).
6. The following times are recorded:

   preheat time - the time from firing the igniters until flames began to spread away from the burning gelled fuel and reached an area of approximately 1 m^2 (10 ft^2);

   ignition time – the time to full ignition (100% flame coverage);

   time to the vigorous (or intense) burn phase;

   time to 50% flame coverage; and,

   extinction time - .the time for the flames to completely extinguish.

7. The apparent density of soot emissions will be observed visually and digitally videoed using the Ringlemann scale
8. After each burn, the residue is allowed to cool. The residue is then collected and weighed.

Each burn will digitally videoed, photographed and observed visually. As well, each experiment will be made available to BSEE personnel in real time by web video broadcast.

Data Management Plan

The data inputs for the small-scale test program are shown in Table 3. Data inputs for the large-scale experiments include existing information on the properties of the fresh ANS crude oil, and data generated by the experiments. The fresh oil properties are available in an Excel spreadsheet that is stored at the SL Ross office in Ottawa.

The data processing that will occur during this Task is presented in Table 9.

Table 15: Data inputs for small-scale experimental program

Dataset	Format	Source	Use Restrictions
Fresh Oil Properties (e.g., density, viscosity, pour point, interfacial tension)	Excel	SL Ross	No restrictions.
Large-scale Experiment Data • Test Conditions ○ Date and time of test ○ Air and water temperature ○ Wave height and period ○ Compressed air flow rate • Test Results ○ Oil and residue mass ○ Burn duration ○ Visual observations	This data will be recorded manually, in ink, on prepared test sheets during the experiments.	This data will be generated by the experiments.	The data from the experiments is the property of CRREL and BSEE.
Large-scale Experiment Video	mp4	This data will be generated by the experiments.	The video of the experiments is the property of CRREL and BSEE.

Table 16: Data processing summary for small-scale experiments

Access and Sharing	Access to data generated by the large-scale experiments will be restricted to the project participants, SL Ross, CRREL and BSEE, and to the EPA. The metadata resulting from the experiments will be presented to CRREL in a summary report.
Data Storage	Test sheets with the manually recorded experimental data will be collected in a binder, which will be stored at CRREL facility for the duration of the testing. Upon completion of the large-scale experimental program, the test sheets will be scanned into a pdf format, and transmitted to the SL Ross office. Video recordings of the experiments will be stored electronically at CRREL with copies transmitted to SL Ross.
Data Processing	Information from the test sheets will be periodically transcribed into an Excel spreadsheet. Data transcription will be audited by a second key project member. Calculation of burn rate and efficiency will be done for each test. The results will be organized in tables to allow comparisons of burn rate and efficiency against the different test conditions.

Data gathered during the experiments will be transferred to an Excel spreadsheet for processing and analysis. The data will be organized into tables to analyse the results for the effects of the test conditions on burn efficiency and soot production. Charts will be prepared to highlight the effects of particular test parameters. Visual observations of the experiments will be used, as needed, to provide further insight into the effectiveness of the augmented linear burn concepts.

The proposed data publishing arrangement is summarised in Table 10.

Table 17: Proposed project metadata publishing arrangements

Title	Summary Data Report on Large-scale Burn Experiments

Description	A report summarising the results and conclusions from the small-scale experiments will be prepared.
Formats	Word, pdf, Excel
Data Storage	Word and pdf versions of the summary report will be provided to CRREL and BSEE by email. Copies of the report and the Excel spreadsheet containing the test data will be stored at the SL Ross office in Ottawa.
Metadata Point of Contact	The point of contact for the project metadata will be the Project Manager, James McCourt.
Restrictions	The summary report is the property of CRREL and BSEE and will not be shared outside of the project personnel.

Quality Control Plan

The following quality control measures will be employed for these experiments.

Initial Calibration Data. A check is made to ensure that data is available to show the initial source of calibration data for each piece of instrumentation used in the project. This includes any calibration information necessary to assure that the calibration data is current for the project.

Pre- and Post-Daily Checks. These are checks that are performed on the instrumentation each morning before testing starts and at the end of the day when testing stops. This is done on all days that testing occurs. Note is made of any unusual conditions that occur

Test Checks and Conditions. These checks ensure that the test plan's instructions on how the experiment is to be done are followed and that the records that are to be made during the experiment are completed accurately.

Significant Occurrences/Variations. This part of the quality checks will be concerned with recording any significant occurrences/variations that might occur during the experiments. These will be immediately reported to the SL Ross Project Manager.

Data Reduction and Validation. All data reduction and validation will be performed in accordance with approved and accepted methods. When non-standard methods are utilized, they shall be included in the Draft Technical Report and sufficiently described so that they can be used by independent sources to duplicate the results. With respect to written material, all draft material will be reviewed by at least one other SL Ross senior staff Professional Engineer before submission to CRREL and BSEE.

Health and Safety Job Hazard Analysis

Introduction

A job hazard analysis is a means of preventing or controlling hazardous conditions associated with testing activity. Analysis begins by determining the basic tasks of a job. Each task is then analysed to identify potential hazards associated with it. It will then be possible to develop control measures for the hazards identified. Prior to any test activity, personnel involved with the test are informed of potential hazards and controls for an understanding of their health and safety responsibilities.

Hazardous Materials

Liquid Hydrocarbons:

- ANS crude oil

Detailed information of the hazardous materials and compounds used or released in the Wave Tank for

these experiments are listed in the Material Safety Data Sheets (MSDS).

All personnel involved in testing will be informed of associated health hazards, as well as the proper personal protective measures required to minimize exposure to the oil and chemicals, in accordance with OSHA Hazard Communication Standard requirements. A Material Safety Data Sheet is maintained for test oils, chemicals or various products, and will be available to each person involved in testing. Eye protection and oil-resistant gloves shall be worn when handling crude oil or herding agent.

Generic Job Safety Analysis

The following table lists basic or generic tasks necessary for the “Large-Scale Linear Augmented Fire Boom In Situ Burn Experiments” project. Hazards associated with the tasks are listed with preventive measures to be followed by affected personnel.

Table 18 - Task Hazard Prevention

TASK	HAZARDS	PREVENTION/CONTROL
1) Materials handling, general set-up	a) Lifting material(s) (muscle strains, back injuries)	a) Use proper lifting techniques; lift with your legs, not your back; get help for heavy loads, use mechanical devices (i.e., fork lift, cranes).
	b) Forklift operations (objects striking)	b) Follow acceptable safe practices for operators. Forklifts will only be operated by CRREL employees trained to operate that specific truck. Mark off areas where Forklifts will be used to restrict other traffic and pedestrians. Use a Ground Guide or a spotter. All forklifts must be examined at least daily before being used. Seatbelts will be utilized at all times while operating a forklift. A vehicle that is damaged, defective or otherwise unsafe must be removed from service.
	c) Crane(s) operations (objects striking)	
	e) Hand/power tools (muscle strains, pinch points, electrocution)	c) Do not stand under raised loads. Do not exceed capacity of crane. Cranes will be operated only by CRREL employees trained to operate that specific crane. Mark off areas where cranes will be lifting restrict pedestrians. All lifting hardware will be inspected at least daily before being used. Any lifting hardware that is damaged, defective or otherwise unsafe must be removed from service.
		e) Use correct tool for the job, use correct PPE and proper body positioning when handling tools. Inspect all power tools to ensure no frayed or exposed wires exist, equipment is grounded and insulated and GFI's extension cords etc. are functioning properly.
2) Wave Tank outfitting (set-up)	a) Rigging from crane (falls)	a) Wear hand protection during rigging.
	b) Cable handling (pinch points)	c) Have appropriate lines of continual communication.

	c) Placing video and still cameras (ladder work)	d) No one permitted under heavy loads.
3) Oil transfer	a) Spilled oil on floors (slip/fall hazard) b) Pressurized equipment/pumps/hoses/ lines (pressure release, objects striking)	a) Clean spills on surfaces immediately. Utilize spill equipment, as required. b) Inspect all equipment prior to use. Do not use damaged equipment. Replace cracked hoses, broken gauges prior to pressurization. Inspect for leaks. Use adequate PPE (hard hat, gloves, and face shield).
4) Oil addition to basin	a) Splashing/spilling oils while transferring to test basin. [Slips/falls, exposure (skin/eyes), exposure (inhalation)] b) Pressure release (object striking, pinch points)	a) Wear appropriate PPE (protective clothes, goggles/face shield, nitrile gloves). Appropriate respirators will be worn as required. Technician will keep deck area as oil-free as possible. b) Utilization of damaged hoses or faulty equipment is prohibited. Check all piping, hoses, hose connections, etc. prior to use. Bleed pressure prior to disconnect. Wear PPE to include protective **c**lothes, goggles/face shield, hard hat, and nitrile gloves.
5) Positioning and Operation of Fire Boom System with Boom Crane	a) Overhead objects b) Crane operations c) Falling objects into water/oil slick	a) Boom truck will be assembled and operated by trained CRREL personnel. b) Hard hats worn when crane positioned and operating. c) Ladder safety person staying ladder during application system operation (if elevated operation required) c) Test drop dummy igniters to assess splash zone.
6) Ignition and burn of contained oil on water	a) Igniter operations b) Flames c) Heat d)Smoke plume	a) Keep all but essential personnel back and upwind/crosswind and essential personnel wear PPE: 1. Anti-slip boots 2. Heavy jackets resilient to ignition 3. Heavy gloves resilient to ignition

		4.. Safety goggles b) Flame/heat impingement on concrete walls minimized by metal flashing an water deluge. c) A total of four fire extinguishers are positioned for each test. d) Two trained firefighters are standing by with extinguishers. e) Keep oil back from protective layer and if ignition occurs allow fire department to extinguish f) Ensure wind is from acceptable direction and at acceptable speed before ignition. g) Fire will naturally cease as fuel is exhausted. If this does not occur, an oil-rated fire extinguisher will be used. h) Site manager for experiment maintains safety cordon and insures rapid response with personnel using fire extinguishers, alerts security and FD as appropriate. i) No burn is to be attempted until Site Manager clears the burn to begin.
5) Refrigeration leak	a) Exposure to anhydrous ammonia in the event of an event of leak	a) Smell ammonia- notify CRREL personnel. b) Ammonia alarm sounds level exceeds 25ppm – evacuate the room.
6) Water Safety	a) Slips, Trips, and Falls.	a) Work areas must remain clear and free of clutter. Ensure equipment, cords, hoses and materials are positioned in a manner to reduce congestion, trip hazards, and ensure accessibility.
7) Electrical	a) Electrical shock	a) Inspect all electric tools, lights, cords and other equipment for damage or wear prior to use. **Do not use damaged equipment.** Report any discrepancies immediately. Tape electrical connections to reduce migration of water at connections. GFCI's are required for all electric tools and lighting.
8) Removal of oil from test basin	a) Oil exposure (skin/eye contact) b) Falls, slips c) Sorbent boom sweeping.	a) Wear protective clothing, goggles/face shields and chemical resistant gloves. b) Use herder and sorbents in Wave Tank c) Put sorbent into garbage bags for weighing and disposal. d) Use secondary containment pallet as additional measure inside of secondary containment area.
9) Health Management	a) Noise	ac) Hearing protection is required when noise levels reach 82 dBA. During high noise activities, such as tool or equipment operations, or over 100 dBA, double hearing protection will be

	b) Soft Tissue Injuries (Back, Shoulder, Arm, Knee, etc.)	used. As a general rule, if employees are required to raise their voice to be heard above operating equipment in normal conversation then hearing protection should be used. Personnel operating and working in the vicinity of chainsaws and augers will wear double hearing protection. b) Work activities will use mechanical lifting/carrying devices whenever possible. If not possible, personnel must exercise proper lifting techniques. Seek assistance for awkward and large loads or loads greater than 50 pounds. Do pre-job stretching and warm-up, use proper SIM techniques, take breaks as necessary and re-energize.

Finally, personal protective equipment guidelines (for items such as hard hats, steel toed boots, and the like) will be followed. The above assessment is based only on generic or basic steps. Chemical Hazards will be discussed based on hazard communication standards with SDS's reviewed.

Safety Data Sheets are available to participants at the CRREL Wave Tank.

Emergency Contacts

SITE LOCATION: US Army Corps of Engineers, Cold Regions Research Engineering Laboratory, 72 Lyme Road, Hanover, New Hampshire, 03755.

CRREL Emergency Telephone Numbers

Name	Title	Organization	Telephone #
Emergency/ Security			911
Security Office	Security	CRREL	4800
Byron Young	Environmental	CRREL	4602
Colin O'Connor	Safety Officer	CRREL	4860
Nathan Lamie	IEF Manager	CRREL	4598
Jared Oren	ERB Supervisor	CRREL	4458
Andre StLouis	FE Supervisor	CRREL	4105

POLICE DEPARTMENT: Hanover Police Department, 46 Lyme Rd., Hanover, NH, Phone 911 (emergency) or 603-643-2222

FIRE DEPARTMENT: Hanover Fire Department, 46 Lyme Rd., Hanover, NH, Phone 911 (emergency) or 603-643-3424

AMBULANCE: Fire Department – Phone 911

HOSPITALS: Alice Peck Day Memorial (APD) (occupational health injuries)
125 Mascoma Street, Lebanon, NH. 03766 Phone 603-448-3121

Dartmouth Hitchcock Medical Center (DHMC)
1 Medical Center Dr, Lebanon, NH 03766 (603) 650-5000

POISON CONTROL CENTER: S/A Hospital above

HAZARDOUS WASTE DISPOSAL/CLEAN-UP CONTRACTORS:

Tradebe Treatment and Recycling of Bridgeport (203)334-1666or (888-276-0887)

North Country Environmental Services (800)479-5299

Clean Harbors (800)645-8265

Personal Protective Equipment

The following personal protective equipment shall be available at all times. Specific use requirements may be found in Section 5.3.

- Work gloves
- Insulated coveralls (Outdoor temperatures average -1° to 13°C or 30° to 55°F)
- Warm hat
- Oil resistant gloves (neoprene, nitrile)
- Eye protection (safety glasses, goggles)
- Safety shoes

- Personal flotation devices (for workboat operations) mandatory
- Life rings
- Splash suits, for basin clean up

Communication Plan

Good communication is essential to the safe execution of the test. The following types of communication tools and skills will be available for use:

- Verbal
- Hand signals

Contingency Plan

In case of medical emergency, fire, or other emergency, it is necessary to notify

- CRREL Security dial 4800

Wave Tank Cleanup and Waste Disposal

The Cold Regions Research and Engineering Laboratory in Hanover is within the US ARMY Corp of Engineers laboratory system. As part of the U.S. ARMY, CRREL is strictly regulated on the management and disposal of hazardous waste generated during research programs. Discarded materials, waste materials, or other field equipment and supplies shall be handled in such a way as to preclude the potential for spreading contamination, creating a sanitary hazard, or causing litter to be left on site. Thought and preparation beforehand can eliminate unnecessary generation and inappropriate management of hazardous waste during the course of the project.

Waste oil, water with waste oil or any contaminated waste derived from the waste crude oil will be handled and disposed per NHDES Hazardous Waste Rules Env-HW, EPA 40 CFR Hazardous waste rules and Regulation No. 200 Environmental Quality U.S. ARMY ENGINEER RESEARCH AND DEVELOPMENT CENTER (ERDC) DISPOSAL OF HAZARDOUS WASTE. To dispose of a known hazardous waste, an MSDS/SDS and generator knowledge or a lab analysis also known as Toxic Characteristic and Leaching Properties (TCLP) are required. Representative samples of the recovered oil and oiled waste will be sent to independent laboratory (Eastern Analytical Laboratory) for characterization and required disposal procedures. The form 1930 needs to be filled out and completed before turn in for disposal to the lab hazardous waste point of contact (John Hebert). The oil waste will be disposed by a certified hazardous waste disposal company. Additional information regarding the hazardous waste program for both NHDES and EPA are as follows:
http://des.nh.gov/organization/divisions/waste/hwcb/

http://www.epa.gov/osw/laws-regs/regs-haz.htm

Potentially contaminated materials, e.g., clothing, gloves, etc., will be bagged or drummed with appropriate labeling affixed as regulated, and segregated for proper disposal.

Non-contaminated materials shall be collected, bagged, and disposed of as normal domestic waste.

Schedule

The following schedule is planned for the Large-Scale Linear Augmented Fire Boom In Situ Burn Experiments:

DATE	**EVENT**
August 31, 2018	Submit First Draft Test Plan to CRREL and BSEE
September 17, 2018	Install Wave Generator and Dry Run Test with Pyroboom
November, 2018	Large-Scale Linear Augmented Fire Boom In Situ Burn Experiments
November 30, 2018	Deliver Raw and Processed Data, Observations and Video Documentation to SL Ross
December 31, 2018	Submission of Summary Data Report to BSEE

References

Alaska Clean Seas. 1991. Long duration test burn: 3M 8-inch fire containment boom. ACS Newsletter. Vol (1), No.1, March 31, 1991. Anchorage.

Buist, I.A., S.G. Potter, B.K. Trudel, S.R. Shelnutt, A.H. Walker, D.K. Scholz, P.J. Brandvik, J. Fritt-Rasmussen, A.A. Allen. 2013. In Situ Burning in Ice-Affected Waters: State of Knowledge Report. Joint Industry Programme Final Report 7.1.1. http://www.arcticresponsetechnology.org/wp-content/uploads/2013/10/Report-7.1.1-OGP_State_of_Knowledge_ISB_Ice_Oct_14_2013.pdf

Franken, P., D. Perry, R Randt, R Petersen, and C. Thorpe. 1992. Combustive management of oil spills -Final report. University of Arizona.

Koseki, H., 2000. Large Scale Pool Fires: Results Of Recent Experiments. Fire Safety Science 6: 115-132.

Kupersmith, J.A. 1995. Trip Report: MSRC Mesoscale Fuel Burn Experiments at SwRI. MSRC R&D Division, Washington, D.C.

Nordvik, A., J. Simmons, J. Burkes, I. Buist, D. Blersch and M. Reed. 1995. Mesoscale In Situ Burn Aeration Tests. MSRC Technical Report 95-017, Washington, DC.

NRT Science and Technology Committee. 1995. Aeration Techniques for In Situ Burning of Oil: Enhancing an Alternative Spill Response Method. https://www.nrt.org/sites/2/files/aeration.pdf

Zhang, C., T. Nedwed, A. Tidwell, N. Urbanski, D. Cooper, I. Buist and R. Belore. 2014. One-Step Offshore Oil Skim And Burn System For Use With Vessels Of Opportunity.IOSC Proc: Vol. 2014, No. 1, pp. 1834-1845.

SAFETY DATA SHEETS

ConocoPhillips

Crude Oil, Sweet

Material Safety Data Sheet

1. PRODUCT AND COMPANY IDENTIFICATION

Product Name:	Crude Oil, Sweet
MSDS Number:	724160
Synonyms:	Crude Oils, Desalted, Sweet Field Crude Petroleum Crude Petroleum Oil Rock Oil Separator Crude Sweet Crude
Intended Use:	Refinery Feed
Responsible Party:	ConocoPhillips 600 N. Dairy Ashford Houston, Texas 77079-1175
MSDS Information:	Phone: 800-762-0942 Email: MSDS@conocophillips.com Internet: http://w3.conocophillips.com/NetMSDS/
Emergency Telephone Numbers:	Chemtrec: 800-424-9300 (24 Hours) California Poison Control System: 800-356-3219

2. HAZARDS IDENTIFICATION

Emergency Overview

DANGER!

Extremely Flammable Liquid and Vapor
May Contain or Release Poisonous Hydrogen Sulfide Gas
Aspiration Hazard
Cancer Hazard

NFPA

Appearance: Amber to Black
Physical Form: Liquid
Odor: Petroleum. Rotten egg / sulfurous

Potential Health Effects
Eye: Contact may cause mild eye irritation including stinging, watering, and redness.

Skin: Contact may cause mild skin irritation including redness and a burning sensation. Prolonged or repeated contact can defat the skin, causing drying and cracking of the skin, and possibly dermatitis (inflammation). Not acutely toxic by skin absorption, but prolonged or repeated skin contact may be harmful (see Section 11).

Inhalation (Breathing): Low to moderate degree of toxicity by inhalation.May contain or release poisonous hydrogen sulfide gas - see Other Comments.

Ingestion (Swallowing): Low degree of toxicity by ingestion. ASPIRATION HAZARD - This material can enter lungs during swallowing or vomiting and cause lung inflammation and damage.

Signs and Symptoms: Effects of overexposure may include irritation of the respiratory tract, irritation of the digestive tract, nausea, vomiting, diarrhea and signs of nervous system depression (e.g., headache, drowsiness, dizziness, loss of coordination, disorientation and fatigue).

Other Comments: This material may contain or liberate hydrogen sulfide, a poisonous gas with the smell of rotten eggs. The smell disappears rapidly because of olfactory fatigue so odor may not be a reliable indicator of exposure. Effects of overexposure include irritation of the eyes, nose, throat and respiratory tract, blurred vision, photophobia (sensitivity to light), and pulmonary edema (fluid accumulation in the lungs). Severe exposures can result in nausea, vomiting, muscle weakness or cramps, headache, disorientation and other signs of nervous system depression, irregular heartbeats, convulsions, respiratory failure, and death.

This material may contain varying concentrations of polycyclic aromatic hydrocarbons (PAHs) which have been known to produce a phototoxic reaction when contaminated skin is exposed to sunlight. The effect is similar in appearance to an exaggerated sunburn, and is temporary in duration if exposure is discontinued. Continued exposure to sunlight can result in more serious skin problems including pigmentation (discoloration), skin eruptions (pimples), and possible skin cancers.

Crude oil can contain trace amounts of heavy metals, some of which may concentrate in vessels and equipment during production and processing operations. While some of these metals are known toxins, the hazard is dependent upon the extent of accumulation. Significant deposits of elemental mercury have the potential to create airborne vapors of the metal, which might result in a hazardous condition. Overexposure to mercury is known to cause neurologic effects and damage the kidneys and developing fetus (See Sections 7 and 8).

Pre-Existing Medical Conditions: Conditions aggravated by exposure may include skin disorders and respiratory (asthma-like) disorders.

See Section 11 for additional Toxicity Information.

3. COMPOSITION / INFORMATION ON INGREDIENTS

Component	CAS	Concentration (wt %)
Crude Oil (Petroleum)	8002-05-9	100
Ethyl Benzene	100-41-4	<2
Benzene	71-43-2	<1
Naphthalene	91-20-3	0-0.9
Hydrogen Sulfide	7783-06-4	<0.2

Crude oil, natural gas and natural gas condensate can contain minor amounts of sulfur, nitrogen and oxygen containing organic compounds as well as trace amounts of heavy metals like mercury, arsenic, nickel, and vanadium. Composition can vary depending on the source of crude.

4. FIRST AID MEASURES

Eye: If irritation or redness develops from exposure, flush eyes with clean water. If symptoms persist, seek medical attention.

Skin: Remove contaminated shoes and clothing and cleanse affected area(s) thoroughly by washing with mild soap and water or a waterless hand cleaner. If irritation or redness develops and persists, seek medical attention.

Inhalation (Breathing): If respiratory symptoms or other symptoms of exposure develop, move victim away from source of exposure and into fresh air. If symptoms persist, seek immediate medical attention. If victim is not breathing, clear airway and immediately begin artificial respiration. If breathing difficulties develop, oxygen should be administered by qualified personnel. Seek immediate medical attention.

Ingestion (Swallowing): Aspiration hazard: Do not induce vomiting or give anything by mouth because this material can enter the lungs and cause severe lung damage. If victim is drowsy or unconscious and vomiting, place on the left side with the head down. If possible, do not leave victim unattended and observe closely for adequacy of breathing. Seek medical attention.

Notes to Physician: At high concentrations hydrogen sulfide may produce pulmonary edema, respiratory depression, and/or respiratory paralysis. The first priority in treatment should be the establishment of adequate ventilation and the administration of 100% oxygen. Animal studies suggest that nitrites are a useful antidote, however, documentation of the efficacy of nitrites in humans is lacking. If the diagnosis of hydrogen sulfide poisoning is confirmed and if the patient does not respond rapidly to supportive care, the use of nitrites may be an effective antidote if delivered within the first few minutes of exposure. For adults the dose is 10 mL of a 3% $NaNO_2$ solution (0.5 gm $NaNO_2$ in 15 mL water) I.V. over 2-4 minutes. The dosage should be adjusted in children or in the presence of anemia, and methemoglobin levels, arterial blood gases, and electrolytes should be monitored closely.

Epinephrine and other sympathomimetic drugs may initiate cardiac arrhythmias in persons exposed to high concentrations of hydrocarbon solvents (e.g., in enclosed spaces or with deliberate abuse). The use of other drugs with less arrhythmogenic potential should be considered. If sympathomimetic drugs are administered, observe for the development of cardiac arrhythmias.

Federal regulations (29 CFR 1910.1028) specify medical surveillance programs for certain exposures to benzene above the action level or PEL (specified in Section (i)(1)(i) of the Standard). In addition, employees exposed in an emergency situation shall, as described in Section (i)(4)(i), provide a urine sample at the end of the shift for measurement of urine phenol.

5. FIRE-FIGHTING MEASURES

NFPA 704 Hazard Class

Health: 1 **Flammability:** 3 **Instability:** 0 (0-Minimal, 1-Slight, 2-Moderate, 3-Serious, 4-Severe)

Unusual Fire & Explosion Hazards: Extremely flammable. This material can be ignited by heat, sparks, flames, or other sources of ignition (e.g., static electricity, pilot lights, mechanical/electrical equipment, and electronic devices such as cell phones, computers, calculators, and pagers which have not been certified as intrinsically safe). Vapors may travel considerable distances to a source of ignition where they can ignite, flash back, or explode. May create vapor/air explosion hazard indoors, in confined spaces, outdoors, or in sewers. Vapors are heavier than air and can accumulate in low areas. If container is not properly cooled, it can rupture in the heat of a fire. Hazardous combustion/decomposition products may be released by this material when exposed to heat or fire. Use caution and wear protective clothing, including respiratory protection.

Extinguishing Media: Dry chemical, carbon dioxide, or foam is recommended. Water spray is recommended to cool or protect exposed materials or structures. Carbon dioxide can displace oxygen. Use caution when applying carbon dioxide in confined spaces. Water may be ineffective for extinguishment, unless used under favorable conditions by experienced fire fighters.

Fire Fighting Instructions: For fires beyond the incipient stage, emergency responders in the immediate hazard area should wear bunker gear. When the potential chemical hazard is unknown, in enclosed or confined spaces, a self contained breathing apparatus should be worn. In addition, wear other appropriate protective equipment as conditions warrant (see Section 8).

Isolate immediate hazard area and keep unauthorized personnel out. Stop spill/release if it can be done with minimal risk. Move undamaged containers from immediate hazard area if it can be done with minimal risk. Water spray may be useful in minimizing or dispersing vapors and to protect personnel. Cool equipment exposed to fire with water, if it can be done with minimal risk. Avoid spreading burning liquid with water used for cooling purposes.

See Section 9 for Flammable Properties including Flash Point and Flammable (Explosive) Limits

6. ACCIDENTAL RELEASE MEASURES

Personal Precautions: Extremely flammable. May contain or release poisonous hydrogen sulfide gas. Keep all sources of ignition and hot metal surfaces away from spill/release. The use of explosion-proof electrical equipment is recommended. Stay upwind and away from spill/release. Notify persons down wind of the spill/release, isolate immediate hazard area and keep unauthorized personnel out. Wear appropriate protective equipment, including respiratory protection, as conditions warrant (see Section 8). See Sections 2 and 7 for additional information on hazards and precautionary measures.

Environmental Precautions: Stop spill/release if it can be done with minimal risk. Prevent spilled material from entering sewers, storm drains, other unauthorized drainage systems, and natural waterways. Use foam on spills to minimize vapors (see Section 5). Use water sparingly to minimize environmental contamination and reduce disposal requirements. Spills into or upon navigable waters, the contiguous zone, or adjoining shorelines that cause a sheen or discoloration on the surface of the water, may require notification of the National Response Center (phone number 800-424-8802).

Methods for Containment and Clean-Up: Notify fire authorities and appropriate federal, state, and local agencies. Immediate cleanup of any spill is recommended. Dike far ahead of spill for later recovery or disposal. Absorb spill with inert material such as sand or vermiculite, and place in suitable container for disposal.

7. HANDLING AND STORAGE

Precautions for safe handling: Avoid breathing gas. Use only outdoors or in well-ventilated area. Wash thoroughly after handling. Use good personal hygiene practices and wear appropriate personal protective equipment.

Open container slowly to relieve any pressure. Bond and ground all equipment when transferring from one vessel to another. Can accumulate static charge by flow or agitation. Can be ignited by static discharge. The use of explosion-proof electrical equipment is recommended and may be required (see appropriate fire codes). Refer to NFPA-704 and/or API RP 2003 for specific bonding/grounding requirements. Do not enter confined spaces such as tanks or pits without following proper entry procedures such as ASTM D-4276 and 29CFR 1910.146. Do not wear contaminated clothing or shoes. Keep contaminated clothing away from sources of ignition such as sparks or open flames.

"Empty" containers retain residue and may be dangerous. Do not pressurize, cut, weld, braze, solder, drill, grind, or expose such containers to heat, flame, sparks, or other sources of ignition. They may explode and cause injury or death. "Empty" drums should be completely drained, properly bunged, and promptly shipped to the supplier or a drum reconditioner. All containers should be disposed of in an environmentally safe manner and in accordance with governmental regulations. Before working on or in tanks which contain or have contained this material, refer to OSHA regulations, ANSI Z49.1, and other references pertaining to cleaning, repairing, welding, or other contemplated operations.

Mercury and other heavy metals may be present in trace quantities in crude oil, raw natural gas, and condensates. Production and processing of these materials can lead to "drop-out" of elemental mercury in enclosed vessels and pipe work, typically at the low point of any process equipment because of its density. Mercury may also occur in other process system deposits such as sludges, sands, scales, waxes, and filter media. Personnel engaged in work with equipment where mercury deposits might occur (confined space entry, sampling, opening drain valves, draining process lines, etc), may be exposed to a mercury hazard (see sections 3 and 8).

Conditions for safe storage: Keep container(s) tightly closed. Use and store this material in cool, dry, well-ventilated areas away from heat, direct sunlight, hot metal surfaces, and all sources of ignition. Store only in approved containers. Post area "No Smoking or Open Flame." Keep away from any incompatible material (see Section 10). Protect container(s) against physical damage. This material may contain or release poisonous hydrogen sulfide gas. In a tank, barge, or other closed container, the vapor space above this material may accumulate hazardous concentrations of hydrogen sulfide. Outdoor or detached storage is preferred. Indoor storage should meet OSHA standards and appropriate fire codes.

8. EXPOSURE CONTROLS / PERSONAL PROTECTION

Component	ACGIH	OSHA	Other:
Crude Oil (Petroleum)	---	---	TWA:100 mg/m³ - 8 hr. ConocoPhillips (ConocoPhillips Guidelines)
Benzene	TWA: 0.5 ppm STEL: 2.5 ppm Skin	Ceiling: 25 ppm STEL: 5 ppm TWA: 1 ppm TWA: 10 ppm	---

8. EXPOSURE CONTROLS / PERSONAL PROTECTION

Naphthalene	TWA: 10 ppm STEL: 15 ppm Skin	TWA: 10 ppm TWA: 50 mg/m³	TWA: 0.2 mg/m³ (as total of 17 PNA's measured by NIOSH Method 5506) (ConocoPhillips Guidelines)
Hydrogen Sulfide	TWA: 10 ppm STEL: 15 ppm	Ceiling: 20 ppm	---

Note: State, local or other agencies or advisory groups may have established more stringent limits. Consult an industrial hygienist or similar professional, or your local agencies, for further information.

Engineering controls: If current ventilation practices are not adequate to maintain airborne concentrations below the established exposure limits, additional engineering controls may be required.

Personal Protective Equipment (PPE):

Eye/Face: The use of eye protection that meets or exceeds ANSI Z.87.1 is recommended to protect against potential eye contact, irritation, or injury. Depending on conditions of use, a face shield may be necessary.

Skin: The use of gloves impervious to the specific material handled is advised to prevent skin contact. Users should check with manufacturers to confirm the performance of their products. Suggested protective materials: Nitrile

Respiratory: Where there is potential for airborne exposure to hydrogen sulfide (H2S) above exposure limits, a NIOSH approved, self-contained breathing apparatus (SCBA) or equivalent operated in a pressure demand or other positive pressure mode should be used. Under conditions where hydrogen sulfide (H2S) is NOT detected, a NIOSH certified air purifying respirator equipped with organic vapor cartridges/canisters may be used.

A respiratory protection program that meets or is equivalent to OSHA 29 CFR 1910.134 and ANSI Z88.2 should be followed whenever workplace conditions warrant a respirator's use. Air purifying respirators provide limited protection and cannot be used in atmospheres that exceed the maximum use concentration (MUC) as directed by regulation or the manufacturer's instructions, in oxygen deficient (less than 19.5 percent oxygen) situations, or other conditions that are immediately dangerous to life and health (IDLH).

If benzene concentrations equal or exceed applicable exposure limits, OSHA requirements for personal protective equipment, exposure monitoring, and training may apply (29CFR1910.1028 - Benzene).

Workplace monitoring plans should consider the possibility that heavy metals such as mercury may concentrate in processing vessels and equipment presenting the possibility of exposure during various sampling and maintenance operations. Implement appropriate respiratory protection and the use of other protective equipment as dictated by monitoring results (See Sections 2 and 7).

Suggestions provided in this section for exposure control and specific types of protective equipment are based on readily available information. Users should consult with the specific manufacturer to confirm the performance of their protective equipment. Specific situations may require consultation with industrial hygiene, safety, or engineering professionals.

9. PHYSICAL AND CHEMICAL PROPERTIES

Note: Unless otherwise stated, values are determined at 20°C (68°F) and 760 mm Hg (1 atm). Data represent typical values and are not intended to be specifications.

Appearance:	Amber to Black
Physical Form:	Liquid
Odor:	Petroleum. Rotten egg / sulfurous
Odor Threshold:	No data
pH:	Not applicable
Vapor Pressure:	0.6-10 psia (Reid VP) @ 100°F
Vapor Density (air=1):	>1
Boiling Point/Range:	-128-1000°F / -89-538°C
Melting/Freezing Point:	No data
Solubility in Water:	Negligible
Partition Coefficient (n-octanol/water) (Kow):	No data
Specific Gravity:	0.7-1.03 @ 60ºF (15.6ºC)
Bulk Density:	5.83-8.58 lbs/gal
Evaporation Rate (nBuAc=1):	No data

Flash Point:	<20°F / <-7°C
Test Method:	(estimate)
LEL (vol % in air):	1.1
UEL (vol % in air):	6.0
Autoignition Temperature:	590°F / 310°C

10. STABILITY AND REACTIVITY

Stability: Stable under normal ambient and anticipated conditions of storage and handling. Extremely flammable liquid and vapor. Vapor can cause flash fire.

Conditions to Avoid: Avoid high temperatures and all sources of ignition. Prevent vapor accumulation.

Materials to Avoid (Incompatible Materials): strong oxidizing agents and nitric acid.

Hazardous Decomposition Products: Combustion can yield carbon monoxide, oxides of nitrogen and sulfur. May contain or liberate poisonous hydrogen sulfide gas.

Hazardous Polymerization: Not known to occur.

11. TOXICOLOGICAL INFORMATION

Chronic Data:

Crude Oil (Petroleum)

Carcinogenicity: Chronic application of crude oil to mouse skin resulted in an increased incidence of skin tumors. IARC concluded in its Crude Oil Monograph that there is limited evidence of carcinogenicity in animals, and that crude oil is not classifiable as to its carcinogenicity in humans (Group 3). It has not been listed as a carcinogen by NTP or OSHA.

Crude Oil (Petroleum)

Reproductive: Dermal exposure to crude oil during pregnancy resulted in limited evidence of developmental toxicity in laboratory animals. Decreased fetal weight and increased resorptions were noted at maternally toxic doses. No significant effects on pup growth or other developmental landmarks were observed postnatally.

n-Hexane

Target Organs: Excessive exposure to n-hexane can result in peripheral neuropathies. The initial symptoms are symmetrical sensory numbness and paresthesias of distal portions of the extremities. Motor weakness is typically observed in muscles of the toes and fingers but may also involve muscles of the arms, thighs and forearms. The onset of these symptoms may be delayed for several months to a year after the beginning of exposure. The neurotoxic properties of n-hexane are potentiated by exposure to methyl ethyl ketone and methyl isobutyl ketone.

Reproductive: Prolonged exposure to high concentrations of n-hexane (>1,000 ppm) has resulted in decreased sperm count and degenerative changes in the testes of rats but not those of mice.

Xylenes

Target Organs: Rats exposed to 800, 1000 or 1200 ppm 14 hours daily for 6 weeks demonstrated high frequency hearing loss. Another study in rats exposed to 1800 ppm 8 hours daily for 5 days demonstrated middle frequency hearing loss.

Reproductive: Both mixed xylenes and the individual isomers produced limited evidence of developmental toxicity in laboratory animals. Inhalation and oral administration of xylene resulted in decreased fetal weight, increased incidences of delayed ossification, skeletal variations and resorptions.

Ethyl Benzene

Carcinogenicity: Rats and mice exposed to 0, 75, 250, or 750 ppm ethyl benzene in a two year inhalation study demonstrated limited evidence of kidney, liver, and lung cancer. Ethyl benzene has been listed as a possible human carcinogen by IARC. Ethyl benzene has not been listed as a carcinogen by NTP, or OSHA.

Benzene

Carcinogenicity: Benzene is known to cause cancer of the blood-forming organs in humans, including acute myelogenous leukemia. It has been identified as a human carcinogen by NTP, IARC and OSHA.

Target Organs: Prolonged or repeated exposures to benzene vapors can cause damage to the blood and blood forming organs, including disorders like leukopenia, thrombocytopenia, and aplastic anemia.

Reproductive: Exposure to benzene during pregnancy demonstrated limited evidence of developmental toxicity in laboratory animals. The effects seen include decreased body weight and increased skeletal variations in rodents. Alterations in hematopoeisis have been observed in the fetuses and offspring of pregnant mice.

Mutagenic Effects: Benzene exposure has resulted in chromosomal aberrations in human lymphocytes and animal bone marrow cells, and DNA damage in mammalian cells in vitro.

Naphthalene

Carcinogenicity: Naphthalene has been evaluated in two year inhalation studies in both rats and mice. The National Toxicology Program (NTP) concluded that there is clear evidence of carcinogenicity in male and female rats based on increased incidences of respiratory epithelial adenomas and olfactory epithelial neuroblastomas of the nose. NTP found some evidence of carcinogenicity in female mice (alveolar adenomas) and no evidence of carcinogenicity in male mice. Naphthalene has been identified as a carcinogen by IARC and NTP.

Acute Data:

Component	Oral LD50	Dermal LD50	Inhalation LC50
Crude Oil (Petroleum)	> 5 g/kg (estimated)	> 2 g/kg (rabbit)	> 5 mg/L
Hydrogen Sulfide	Not Applicable	Not Applicable	LC50 (rat) = 1500 mg/m^3/15 min

12. ECOLOGICAL INFORMATION

Not evaluated.

13. DISPOSAL CONSIDERATIONS

13. DISPOSAL CONSIDERATIONS

The generator of a waste is always responsible for making proper hazardous waste determinations and needs to consider state and local requirements in addition to federal regulations.

This material, if discarded as produced, would not be a federally regulated RCRA "listed" hazardous waste. However, it would likely be identified as a federally regulated RCRA hazardous waste for the following characteristic(s) shown below. See Sections 7 and 8 for information on handling, storage and personal protection and Section 9 for physical/chemical properties. It is possible that the material as produced contains constituents which are not required to be listed in the MSDS but could affect the hazardous waste determination. Additionally, use which results in chemical or physical change of this material could subject it to regulation as a hazardous waste.

Container contents should be completely used and containers should be emptied prior to discard. Container residues and rinseates could be considered to be hazardous wastes.

EPA Waste Number(s)
- D001 - Ignitability characteristic
- D018 - Toxicity characteristic (Benzene)

14. TRANSPORTATION INFORMATION

U.S. Department of Transportation (DOT)

Shipping Description:	***The following shipping descriptions assume the boiling point is above 68° F (35° C)*** Petroleum crude oil, 3, UN1267, I ***or*** II
Non-Bulk Package Marking:	Petroleum crude oil, UN1267
Non-Bulk Package Labeling:	Flammable liquid
Bulk Package/Placard Marking:	Flammable / 1267
Packaging - References:	49 CFR 173.150; 173.201; 173.243 ***[PG I]*** ***-or-*** 49 CFR 173.150; 173.202; 173.242 ***[PG II]*** ***(Exceptions; Non-bulk; Bulk)***
Hazardous Substance:	See Section 15 for RQ`s
Emergency Response Guide:	128
Note:	Packing group is dependent on boiling point (BP) of the material: I if BP <=95°F; II if BP > 95°F ***Shipping description may be modified by placing the UN or NA number as the first element. This order becomes mandatory on January 1, 2013.***

International Maritime Dangerous Goods (IMDG)

Shipping Description:	UN1267, Petroleum crude oil, 3, I ***or*** II, (FP° C cc), *[where FP is the material's flash point in degrees Celsius closed cup]*
Non-Bulk Package Marking:	Petroleum crude oil, UN1267
Labels:	Flammable liquid
Placards/Marking (Bulk):	Flammable / 1267
Packaging - Non-Bulk:	P001
EMS:	F-E, S-E
Note:	Federal compliance requirements may apply. See 49 CFR 171.12.

International Civil Aviation Org. / International Air Transport Assoc. (ICAO/IATA)

UN/ID #:	UN1267
Proper Shipping Name:	Petroleum crude oil
Hazard Class/Division:	3
Subsidiary risk:	None
Packing Group:	I ***or*** II
Non-Bulk Package Marking:	Petroleum crude oil, UN1267
Labels:	Flammable liquid
ERG Code:	3H
Note:	Federal compliance requirements may apply. See 49 CFR 171.11.

14. TRANSPORTATION INFORMATION

	LTD. QTY	Passenger Aircraft	Cargo Aircraft Only
Packaging Instruction #:	None - ***[PG I]*** Y305 - ***[PG II]***	302 - ***[PG I]*** 305 - ***[PG II]***	303 - ***[PG I]*** 307 - ***[PG II]***
Max. Net Qty. Per Package:	None ***[PG I]*** 1L ***[PG II]***	1L ***[PG I]*** 5 L ***[PG II]***	30 L ***[PG I]*** 60 L ***[PG II]***

15. REGULATORY INFORMATION

CERCLA/SARA - Section 302 Extremely Hazardous Substances and TPQs (in pounds):
This material contains the following chemicals subject to the reporting requirements of SARA 302 and 40 CFR 372:

Component	TPQ	EPCRA RQ
Hydrogen Sulfide	500 lb	100 lb

CERCLA/SARA - Section 311/312 (Title III Hazard Categories)

Acute Health:	Yes
Chronic Health:	Yes
Fire Hazard:	Yes
Pressure Hazard:	No
Reactive Hazard:	No

CERCLA/SARA - Section 313 and 40 CFR 372:
This material contains the following chemicals subject to the reporting requirements of Section 313 of SARA Title III and 40 CFR 372:

Component	Concentration (wt %)	de minimis
n-Hexane	0-5	1.0%
Xylenes	0-3	1.0%
Ethyl Benzene	<2	0.1%
Benzene	<1	0.1%
Naphthalene	0-0.9	0.1%

EPA (CERCLA) Reportable Quantity (in pounds):
EPA's Petroleum Exclusion applies to this material - (CERCLA 101(14)).

California Proposition 65:
Warning: This material may contain detectable quantities of the following chemicals, known to the State of California to cause cancer, birth defects or other reproductive harm, and which may be subject to the requirements of California Proposition 65 (CA Health & Safety Code Section 25249.5):

Component	Type of Toxicity
Ethyl Benzene	Cancer
Benzene	Cancer Developmental Toxicant Male Reproductive Toxicant
Naphthalene	Cancer
Toluene	Developmental Toxicant
Various Polycyclic Aromatic Hydrocarbons	Skin Cancer

Canadian Regulations:
This product has been classified in accordance with the hazard criteria of the Controlled Products Regulations (CPR) and the MSDS contains all the information required by the Regulations.

WHMIS Hazard Class
B2 - Flammable Liquids
D2B

National Chemical Inventories:
All components are either listed on the US TSCA Inventory, or are not regulated under TSCA.
All components are either on the DSL, or are exempt from DSL listing requirements.

U.S. Export Control Classification Number: 1C981

16. OTHER INFORMATION

Issue Date:	13-Mar-2008
Status:	Final
Previous Issue Date:	07-Jan-2008
Revised Sections or Basis for Revision:	NFPA ratings (Section 2)
MSDS Number:	724160

MSDS Legend:
ACGIH = American Conference of Governmental Industrial Hygienists; CAS = Chemical Abstracts Service Registry; CEILING = Ceiling Limit (15 minutes); CERCLA = The Comprehensive Environmental Response, Compensation, and Liability Act; EPA = Environmental Protection Agency; IARC = International Agency for Research on Cancer; LEL = Lower Explosive Limit; NE = Not Established; NFPA = National Fire Protection Association; NTP = National Toxicology Program; OSHA = Occupational Safety and Health Administration; PEL = Permissible Exposure Limit (OSHA); SARA = Superfund Amendments and Reauthorization Act; STEL = Short Term Exposure Limit (15 minutes); TLV = Threshold Limit Value (ACGIH); TWA = Time Weighted Average (8 hours); UEL = Upper Explosive Limit; WHMIS = Worker Hazardous Materials Information System (Canada)

Disclaimer of Expressed and implied Warranties:
The information presented in this Material Safety Data Sheet is based on data believed to be accurate as of the date this Material Safety Data Sheet was prepared. HOWEVER, NO WARRANTY OF MERCHANTABILITY, FITNESS FOR ANY PARTICULAR PURPOSE, OR ANY OTHER WARRANTY IS EXPRESSED OR IS TO BE IMPLIED REGARDING THE ACCURACY OR COMPLETENESS OF THE INFORMATION PROVIDED ABOVE, THE RESULTS TO BE OBTAINED FROM THE USE OF THIS INFORMATION OR THE PRODUCT, THE SAFETY OF THIS PRODUCT, OR THE HAZARDS RELATED TO ITS USE. No responsibility is assumed for any damage or injury resulting from abnormal use or from any failure to adhere to recommended practices. The information provided above, and the product, are furnished on the condition that the person receiving them shall make their own determination as to the suitability of the product for their particular purpose and on the condition that they assume the risk of their use. In addition, no authorization is given nor implied to practice any patented invention without a license.

Appendix D – Large-scale Test Protocol

The test procedure for a Linear Augmented Burn experiment in the CRREL wave tank was as follows:

9. The specified volume of oil (35 liters) was measured out and the weight of oil recorded.
10. The oil was transferred into the linear boom containment area using a spill plate.
11. The ambient wind speed was recorded using a hand-held anemometer at a height of about 2 m above the surface of the oil in the containment area. Weather data was retrieved later from a nearby recording weather station operated by CRREL (see Figure 26 for location) throughout the experiments. The temperature of the air and water was also recorded.
12. The water pump for the deluge cooling of the tank was started.
13. The air compressor engine was started and left idling.
14. The video cameras and still cameras were initiated.
15. The oil was ignited by hand with a propane torch mounted on a pole.
16. Once the flame had spread to cover the entire surface of the slick, the compressed air augmentation system was activated (if required for the test) and the waves turned on at the desired profile setting (if required for the test).
17. The following times were recorded:

    preheat times - the time from firing the igniters until flames began to spread away from the ignition point and reaches 10% and 50% flame coverage;
    ignition time – the time to full involvement (100% flame coverage);
    time to the vigorous (or intense) burn phase;
    time to 90%, 50% and 10% flame coverage; and,
    extinction time - the time for the flames to completely extinguish.
18. The apparent density of soot emissions was observed visually, manually noted, and electronically measured with a program running on a cell phone.
19. After extinction the air compressor was stopped and the video and still cameras turned off.
20. The water deluge pump was stopped.
21. After each burn, the residue was allowed to cool. The residue was then collected with preweighed sorbent pads and then weighed in a garbage bag immediately after.
22. The sorbent pads were then removed from the garbage bag and hung up to dry for 24 hours, placed back in the garbage bag and then reweighed.
23. The weight of oil samples for the U.S. EPA was recorded.

Appendix E – Analysis of Emissions and Residue from Methods to Improve Combustion Efficiency of In Situ Oil Burns- EPA Final Report

Analysis of Emissions and Residue from Methods to Improve Combustion Efficiency of *In Situ* Oil Burns

Innovative fire and fuel configurations to optimize in situ burning volumes and efficiencies

Final Report

August 9, 2019

Dr. Brian Gullett
US EPA, Office of Research and Development, National Risk Management Research Laboratory, Air and Energy Management Division

Dr. Johanna Aurell
University of Dayton Research Institute, Power & Energy Division, Energy and Environmental Sciences

Dr. Amara Holder
US EPA, Office of Research and Development, National Risk Management Research Laboratory, Air and Energy Management Division

Dr. Robyn Conmy
US EPA, Office of Research and Development, National Risk Management Research Laboratory, Land and Materials Management Division

Dr. Devi Sundaravadivelu
Pegasus Technical Services, Inc.

ABSTRACT

The efficiency of at-sea surface oil burns was determined while testing varied boom configurations and air-assist nozzles to improve combustion. Tests were conducted in a 47 ft x 8 ft x 8 ft tank under both calm and wave-action conditions. Measurements of emissions and residual of uncombusted oil were made to characterize variations in boom length/width ratios, injection air, nozzle angle, and presence or absence of waves. Combustion tests were done with 30 L of Alaska North Slope oil within an outdoor, fresh water, 16,700-gallon tank. The combustion plume was sampled with a crane-suspended instrument system. Combustion efficiencies based on unburned carbon in the plume ranged from 85% to 93%. Efficiencies based on oil mass loss ranged from 89% to 99%. A 3-fold variation in $PM_{2.5}$ emission factors was observed from the test conditions. Results suggest that the most effective burns in terms of reduced combustion efficiency and oil consumed were those that have high length to width boom ratios and injection air. Post-burn, residual oil samples were collected and analyzed.

TABLE OF CONTENTS

TABLE LIST

FIGURE LIST

ACRONYMS

AAE	Absorption angstrom exponent
AEMD	Air and Energy Management Division
BC	Black carbon
BSEE	Bureau of Safety and Environmental Enforcement
BTEX	Benzene, toluene, ethylbenzene, xylene
CH_4	Methane
CO	Carbon monoxide
CO_2	Carbon dioxide
CRREL	Cold Regions Research and Engineering Laboratory
DCM	Dichloromethane
DNPH	2,4-Dinitrophenylhydrazine
EC	Elemental Carbon
ED-XRF	Energy dispersive x-ray fluorescence spectrometry
ELPI	Electrical Low Pressure Impactor
EPA	Environmental Protection Agency
FID	Flame Ionization detector
GC	Gas Chromatography
GFAA	Graphite furnace atomic absorption
HPLC	High-Pressure Liquid Chromatography
HRGC	High resolution gas chromatography
HRMS	High resolution mass spectrometry
ICP	Inductively coupled plasma mass spectrometry
LOD	Limit of detection
MCE	Modified Combustion Efficiency
MS	Mass spectrometry
MSD	Mass selective detector
ND	Not detected
NDIR	Non-dispersive infrared
NIOSH	National Institute for Occupational Safety and Health
NIST	National Institute of Standards and Technology
NRMRL	National Risk Management Research Laboratory
NS	Not sampled
OC	Organic Carbon
OD	Outer diameter
ORD	Office of Research and Development
PAHs	Polycyclic aromatic hydrocarbons
Pb	Lead
PCDD/PCDF	Polychlorinated dibenzo-p-dioxins/ polychlorinated dibenzofurans
PCF	Photometric calibration factor
PM	Particulate matter

PM_{10}	Particulate matter, with diameter equal to or less than 10 µm
$PM_{2.5}$	Particulate matter, with diameter equal to or less than 2.5 µm
PN	Particle number
PUF	Polyurethane foam plug
RH	Relative humidity
RPD	Relative Percent Difference
RSD	Relative Standard Deviation
SOP	Standard operating procedure
SP2	Single particle soot photometer
Stand. Dev.	Standard deviation
TC	Total Carbon
TEQ	Toxic equivalent
TOA	Thermal-optical analysis
TPH	total petroleum hydrocarbons
TSP	Total suspended particles
UDRI	University of Dayton Research Institute
UVPM	Ultra violet particulate matter
VOCs	Volatile Organic Compounds

1 INTRODUCTION

At-sea oil spills are often treated by boom-aided herding and concentration of surface oils followed by purposeful ignition at the apex of the U-shaped boom system. These *in situ* oil burns are employed to mitigate the potential environmental impact of floating oil. One undesirable consequence of the burns is the black plume formed by the combustion by-products. Recent studies have begun to characterize the plume pollutants through at-sea (Aurell and Gullett, 2010; Gullett et al., 2016) and laboratory-based measurements (Gullett et al., 2017) and found that emissions from burning oil are comprised of fine particulate matter (<2.5 μm mass median diameter, $PM_{2.5}$) and gaseous components. Measurements during the Deepwater Horizon disaster in the Gulf of Mexico found that 7.5% of the oil mass burned was emitted as fine particle mass into the atmosphere (Aurell and Gullett, 2010). These particles were 82% elemental carbon (EC) to which were bound polycyclic aromatic hydrocarbons (PAHs) at concentrations of 68 μg/g particle mass (Gullett et al., 2016). Trace amounts of polychlorinated dibenzodioxins and dibenzofurans (PCDDs/PCDFs) were also found (Aurell and Gullett, 2010).

A recent laboratory study (Gullett et al., 2017) with Bayou Sweet crude simulated the Deepwater Horizon burns, finding ~6% of the oil by mass became a particle emission of median diameter 1 μm, over 90% of which was light absorbing black carbon (BC). The gas phase modified combustion efficiency declined throughout the burns to 97.8%; incorporation of the carbon within the particle emissions and unburnt residue (in this case, 29% by mass) would significantly lower this efficiency.

Efforts to improve the combustion efficiency of *in situ* oil burns aim to reduce the amount of PM and trace pollutants released in the plume, alleviating concerns related to inhalation and environmental exposure, as well as reducing the unburnt oil residues. Methods of increasing combustibility include limiting heat loss from the burning oil layer to the water below and increasing air and heat penetration to the burning oil plume.

Limited research suggests that smoke yield (mass of PM/mass of oil burned) decreases below oil slick diameters of 3 m, due to the ability of the convective, rising plume to entrain combustion air into its core, enhancing combustion (Koseki, 2000). Values for smoke yield range from 0.055 to 0.2 kg smoke/kg oil burned for 0.09 m and 3 m pan sizes, respectively (Koseki, 2000). This suggests that alteration of the boom geometry, in combination with mechanically-enhanced aeration, may improve combustion efficiency while minimizing residues. In this work, a narrow, linear boom geometry was tested for its ability to enhance combustion by shortening the oil plume core thickness, allowing greater air penetration and radiant heat feedback to the burning oil. This geometry, as well as addition of nozzle-supplied compressed air at the boom/oil interface, formed the basis of the second set of technologies studied.

This work will characterize combustion efficiencies of oil burning technology concepts by sampling and quantifying the pollutants and unburned residues. This technology was tested on an outdoor water tank. Results were used to determine emission factors, or the mass amount of a pollutant per amount of oil burned as well as the residue constituent per mass of oil burned.

2 MATERIALS AND METHODS

2.1 Test Location and Set-up

Testing took place at the U.S. Army Corps of Engineers, Cold Regions Research and Engineering Laboratory (CRREL) located in Hanover, New Hampshire. The facility used for the testing was the CRREL in-ground tank shown in the background of Figure 2-1. The interior dimensions of the wave tank are 47ft x 8ft x 8ft. The beach end is tapered and the water level is 6.5ft so the operating capacity is roughly 16,700 gallons. To simulate at-sea, *in situ* oil burning, crude oil was floated on the surface of the water-filled tank and ignited by CRREL. For each burn test, members of CRREL prepared the area and the burn tank with the test oil and then began the burn. CRREL handled oil storage, transport, ignition, and post-residue-collection cleanups. Tests were conducted from November 5-9, 2018 during mostly sunny days with temperatures ranging from 9ºC to 23ºC.

Figure 2-1. U.S. Army Corps of Engineers wave tank.

The mass of oil added and residue recovered was measured by CREEL to allow burn removal efficiency to be calculated. Burns were videotaped and timed by CRREL to permit estimates of burn rate and smoke quality.

The burn plume was sampled using an EPA instrument system suspended from a crane and maneuvered into the plume. Slight movements of the crane boom angle, rotational position, and cable length kept the instruments in the plume to accommodate wind shifts. The sampling system was mounted on an aluminum skid as shown in Figure 2-2.

Figure 2-2. U.S. EPA's emission instrument system mounted on an aluminum skid.

2.2 Test Matrix

A test program consisting of the following conditions with different boom configurations and nozzle locations was undertaken, with replicates of one test configuration resulting in a total of sixteen burns (

Table 2-1). The Boom Ratio is the ratio of the boom length to boom width and was varied from 1:1 to 9:1. Air-assist nozzles were affixed to the boom and angled directly across the oil slick (90^{o}), angled up over the oil slick (+45^{o}), and angled down toward the oil (-45^{o}). In addition, the presence or absence of waves was tested.

1. Control (no air or waves)
2. Air
3. Waves
4. Air and waves

Table 2-1. Test Matrix.

Burn Number	Date	Test Condition	Configuration		Mass initial oil (kg)
			Boom Ratio	Nozzle location	
1	11/5/2018	Control	1:1	No nozzle	31.0720
2	11/5/2018	Air	1:1	90°	31.0715
3	11/5/2018	Waves	1:1	No nozzle	31.1195
4	11/6/2018	Air and Waves	1:1	90°	31.0688
5	11/6/2018	Air and Waves	1:1	+45°	32.5236
6	11/7/2018	Control	9:1	No nozzle	31.0659
7	11/7/2018	Air	9:1	+45°	31.1188
8	11/7/2018	Waves	9:1	No nozzle	31.0647
9	11/7/2018	Air and Waves	9:1	+45°	31.0670
10	11/8/2018	Control	4:1	No nozzle	31.0710
11	11/8/2018	Air	4:1	+45°	31.0679
12	11/8/2018	Waves	4:1	No nozzle	31.1109
13	11/8/2018	Air and Waves	4:1	+45°	31.1118
14	11/8/2018	Air and Waves	4:1	-45°	31.0640
15	11/9/2018	Air and Waves	9:1	+45°	31.0620
16	11/9/2018	Air and Waves	9:1	+45°	31.0850

Configuration: Boom ratio = boom length/width, Nozzle location - degree of air nozzle to water/oil surface

2.3 Target Emission Compounds

Target compounds include carbon monoxide (CO), carbon dioxide (CO_2), particulate matter less than 2.5 µm ($PM_{2.5}$), BC and ultraviolet (light absorbing) PM (UVPM), EC/OC and total carbon (TC), PAHs, PCDDs/PCDFs, and volatile organic compounds (VOCs) including carbonyls.

Targeted emissions and their sampling methods are listed in Table 2-2. The number of batch samples collected for each test configuration is shown in Table 2-3.

Table 2-2. Oil Burn Emission Targets

Analyte	Method	Frequency
CO_2	LiCOR-820, NDIR	Continuous

Analyte	Method	Frequency
CO	Electrochemical cell	Continuous
$PM_{2.5}$	Impactor/filter/gravimetric	Batch
PM by size	TSI DustTrak DRX	Continuous
PM size	Electrical Low-Pressure Impactor	Continuous
PCDD/PCDF	Quartz filter/PUF, HRMS	Batch
PAH	Quartz filter/PUF/XAD/PUF, HRMS	Batch
VOCs	SUMMA cannister	Batch
BC	Aethalometer, MA200/MA350	Continuous
UVPM	Aethalometer, MA200/MA350	Continuous
PM absorption and scattering	Photoacoustic Soot Spectrometer	Continuous
BC size distribution	Single Particle Soot Photometer	Continuous
EC/OC/TC	Quartz filter	Batch
Carbonyls	DNPH cartridges	Batch

Table 2-3. Number of batch samples collected in each test configuration.

Burn		Configuration		No. of collected samples					
No.	Test Condition	Boom Ratio	Nozzle Location	$PM_{2.5}$	EC/OC/TC	PAH	PCDD/ PCDF	VOC	Carbonyls
1	Control	1:1	No nozzle	2	2	1	1	1	
2	Air	1:1	90	2	2	1	1	1	
3	Waves	1:1	No nozzle	2	2	1	1	1	
4	Air and Waves	1:1	90	2	2	1	1	1	1
5	Air and Waves	1:1	+45	2	2	1		1	1
6	Control	9:1	No nozzle	2	2	1	1	1	1
7	Air	9:1	+45	2	2	1		1	1
8	Waves	9:1	No nozzle	2	2	1		1	1
9	Air and Waves	9:1	+45	2	2	1		1	1
10	Control	4:1	No nozzle	2	2	1		1	1
11	Air	4:1	+45	2	2	1		1	1
12	Waves	4:1	No nozzle	2	2	1		1	1
13	Air and Waves	4:1	+45	2	2	1		1	
14	Air and Waves	4:1	-45	2	2	1	1		
15	Air and Waves	9:1	+45	2	2	1	1	1	
16	Air and Waves	9:1	+45	2	2	1		1	
	Ambient			1	1	1		1	2
	Sum			**33**	**33**	**17**	**7**	**16**	**11**

2.4 Calculations

2.4.1 Emission Factors in mass analyte per mass initial oil

Measurements were used to determine emission factors based on the carbon balance method, which uses the ratio of the sampled pollutant mass to the sampled carbon mass (determined from CO + CO_2 measurements and, where possible, TC from $PM_{2.5}$ analyses) and the carbon percentage of the fuel (85%). The resultant emission factors are expressed as mass of pollutant per mass of oil burned (Equation 1).

$$Emission\ Factor_{initial} = Fc\ x \frac{Analyte_{ij}}{C_j} \qquad Equation\ 1$$

Where:

$EF_{initial}$ = The Emission Factor for target analyte *i* (mg $Analyte_i$/kg oil initial)
Fc = Carbon fraction in the oil (0.85)
$Analyte_{ij}$ = background-corrected concentration (mg $Analyte_i/m^3$) of the target analyte *i* collected from the volume element *j* of the plume.
C_j = background-corrected concentration of carbon (kg Carbon/m^3) collected from volume element *j* of the plume

2.4.2 Emission Factors in mass analyte per mass oil consumed

An alternative emission factor was calculated taking the oil not consumed into consideration as shown in Equation 2.

$$Emission\ Factor_{Consumed} = EF_{initial}\ x \frac{mass\ oil}{mass\ oil\ x oil\ mass\ loss} \qquad Equation\ 2$$

Where:

$Emission\ Factor_{consumed}$ = The Emission Factor for target analyte *i* (mg $Analyte_i$/kg oil consumed)
$EF_{initial}$ = The Emission Factor for target analyte *i* (mg $Analyte_i$/kg oil initial)
mass oil = mass of oil initial
oil mass loss = fraction of oil consumed in the burn

2.4.3 Modified Combustion Efficiency

The Modified Combustion Efficiency (MCE) was used to calculate how well the oil burned.

$$MCE = \frac{CO2}{CO_2 + CO + Total\ Carbon} \qquad Equation\ 3$$

Where:

MCE = modified combustion efficiency

CO_2 = carbon dioxide in the plume in ppm
CO = carbon monoxide in the plume in ppm
Total Carbon = total carbon in the particulates (TC)

2.4.4 Data Variability

Standard deviation (Stand. Dev.), relative standard deviation (RSD), and relative percent difference (RPD) were used as a measure of dispersion, calculations shown in Equations 4 to 6.

$$tan\ ar\ D\ iation = \Sigma(\frac{\overline{\ \ ^{2}}}{(n-1)} \qquad \textit{Equation 4}$$

where:

x = each sample value
$\bar{x}$ = mean value of samples
n = number of samples

$$RD(\%) = 100x\frac{Standard\ Deviation}{Sample\ Average} \qquad \textit{Equation 5}$$

$$RPD\ (\%) = 100\ x\ \frac{1-\ 2}{\frac{x1+x2}{2}} \qquad \textit{Equation 6}$$

where:
x_1 = sample value one
x_2 = sample value two

3 MEASUREMENT AND QUALITY ASSURANCE PROCEDURES

3.1 CO_2 measurements

The CO_2 was continuously measured using a non-dispersive infrared (NDIR) instrument (LI-820 model, LI-COR Biosciences, Lincoln, USA). These units are configured with a 14 cm optical bench, giving it an analytical range of 0-20,000 ppm with an accuracy specification of less than 3% of reading. The LI-820 calibration range was set to 0-4,581 ppm and was calibrated for CO_2 on a daily basis in accordance with EPA Method 3A (2017b). Concentration was recorded on the onboard computer using the FlyerDAQ program, a LabView generated data acquisition and control program.

CO_2 was used to calculate the dilution ratio achieved in the dilution system. A liquid nitrogen dewar was used to supply high pressure nitrogen as a diluent, thus the amount of CO_2 in the diluted sample was used to calculate the dilution ratio. The CO_2 concentration in the diluted

sample was monitored continuously with a second LI-820 and compared to the undiluted CO_2 concentration.

All gas cylinders used for calibration were certified by the suppliers that they are traceable to National Institute of Standards and Technology (NIST) standards.

3.2 CO measurements

The CO sensor (e2V EC4-500-CO) was an electrochemical gas sensor (SGX Sensortech, Essex, United Kingdom) which measures CO concentration by means of an electrochemical cell through CO oxidation and changing impedance. The E2v CO sensor has a CO detection range of 1-500 ppm with resolution of 1 ppm. The temperature and relative humidity (RH) operating range was -20 to +50°C and 15 to 90% RH, respectively. The response time is less than 30 seconds. Output is non-linear from 0 to 500 ppm. A calibration curve has been calculated in the EPA Metrology Laboratory at 0 to 100 ppm with ±2 ppm error using EPA Method 3A (2017b). The sensor was calibrated for CO on a daily basis in accordance with U.S. EPA Method 3A (2017b).

All gas cylinders used for calibration were certified by the suppliers that they are traceable to NIST standards.

3.3 $PM_{2.5}$

$PM_{2.5}$ was sampled with SKC impactors using 47 mm tared Teflon™ filters with a pore size of 2.0 µm via a Leland Legacy sample pump (SKC Inc., USA) with a constant airflow of 10 L/min. PM was measured gravimetrically following the procedures described in 40 CFR Part 50 (1987). Particles larger than 2.5 µm in the $PM_{2.5}$ impactor were collected on an oiled 37 mm impaction disc mounted on the top of the first filter cassette. The Teflon™ filters were pre- and post-weight by Chester LabNet. The Leland Legacy Sample pump was calibrated with a Gilibrator Air Flow Calibration System (Sensidyne LP, USA).

3.4 Particulate Size Characterization, Black Carbon, and Optical Measurements

The emission probe for PM size characterization, BC, and optical properties were collocated with the flyer suspended in the plume. The PM sample was diluted using a porous probe diluter and an eductor mounted next to the flyer and then transported through a conductive teflon sample hose (1/2 in inner diameter, 100 ft length) to the instrumentation at ground level. Concentrations at the ground are corrected for particle losses in the sample line based on laboratory calibrations with a known aerosol concentration and size distribution.

Particle size distribution, BC concentration and size, and particle optical properties were measured from the diluted sample line. Particle size distribution was measured continuously with an Electrical Low Pressure Impactor (ELPI, Dekati, Kangasala, Finland). The ELPI sampled aerosols on aluminum foil substrates over 13 size stages at a constant airflow of 10 L/min. The charge collected on each substrate is converted to a particle mass to derive a particle size distribution.

The BC size distribution was measured with a Single Particle Soot Photometer (SP2, Droplet Measurement Technologies, Longmont, CO). The SP2 uses an intra-cavity laser to irradiate single particles resulting in a laser induced incandescence, which is measured with a detector. Individual particle mass is proportional to the incandescence signal and is used to generate a BC mass distribution. Additionally, scattered laser light is used to optically size particles.

3.5 Metals

The PM collected on the 47 mm Teflon™ $PM_{2.5}$ filter at 10 L/min was also appropriate for the determination of metals. EPA Compendium Method I0-3.3(1999b) specifies analysis by energy dispersive x-ray fluorescence spectrometry (ED-XRF). This method is compatible with particulate on filters, is quite sensitive, and is non-destructive. This means that the PM and substrate survive the analysis intact; and may be archived or analyzed by other methods, such as more expensive inductively coupled plasma mass spectrometry (ICP) or Graphite Furnace atomic absorption (GFAA) if necessary. Filters were analyzed by Chester LabNet using XRF methods for a full-metal scan.

Thin film standards were used for calibration because they most closely resemble the layer of particles on a filter. Thin films standards are typically deposited on Nuclepore™ substrates.

A background spectrum generated by the filter itself was subtracted from the X-ray spectrum prior to extracting peak areas. Background spectra was obtained for each filter lot used for sample collection. The background shape standards which are used for background fitting were created at the time of calibration. If a new lot of filters was used, a new background spectra was obtained. A minimum of 20 clean blank filters from each filter lot were kept in a sealed container and were used exclusively for background measurement and correction. The spectra acquired on individual blank filters were added together to produce a single spectrum for each of the secondary targets or fluorescing compounds used in the analysis of lead (Pb). Individual blank filter spectra which show atypical contamination were excluded from the summed spectra. The summed spectra were fitted to the appropriate background during spectral processing. Background correction was automatically included during spectral processing of each sample.

3.6 Continuous PM

Continuous PM was sampled with a DustTrak DRX Model 8533 (TSI Inc., USA) on the diluted sample line. This instrument measured light scattering by aerosols as they intercept a laser diode and has the capability of simultaneous real time measurement (every second) of PM_1, $PM_{2.5}$, Respirable (PM_4), PM_{10} and Total PM (up to 15 µm). The aerosol concentration range for the DustTrak DRX is 0.001-150 mg/m^3 with a resolution of ±0.1% of reading. The flow accuracy is ±5% of internal flow controlled. Concurrently, an enclosed, 37-mm pre-weighed filter cassette provides a simultaneous total suspended particles (TSP) gravimetric sample. The total flow rate is 3 L/min where 1/3 of the flow rate is used for the continuous measurements and 2/3 is used for the gravimetric sample. The enclosed gravimetric sample was used to conduct a custom photometric calibration factor (PCF) for the Total PM. The DustTrak DRX was factory calibrated to the respirable fraction, with a PCF value of 1.00. A custom PCF is conducted as per manufacturer's recommendations for $PM_{2.5}$ using the simultaneously sampled $PM_{2.5}$ by filter impactor concentrations (averaged continuous $PM_{2.5}$ concentration divided by $PM_{2.5}$ by filter mass concentration). This factor is applied to scale the real time data.

3.7 Black Carbon, Total Carbon, Elemental Carbon, Organic Carbon

BC was measured with an MA350 microaethalometer (AethLabs, USA) from the diluted sample line. The microaethalometer is a small, portable, hand-held instrument capable of measuring BC concentration, the instrument measures light attenuation of particles deposited on a filter at five wavelengths (375, 470, 528, 625, 880 nm). The attenuation at the different wavelengths can be used to indicate differing sources of BC. The MA350 is capable of sampling in increments of 1, 10, 60, or 300 seconds from 0-1 mg BC/m^3. The optical response of these instruments is factory calibrated. The pump flow was calibrated before leaving for the field via a TSI flow calibrator. The MA350 is equipped with a filter cartridge that can advance to a new filter spot after PM loads the previous spot to a set attenuation (100). Integrated filter samples were taken at each measurement location and stored for gravimetric or thermal-optical analysis.

OC/EC/TC was sampled with a SKC $PM_{2.5}$ impactor using 37 mm quartz filter via a Leland Legacy sample pump (SKC Inc., USA) with a constant airflow of 3 L/min. Particles larger than 2.5 µm in the $PM_{2.5}$ impactor were collected on an oiled 37 mm impaction disc mounted on the top of the first filter cassette. The Leland Legacy sample pump was calibrated with a Gilibrator Air Flow Calibration System (Sensidyne LP, USA). The OC/EC/TC was analyzed via a modified thermal-optical analysis (TOA) using NIOSH Method 5040 (1999e) and Khan et al. (Khan et al., 2012).

3.8 Volatile Organic Compounds and Carbonyls

SUMMA® canisters were used for collection of VOCs via EPA Method TO-15 (1999d). Sampling for VOCs was accomplished using laboratory-supplied 6 L SUMMA® equipped with a manual valve, metal filter (frit), pressure gauge, pressure transducer, and an electronic solenoid valve. The canisters were analyzed by ALS, NY. The canisters were also used for analysis of CO, CO_2, and methane (CH_4) by GC/ flame ionization detector (FID) according to EPA Method 25 . Method 25 also specifies gas sample collection by evacuated cylinder determines the SUMMA®'s sampling rate.

Carbonyls were sampled with 2,4-Dinitrophenylhydrazine (DNPH) coated silica cartridges (Sigma-Aldrich, PN 505323) using EPA Method TO-11A (1999a). The cartridge flow was controlled by a calibrated a pump downstream of the cartridge at a sampling flow rate of 1 L/min. Two background samples were taken. DNPH cartridges were extracted with carbonyl-free acetonitrile and analyzed by High-Pressure Liquid Chromatography (HPLC) on an Agilent 1100 HPLC with a Diode Array Detector in accordance with EPA Method TO-11A (1999a).

3.9 Polyaromatic Hydrocarbons

PAHs were sampled using a polyurethane foam (PUF)/XAD-2/PUF sorbent preceded by a quartz microfiber filter with a sampling rate of 5 L/min (Leland Legacy pump (SKC Inc., Eighty Four, PA, USA)). The PUF/XAD-2/PUF cartridge was purchased pre-cleaned from Supelco (USA). The glass cartridge was 2.2 cm in outer diameter (OD) and 10 cm long with 1.5 g of XAD-2 sandwiched between two 3-cm PUF plugs. The Leland Legacy sample pump was calibrated with a Gilibrator Air Flow Calibration System (Sensidyne LP, St. Petersburg FL, USA).

The target PAH compounds (naphthalene, acenaphthylene, acenaphthene, fluorene, phenanthrene, anthracene, fluoranthene, pyrene, benzo(a)anthracene, chrysene, benzo(b)fluoranthene, benzo(k)fluoranthene, benzo(a)pyrene, indeno(1,2,3-cd)pyrene, dibenz(a,h)anthracene, benzo(ghi)perylene) were analyzed using a modified EPA Method 8270D (2007). Modifications to the method included use of a pre-sampling, pre-extraction, and pre-analysis spike. Labeled standards for PAHs were added to the XAD-2 trap before the sample was collected. The detection limit was approximately 0.2 µg/sample. Surrogate recoveries were measured relative to the internal standards and are a measure of the sampling train collection efficiency.

All pre-extraction standard recoveries and pre-sampling recoveries were 65-143% and 87-115%, respectively. There are no set method criteria recoveries as this is a modified sampling method.

When comparing these pre-extraction recoveries and pre-sampling recoveries to the PCDD/PCDF method criteria of 25-130% and 70-130%, respectively, we were slightly over the criteria for one of the internal standard spikes (chrysene) in the background sample. A one-hour background sample for ambient PAH was collected for analysis. The PAH concentrations in the collected plumes samples were 600-2500 times higher than the ambient background sample's concentrations.

3.10 Polychlorinated Dibenzodioxins and Furans

PCDDs/PCDFs were collected onto a quartz microfiber filter (20.3×25.4 cm) and PUF plug using a low voltage Windjammer brushless direct current blower (AMETEK Inc., Berwyn, USA) with a nominal sampling rate of 0.85 m^3/min following EPA Method TO-9A (1999c). The PUF was cleaned before use by solvent extraction with dichloromethane and dried with flowing nitrogen to minimize contamination of the media with the target analytes and remove unreacted monomer from the sorbent.

PCDDs/PCDFs samples were cleaned up and analyzed using an isotope dilution method based on EPA Method 23 (1996). Concentrations were determined using high resolution gas chromatography/high resolution mass spectrometry (HRGC/HRMS) with a Hewlett-Packard GC 6890 Series coupled to a Micromass Premier mass spectrometer (Waters Corp., Milford, MA, USA) with an RTX-Dioxin 2, 60 m × 0.25 mm × 0.25µm film thickness column (Restek Corp., Bellefonte, PA, USA). Method 8290 (Agency., February 2007) was followed for analysis of tetra- through octa-CDDs/Fs. The standard used for chlorinated dioxin/furan identification and quantification was a mixture of standards containing tetra- to octa-PCDD/F native and 13C-labeled congeners designed for modified EPA Method 23 (1996) (ED-2521, EDF-4137A, EDF-4136A, EF-4134, ED-4135, CIL Cambridge Isotope Laboratories Inc., U.S.A.). The PCDD/F calibration solutions were prepared by EPA and contained native PCDD/F congeners at concentrations from 1 (ICAL-1)-100 (I-CAL6) ng/mL.

All pre-extraction standard recoveries were 58-178% which is slightly outside the method criteria (25-130%) and pre-sampling recoveries were 95-150% also slightly the criteria of the method (70-130%). A one-hour background sample for ambient PCDD/PCDF was collected for analysis during previous on-site testing in May. The PCDDs/PCDFs concentrations in the collected plumes samples were relatively low although more than 51 times higher than the ambient background sample's concentrations.

3.11 Oil/Water Residue Analysis

Post burn residue samples were collected with oil absorbent pads and analyzed for monoaromatic hydrocarbons (i.e., benzene, toluene, ethylbenzene and xylene; BTEX), PAHs, alkanes (C10-C35 normal aliphatics, and branched alkanes [pristine and phytane]) and total petroleum hydrocarbons (TPH; as total extracted petroleum hydrocarbons). PAHs analyzed included 2-4

ring compounds and their alkylated homologs (i.e., C0-C4 naphthalenes, C0-C4 phenanthrenes, C0-C3 fluorenes, C0-C4 dibenzothiophenes, C0-C4 napthabenzothiophenes, C0-C4 pyrenes and C0-C4 chrysenes). Concentrations of the detected alkanes and PAHs were summed to compute total alkane and PAH concentrations, respectively. In addition to the burn residue sample, a one-liter water sample was also collected from the tank at the end of each burn and analyzed for hydrocarbon components.

For the burn residue, analysis for BTEX was performed by adding 0.25×0.25-inch oil-soaked absorbent pads from each burn to a vial and spiking with a deuterated BTEX mix, surrogate mix and internal standards. The samples were then quantified using an Agilent 7890A GC with a 5975C mass selective detector (MSD) with Triple Axis Detector and CombiPal autosampler (CTC Analytics) following EPA Method 524.3 (2009) modified to perform head space analysis instead of purge and trap. For PAHs and alkanes measurements, 1×1-inch pads from each burn were spiked with a labeled surrogate mix and extracted with dichloromethane (DCM). The extracts were quantified using an Agilent 6890N GC with an Agilent 5975 MSD and an Agilent 7683 series autosampler, equipped with a DB-5 capillary column by J&W Scientific (30 m, 0.25 mm I.D., and 0.25 mm film thickness) and a splitless injection port as per EPA NRMRL-LMMD-34-0 SOP. Similarly, DCM extracts were prepared (without surrogates) for TPH analysis. The fuel used for the burn experiment (Alaska North Slope, provided by Bureau of Safety and Environmental Enforcement, BSEE) was used to prepare a six-point calibration curve for quantification. An Agilent 7890B GC equipped with an FID and 7693 autosampler following EPA Method 8015B (n.d.) was used for the analysis. One pad sample per burn was extracted and analyzed in triplicate.

The tank water samples were evaluated for BTEX by adding 15 mL of the sample and spiking with a deuterated BTEX mix, surrogate mix and internal standards. The samples were then measured using the head space method described above. The remaining water sample was split into two (~ 500 mL each) and extracted with DCM and analyzed for alkanes, PAHs, and TPH using the aforementioned GC-MS and GC-FID methods respectively. One water sample was collected and analyzed per burn.

4 RESULTS AND DISCUSSION

4.1 Oil Residue

The mass loss in Table 4-1 was derived by CRREL and used in this report to calculate the emission factor in mass pollutant per mass consumed oil, see Equation 2 in Chapter 2.4.2. The mass loss varied from 88.8% to 99.6%, Figure 4-1. The three replicate runs of configuration “Air and Waves 9:1 +45°” had an average mass loss of 90.2%±1.4 resulting in an RSD of 1.6% indicating a very good reproducibility. The mass loss data are also plotted chronologically in Figure 4-1.

Table 4-1. Oil residue in each test.

Burn Number	Test Condition	Boom Ratio	Nozzle location	Mass initial oil (kg)	Mass loss (%)
1	Control	1:1	No nozzle	31.0720	94.3
2	Air	1:1	90°	31.0715	95.5
3	Waves	1:1	No nozzle	31.1195	91.5
4	Air and Waves	1:1	90°	31.0688	94.4
5	Air and Waves	1:1	45°	32.5236	95.0
6	Control	9:1	No nozzle	31.0659	99.6
7	Air	9:1	+45°	31.1188	98.7
8	Waves	9:1	No nozzle	31.0647	94.9
9	Air and Waves	9:1	+45°	31.0670	89.2
10	Control	4:1	No nozzle	31.0710	97.1
11	Air	4:1	+45°	31.0679	96.4
12	Waves	4:1	No nozzle	31.1109	89.2
13	Air and Waves	4:1	+45°	31.1118	90.5
14	Air and Waves	4:1	-45°	31.0640	88.8
15	Air and Waves	9:1	+45°	31.0620	89.5
16	Air and Waves	9:1	+45°	31.0850	91.8

[a] Measured from collected oil residue by CRREL.

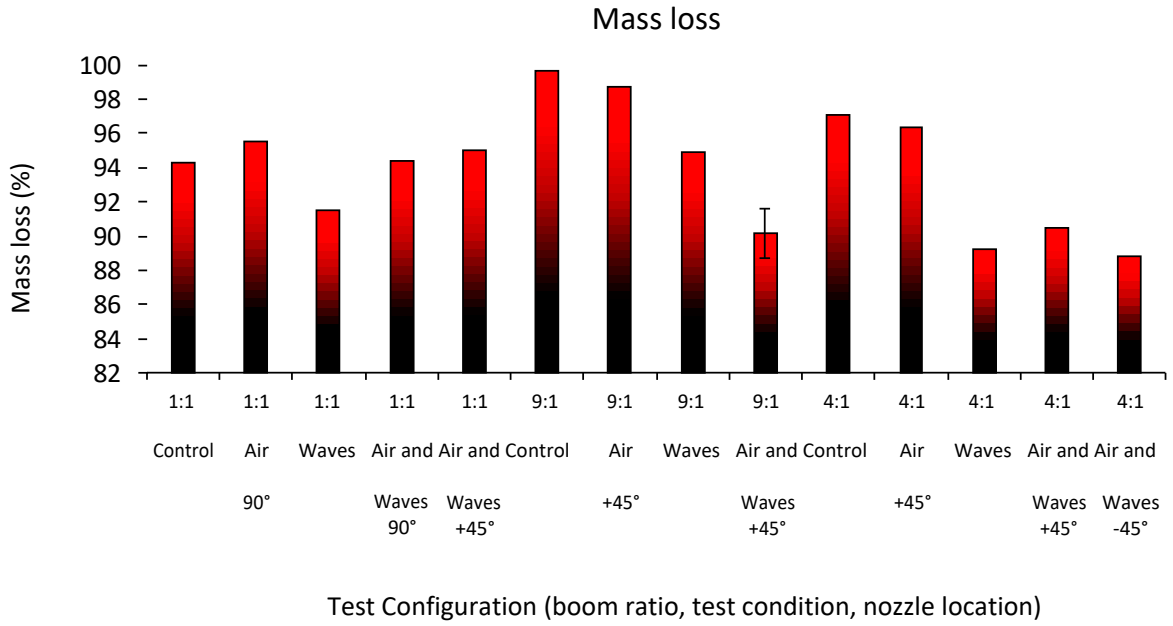

Figure 4-1. Mass loss in each test configuration. Error bar equal 1 Stand. Dev.

4.2 Combustion Gases

Continuous measurements of CO and CO_2 were made throughout each burn. Figure 4-2 shows a typical trace with the resulting time-resolved MCE plotted as dashed lines. The MCE declines throughout the burn likely reflecting the initially more complete oxidation of the burning volatile components of the oil. While the time-resolved concentrations of CO and CO_2 appear to increase with time, this could simply be due to crane operator more successfully positioning the sampler in the "thicker" parts of the plume.

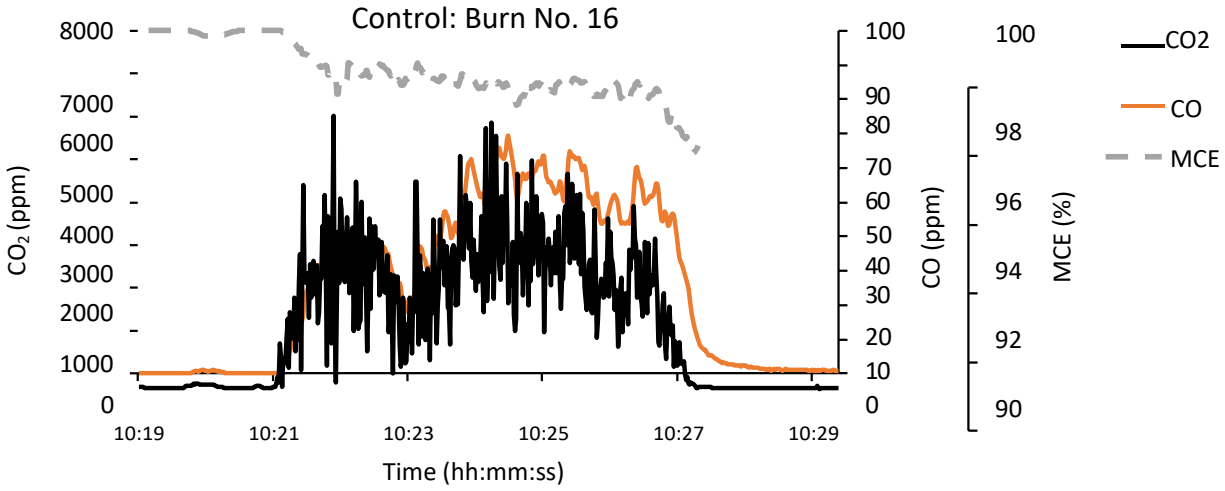

Figure 4-2. A typical CO_2 and CO concentration trace (data frequency 1 second) with corresponding MCE (10 seconds moving average) during air and waves 9:1 +45°, burn no. 16., MCE calculated using CO_2 and CO.

The PM particles were analyzed for solid phase carbon (EC) to determine the Total Carbon (TC) content. When the TC fraction was coupled with the PM emission rate, a particle-phase carbon emission rate is calculated. When this value is combined with carbon from CO and CO_2, values for "MCE with TC" result. Figure 4-3 shows chronological run date for MCE values both with and without TC as well as TC. When MCE is calculated with TC, MCE values decrease up to about 30-40%, indicating a significant unburnt carbon content emission in the particles. Figure 4-4 repeats this figure but uses oil mass loss instead of MCE as the ordinate value. Mass loss varies between 88% to 98%.

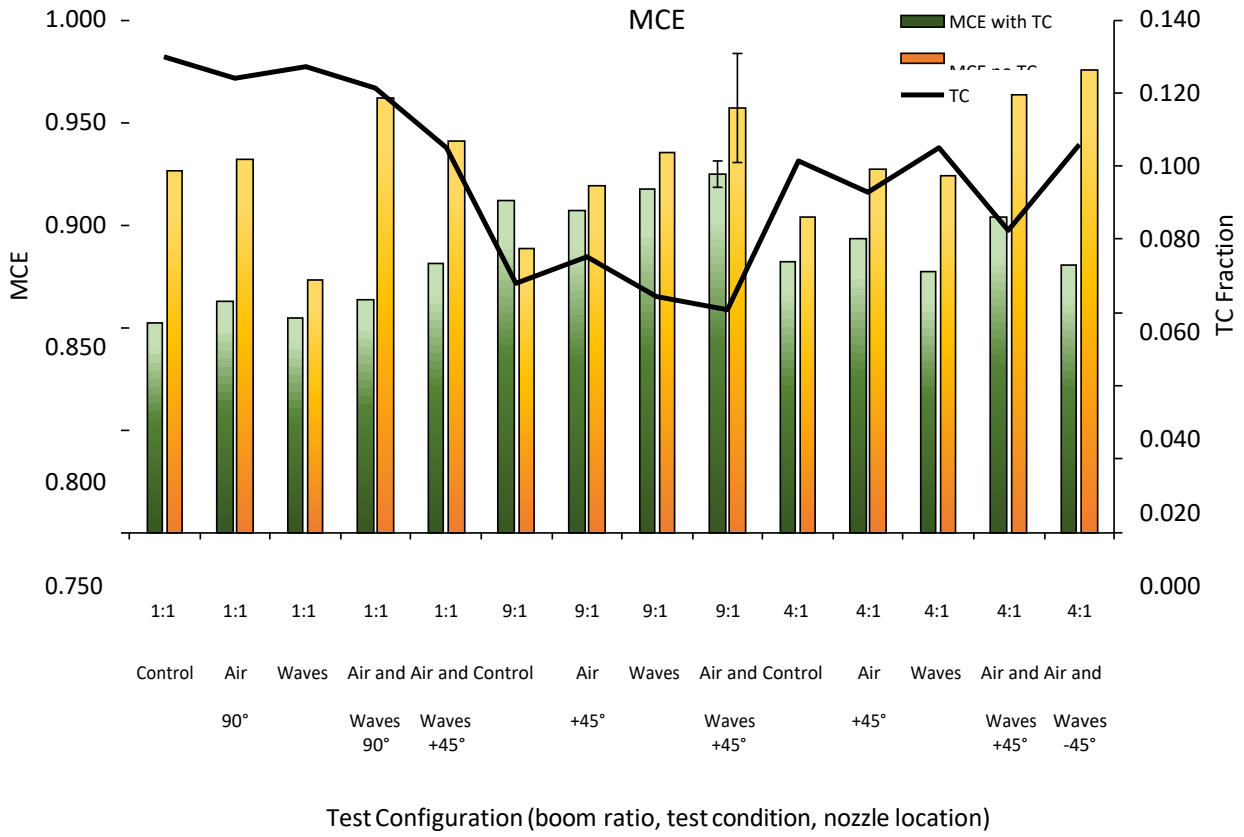

Figure 4-3. Modified combustion efficiency and TC in each of the test categories. MCE calculated with and without TC from particles. Error bar equal 1 Stand. Dev.

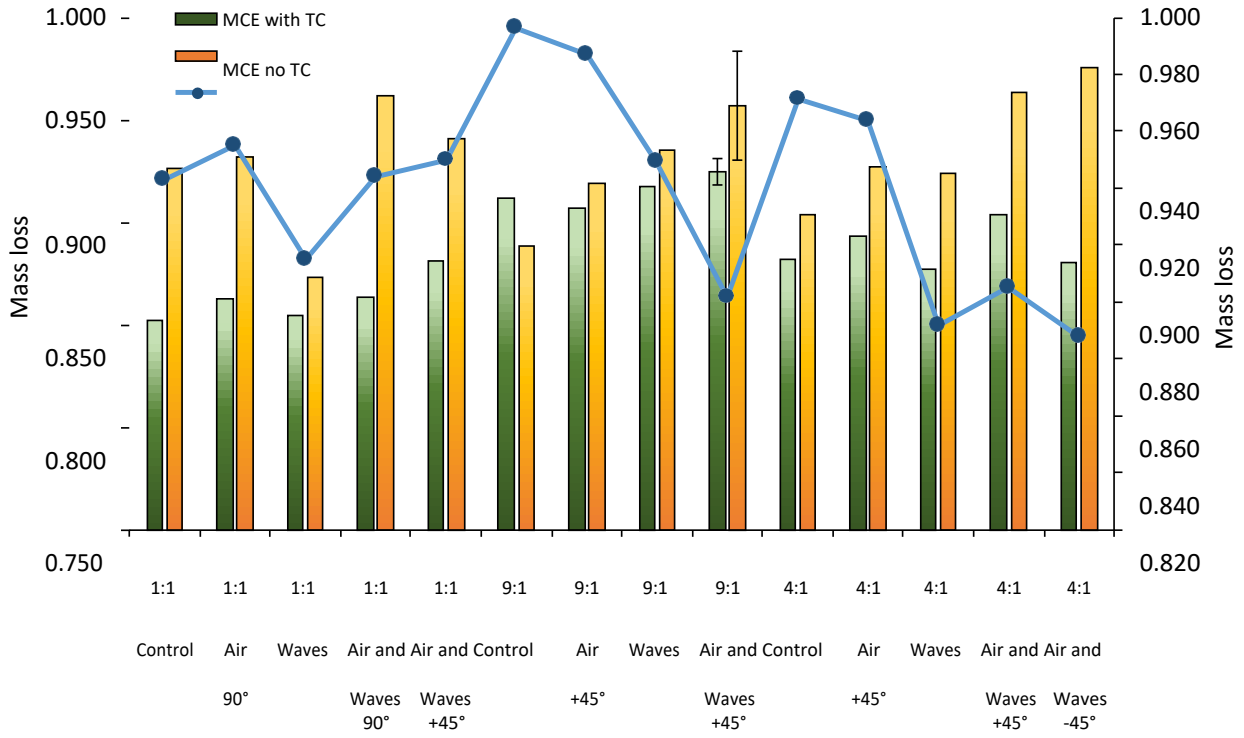

Figure 4-4. Modified combustion efficiency and oil mass loss in each of the test categories. MCE calculated with and without TC from particles. Error bar equal 1 Stand. Dev.

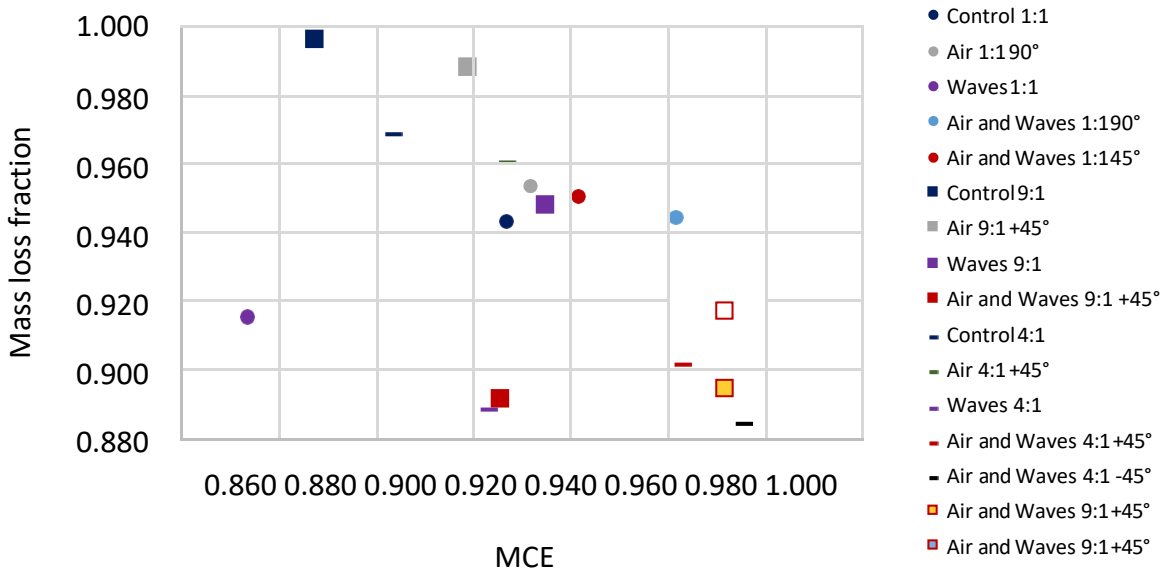

Figure 4-5. MCE (without TC from particles) versus mass loss for all tests.

The oil mass loss was compared with the MCE for all of the tests in Figure 4-5. The majority of the tests show that higher MCE values correspond to lower oil mass loss. This suggests a more efficient burn but of less oil.

The complete set of gas phase emission factors for each of the 16 tests are included in Table 4-2, along with a compilation of the one triplicate test condition and summary statistics for the whole test program.

Table 4-2. CO, CO_2, and CH_4 emission factors from each of the test configurations.

Test Condition	Configuration		CO_2	CO	CH_4	CO_2	CO	CH_4
	Boom Ratio	Nozzle Location	g/kg oil initial	g/kg oil initial	g/kg oil initial	g/kg oil consumed	g/kg oil consumed	g/kg oil consumed
Control	1:1	No nozzle	2261	30	2.2	2398	31	2.3
Air	1:1	90°	1933	19	1.0	2025	20	1.0
Waves	1:1	No nozzle	2468	33	1.8	2697	36	2.0
Air and Waves	1:1	90°	2690	30	0.6	2850	32	0.6
Air and Waves	1:1	+45°	2165	20	0.8	2279	22	0.8
Control	9:1	No nozzle	2676	39	2.0	2687	39	2.0
Air	9:1	+45°	2781	32	0.8	2818	32	0.8
Waves	9:1	No nozzle	2597	33	0.7	2737	34	0.8
Air and Waves	9:1	+45	2824	27	1.0	3166	30	1.1
Control	4:1	No nozzle	2635	11	1.8	2714	12	1.9
Air	4:1	+45°	2653	27	0.6	2752	28	0.7
Waves	4:1	No nozzle	2534	31	1.2	2841	34	1.3
Air and Waves	4:1	+45°	2555	24	0.6	2823	27	0.7
Air and Waves	4:1	-45°	2513	24	NS	2830	27	NS
Air and Waves	9:1	+45°	2634	25	0.7	2943	28	0.8
Air and Waves	9:1	+45°	2796	30	0.8	3045	32	0.8
Air and Waves (Burn #s 9,15,16)	9:1	+45° Avg.	2751	27	0.8	3052	30	0.9
		Stand. Dev.	102	2.2	0.15	112	2.1	0.17
		RSD (%)	3.7	8.3	17.6	3.7	6.8	18.6

NS = not sampled. CH_4 emission factor derived from SUMMA canister.

4.3 Oil Consumption and Modified Combustion Efficiency

Table 4-3 groups the burn runs by similar test condition and reports the average oil consumption (weight loss) and the MCE. The Control and Air (only) test conditions have higher oil weight loss than all other conditions at 97.00% and 96.87%. These values are considered indistinguishable given the data variance. The presence of Waves, regardless of Air or Boom Ratio condition, always lowers the oil weight (Figure 4-6). Higher Boom Ratios have higher MCE values than lower Boom Ratios (Table 4-7). This is true for oil weight loss but only in the absence of waves. This Boom Ratio effect is possibly due to more efficient air penetration into the flame zone due to the thinner oil slick configuration.

Table 4-3. Average Oil Weight Loss and MCE with TC by Test Condition

Test Condition	Wt loss, %	MCE, unitless
Control*	97.00	0.88
Waves*	91.87	0.88
Air and Waves*	91.31	0.90
Air*	96.87	0.89
All 1:1 Boom Ratio	94.14	0.86
All 4:1 Boom Ratio	92.40	0.89
All 9:1 Boom Ratio	93.95	0.92
Control, 1:1	94.30	0.85
Control, 4:1	97.10	0.88
Control, 9:1	99.60	0.91
Air, 1:1	95.50	0.86
Air, 4:1	96.40	0.89
Air, 9:1	98.70	0.91
Waves, 1:1	91.50	0.85
Waves, 4:1	89.20	0.88
Waves, 9:1	94.90	0.92
Air and Waves, 1:1[#]	94.70	0.87
Air and Waves, 4:1[#]	89.65	0.89
Air and Waves, 9:1[#]	90.17	0.92

*All three Boom Ratios

[#]All nozzle configurations

The oil mass loss and MCE results were further analyzed by grouping Control, Air, Waves, and Air and Waves tests from Table 4-3 and plotting them versus Boom Ratio in Figure 4-6. Higher Boom Ratios tended to result in higher oil weight loss unless waves were present. For MCE (with TC), however, higher Boom Ratios resulted in more efficient combustion under all groupings (Figure 4-7).

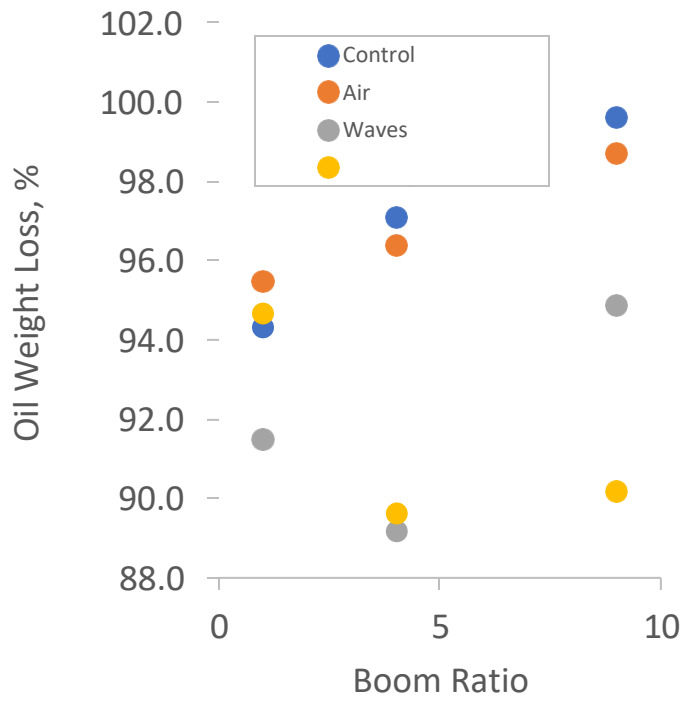

Figure 4-6. The effect of Boom Ratio on oil weight loss for major test conditions.

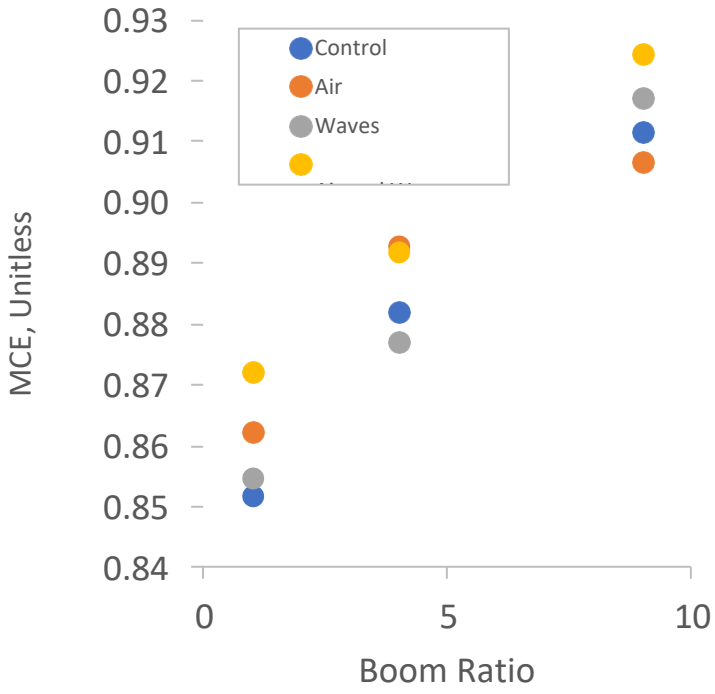

Figure 4-7. The effect of Boom Ratio on MCE with TC for major test conditions.

4.4 $PM_{2.5}$

Figure 4-8 indicates that the higher MCE (with TC) burn efficiencies are experienced with the Air and Waves, 4:1 and 9:1 boom configuration, $\pm 45^0$ scenarios. These higher burn efficiencies result in lower $PM_{2.5}$ emission factors. When these $PM_{2.5}$ emission factors are plotted in Figure 4-9 against the amount of oil consumed (mass loss from Table 4-1) the 9:1 ratio control and air (+45°) scenarios without waves results in the highest oil consumption.

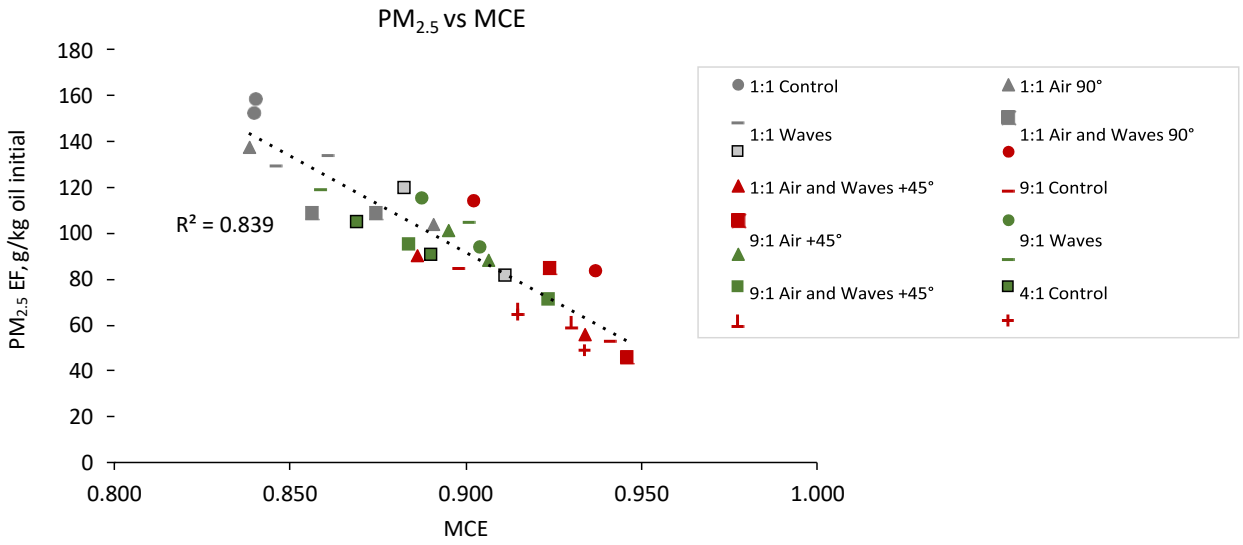

Figure 4-8. Change of $PM_{2.5}$ emission factor with modified combustion efficiency (MCE). Total carbon (TC) included in the emission factor and MCE calculations. Marker colors indicate boom configuration settings; Grey 1:1, Red 9:1, and Green 4:1. Two $PM_{2.5}$ samples per test, one in the first part and one in the second part of the burn.

When the $PM_{2.5}$ emission factor is compared with MCE (with TC) a clear relation exists, showing that higher MCE values lead to lower $PM_{2.5}$ emission factors. These are all associated with the higher (9:1) boom ratios (Figure 4-10). These same $PM_{2.5}$ values when plotted against Oil Mass loss, show no apparent trends (Figure 4-11).

Finally, the $PM_{2.5}$ emission factor data versus test condition are shown in Table 4-4

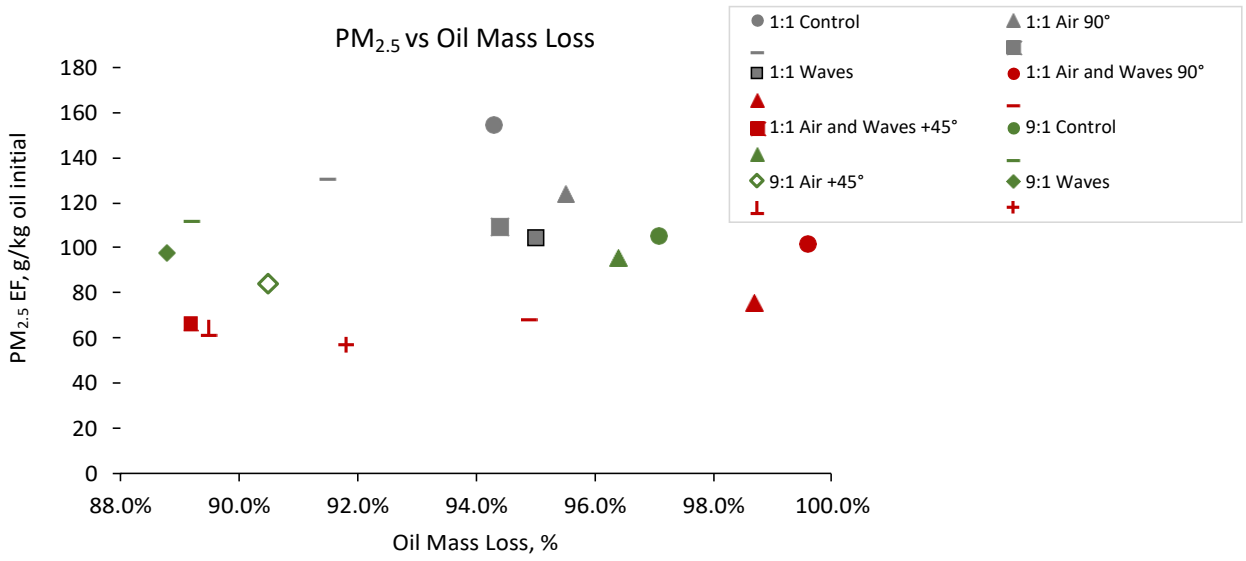

Figure 4-9. Change of $PM_{2.5}$ emission factor (g $PM_{2.5}$ per original oil mass) with oil mass loss. Marker colors indicate boom configuration settings; Grey 1:1, Red 9:1, and Green 4:1. $PM_{2.5}$ emission factor average of two samples per test.

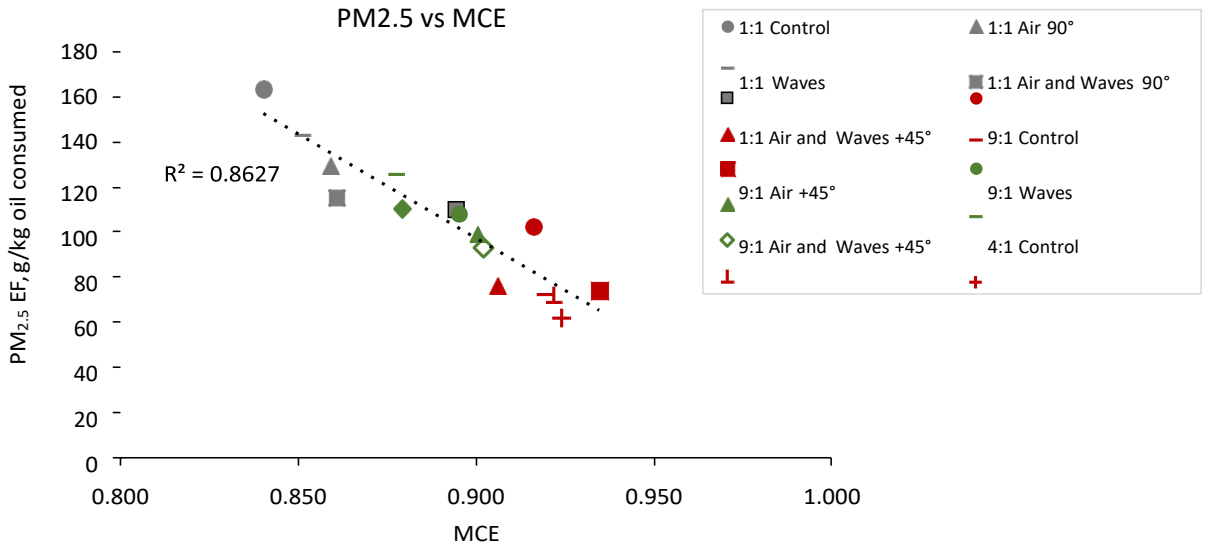

Figure 4-10. $PM_{2.5}$ emission factor (g $PM_{2.5}$ per oil mass lost) based on oil consumed versus oil mass loss. Marker colors indicate boom configuration settings; Grey 1:1, Red 9:1, and Green 4:1. $PM_{2.5}$ emission factor average of two samples per test.

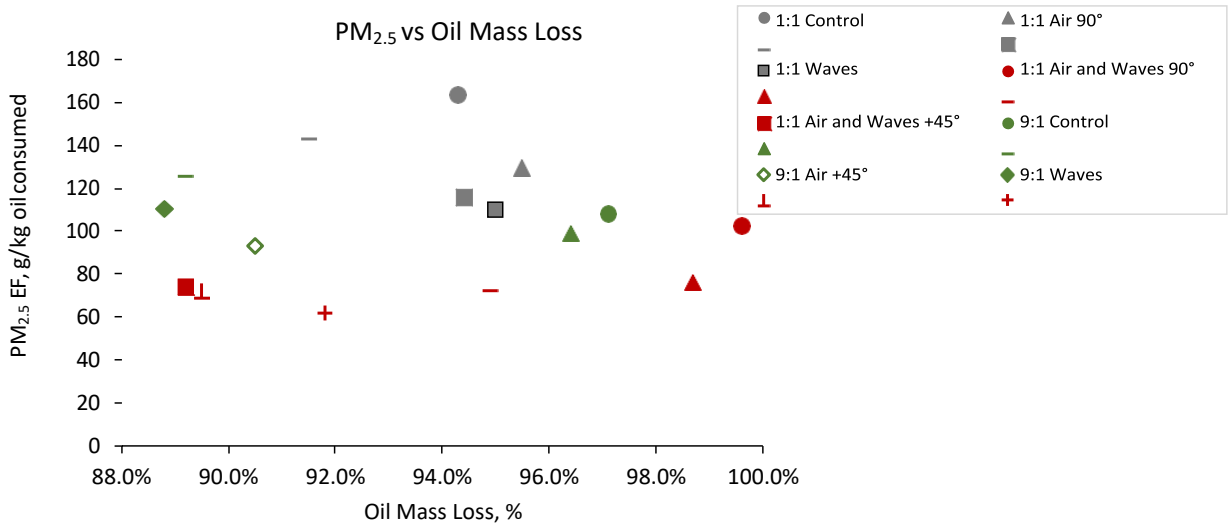

Figure 4-11. $PM_{2.5}$ emission factor based on oil consumed versus MCE. Grey 1:1, Red 9:1, and Green 4:1. $PM_{2.5}$ emission factor average of two samples per test.

Table 4-4. $PM_{2.5}$ emission factors from each test configuration.

Burn No.	Test Condition	Configuration		$PM_{2.5}$	$PM_{2.5}$
		Boom Ratio	Nozzle Location	g/kg oil initial	g/kg oil consumed
1	Control	1:1	No nozzle	154	163
2	Air	1:1	90°	124	130
3	Waves	1:1	No nozzle	134	146
4	Air and Waves	1:1	90°	109	115
5	Air and Waves	1:1	+45°	104	110
6	Control	9:1	No nozzle	102	102
7	Air	9:1	+45°	75	76
8	Waves	9:1	No nozzle	72	75
9	Air and Waves	9:1	+45°	66	74
10	Control	4:1	No nozzle	105	108
11	Air	4:1	+45°	95	99
12	Waves	4:1	No nozzle	115	129
13	Air and Waves	4:1	+45°	84	93
14	Air and Waves	4:1	-45°	98	110
15	Air and Waves	9:1	+45°	65	72
16	Air and Waves	9:1	+45°	57	62
9,15,16	Air and Waves	9:1	+45° Avg.	62	69
			Stand. Dev.	5.0	6.6
			RSD (%)	8.0	9.5

4.5 Total Carbon, Elemental Carbon and Organic Carbon

Analysis of the particles for OC, EC, and TC is reported in Table 4-5. The amount of TC to all carbon sampled was 9.3% ± 2.4 with an RSD of 31%. On average, 83% of all the particle mass was carbonaceous, and of this carbon, 86% by mass was EC. The fraction of the PM that was carbonaceous was generally constant and did not show any clear trends with the boom configuration, nozzle location, or waves. The average OC, EC, TC values of Burns 1-16 are 20.1, 75.7, and 90.8 g/kg oil consumed, respectively compared with values of 4.1, 49.0 and 53.0 g/kg oil consumed from 1 m^2 pan burns using the same sampling and analytical methods (Gullett et al., 2017). Additionally, the particles emitted from the much smaller pool size in Gullett et al. (2017) were 91% carbonaceous and of that were 92% EC. These value differences are likely due to the many distinctions between the test conditions including pool size, oil type, and oil thickness. Particle samples from the *in situ* burns during the Deepwater Horizon disaster showed 82% of the carbonaceous material was EC (Gullett et al. 2016), similar to the ratios observed in this work.

Table 4-5. Total carbon, elemental carbon, and organic carbon emission factors.

Burn No.	Test Condition	Configuration		OC	EC	TC	OC	EC	TC
		Boom Ratio	Nozzle Location	g/kg oil initial			g/kg oil consumed		
1	Control	1:1	No nozzle	31.9	97.1	130.2	33.9	103.0	138.0
2	Air	1:1	90°	23.6	102.3	114.3	24.7	107.1	119.7
3	Waves	1:1	No nozzle	22.0	103.2	122.1	24.1	112.8	133.5
4	Air and Waves	1:1	90°	67.3	54.1	115.2	71.2	57.3	122.0
5	Air and Waves	1:1	+45°	35.4	70.3	93.3	37.3	74.0	98.2
6	Control	9:1	No nozzle	12.3	52.2	58.4	12.4	52.5	58.7
7	Air	9:1	+45°	8.6	63.5	64.7	8.7	64.4	65.6
8	Waves	9:1	No nozzle	6.7	51.9	54.8	7.0	54.7	57.7
9	Air and Waves	9:1	+45°	5.3	42.4	45.8	6.0	47.6	51.3
10	Control	4:1	No nozzle	16.7	81.5	91.7	17.2	83.9	94.5
11	Air	4:1	+45°	12.6	75.1	84.1	13.0	77.9	87.2
12	Waves	4:1	No nozzle	22.3	79.2	96.1	25.1	88.8	107.7
13	Air and Waves	4:1	+45°	6.8	71.3	72.7	7.6	78.8	80.4
14	Air and Waves	4:1	-45°	14.2	86.6	99.3	16.0	97.5	111.9
15	Air and Waves	9:1	+45°	8.0	52.1	58.8	9.0	58.2	65.7
16	Air and Waves	9:1	+45°	8.0	48.9	55.2	8.7	53.3	60.1
9,15,16	Air and Waves	9:1	+45° Avg.	10	64	71	8	53	59
			Stand. Dev.	4.0	20.0	24.7	1.7	5.3	7.3
			RSD (%)	41.5	31.5	34.8	21.0	10.0	12.3

4.6 Particle Size Characterization, Black Carbon, and Optical Measurements

The particle size distributions for each burn were approximately constant during the burn; a typical average distribution is shown in Figure 4-12 below and the complete data results are shown in Table 4-6. The number concentration was dominated by the smallest particles (< 100 nm). The total particle number concentration (PN), geometric standard deviation (σ_g), and median diameter (d_g) showed a slight decreasing trend with increasing MCE, i.e., less particles, smaller median size, and a more narrow distribution were emitted as the MCE increased (Figure 4-13). However, the correlations with MCE were low (PN $r^2 = 0.095$, d_g $r^2 = 0.059$, $\sigma_g = 0.15$).

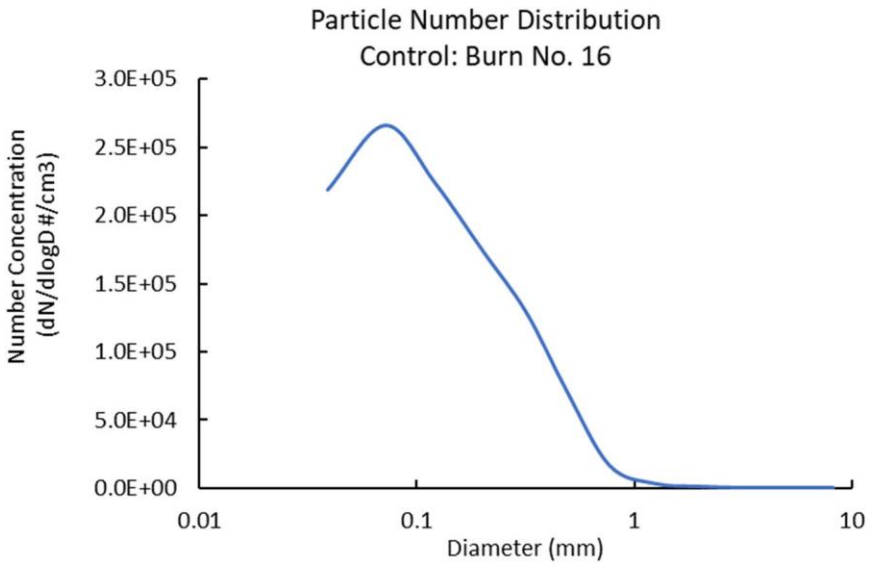

Figure 4-12. Particle number distribution for Burn No. 16; Air and Waves 9:1 Boom Ratio and Nozzle Location +45°.

Table 4-6. Particle number (PN), median diameter (d_g) and geometric standard deviation (σ_g).

Burn No.	Test Condition	Configuration		PN	PN	Dg	σg
		Boom Ratio	Nozzle Location	g/kg oil initial	g/kg oil consumed	(nm)	
1	Control	1:1	No nozzle	3.34×10^{16}	2.21×10^{16}	99	3.08
2	Air	1:1	90°	1.26×10^{16}	1.03×10^{16}	135	3.01
3	Waves	1:1	No nozzle	$2.03.\times10^{16}$	1.96×10^{16}	132	2.90
4	Air and Waves	1:1	90°				
5	Air and Waves	1:1	+45°	1.50×10^{16}	1.41×10^{16}	126	2.74

6	Control	9:1	No nozzle		2.02×10^{16}	1.91×10^{16}	112	2.74
7	Air	9:1	+45°		2.06×10^{16}	1.64×10^{16}	115	2.79
8	Waves	9:1	No nozzle		1.62×10^{16}	1.58×10^{16}	145	2.61
9	Air and Waves	9:1	+45°		1.43×10^{16}	1.57×10^{16}	126	2.80
10	Control	4:1	No nozzle		2.50×10^{16}	2.82×10^{16}	78	2.90
11	Air	4:1	+45°		2.6×10^{16}	2.93×10^{16}	81	2.93
12	Waves	4:1	No nozzle		1.81×10^{16}	2.04×10^{16}	92	3.05
13	Air and Waves	4:1	+45°		2.08×10^{16}	2.25×10^{16}	90	3.00
14	Air and Waves	4:1	-45°		1.19×10^{16}	1.22×10^{16}	111	3.57
15	Air and Waves	9:1	+45°		2.14×10^{16}	2.31×10^{16}	74	3.24
16	Air and Waves	9:1	+45°		1.71×10^{16}	1.56×10^{16}	74	3.22
9,15,16	Air and Waves	9:1	+45°	Avg.	1.65×10^{16}	1.70×10^{16}	110	3.14
				Stand. Dev.	4.80×10^{15}	5.55×10^{15}	36	0.49
				RSD (%)	29	32.6	33	15.7

The continuous $PM_{2.5}$ concentration was strongly correlated with the filter based $PM_{2.5}$ (r^2 = 0.91). The BC (full data shown in

Table 4-7) was also moderately correlated with the elemental carbon concentration (r^2 = 0.48). The poorer correlation may indicate varying optical properties as BC is an optical-based measurement and EC is a thermal-based measurement. The BC measurements at five wavelengths was used to calculate the absorption angstrom exponent (AAE), which can be used to distinguish among combustion sources. The AAE was less than one, which has been observed before from crude oil burns, indicating that the particles emitted from oil burning have larger spherules than other combustion sources like diesel exhaust. The AAE increases with MCE, showing that the particle structure changes as the combustion improves. This change in AAE trends with the MCE throughout the burn as shown in the Figure 4-13.

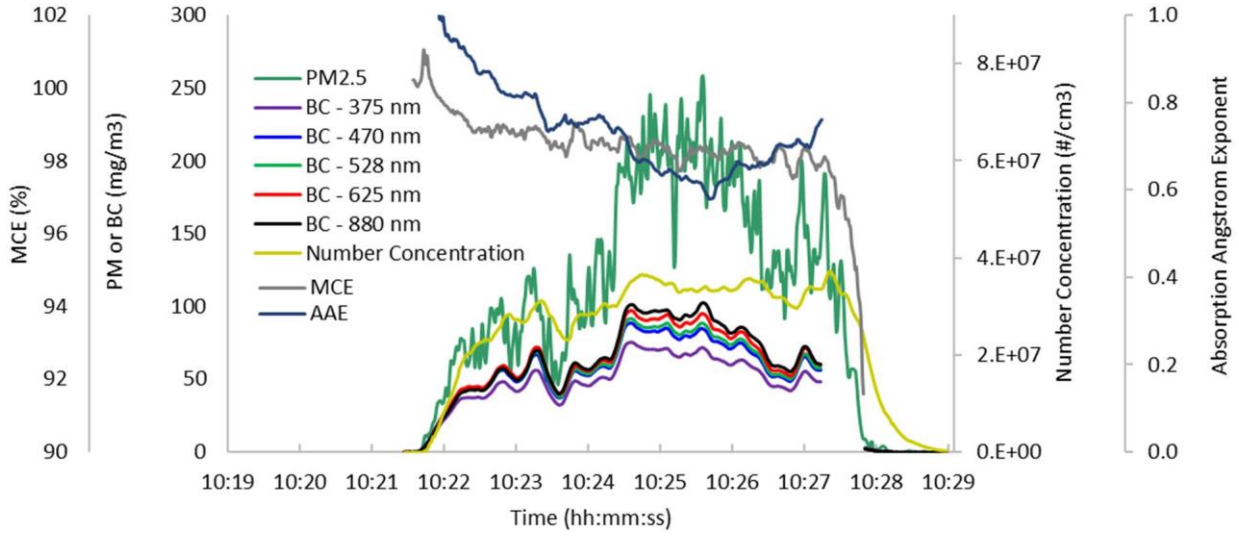

Figure 4-13. A typical $PM_{2.5}$, black carbon (BC), and number concentration trace (data frequency 1 second) with corresponding MCE (10 seconds moving average) and absorption angstrom exponent during air and waves 9:1 +45°, Burn No. 16., MCE calculated using CO_2 and CO.

Table 4-7. Black carbon (BC) emission factors and the absorption angstrom exponent (AAE).

Burn No.	Test Condition	Configuration		BC (880 nm) g/kg oil initial	BC (880 nm) g/kg oil consumed	AAE
		Boom Ratio	Nozzle Location			
1	Control	1:1	No nozzle	165.1	152.9	0.57
2	Air	1:1	90°	115.6	89.4	0.37
3	Waves	1:1	No nozzle	128.6	123.5	0.44
4	Air and Waves	1:1	90°			
5	Air and Waves	1:1	+45°	102.7	96.2	0.56
6	Control	9:1	No nozzle	67.7	55.5	0.78
7	Air	9:1	+45°	66.3	49.0	0.69
8	Waves	9:1	No nozzle	62.6	52.2	0.83
9	Air and Waves	9:1	+45°	46.0	45.5	0.79
10	Control	4:1	No nozzle	70.2	66.3	0.63
11	Air	4:1	+45°	62.8	65.0	0.59
12	Waves	4:1	No nozzle	54.9	55.7	0.67
13	Air and Waves	4:1	+45°	52.6	51.5	0.65
14	Air and Waves	4:1	-45°	41.2	42.0	0.42
15	Air and Waves	9:1	+45°	47.0	48.6	0.85

16	Air and Waves	9:1	+45°		35.7	32.0	0.79
9,15,16	Air and Waves	9:1	+45°	Avg.	50.3	47.6	0.70
				Stand. Dev.	11.1	5.2	0.25
				RSD (%)	22.1	10.9	35.03

4.7 Volatile Organic Compounds

VOC emission factors are reported in Table 4-8. Non-detectable VOCs (those VOCs that were analyzed by not detected are shown in carbonyls in

1,2-Dichloro-1,1,2,2-tetrafluoroethane	Vinyl Chloride
Bromomethane	Chloroethane
2-Propanol (Isopropyl Alcohol)	1,1-Dichloroethene
3-Chloro-1-propene (Allyl Chloride)	trans-1,2-Dichloroethene
1,1-Dichloroethane	Methyl tert-Butyl Ether
Vinyl Acetate	cis-1,2-Dichloroethene
Chloroform	1,2-Dichloroethane
1,1,1-Trichloroethane	1,2-Dichloropropane
Bromodichloromethane	Trichloroethene
1,4-Dioxane	Methyl Methacrylate
cis-1,3-Dichloropropene	4-Methyl-2-pentanone
trans-1,3-Dichloropropene	1,1,2-Trichloroethane
2-Hexanone	Dibromochloromethane
1,2-Dibromoethane	Tetrachloroethene
Chlorobenzene	Bromoform
1,1,2,2-Tetrachloroethane	Benzyl Chloride
1,3-Dichlorobenzene	1,4-Dichlorobenzene
1,2-Dichlorobenzene	1,2-Dibromo-3-
1,2,4-Trichlorobenzene	Hexachlorobutadiene

Table 4-10. Volatile carbonyl emission factors are included within Table 4-10. Emission factors, particularly for VOCs, are often proportional to the MCE, as shown for benzene in Figure 4-14, below. Tests on a 1 m^2 oil slick resulted in a average benzene emission factor of 1,120 mg/kg oil initial at an MCE of 0.978 (Gullett et al., 2017), a value higher than observed here and likely due to the difference in oil and combustion conditions.

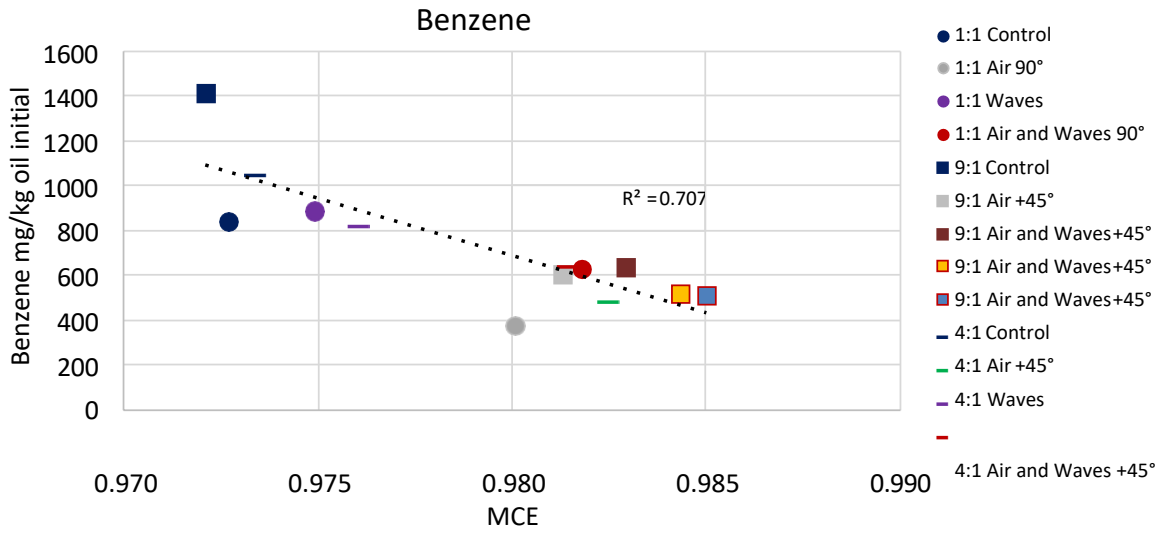

Figure 4-14. MCE versus benzene emission factor for all tests and configurations.

Table 4-8. VOC emission factors in mg/kg initial oil. Detected compounds only.

	1:1 C	1:1 A/90	1:1 W	1:1 AW/90	1:1 AW/+45	9:1 C	9:1 A/+45	9:1 W	9:1 AW/+45	4:1 C	4:1 A/+45	4:1 W	4:1 AW/+45	9:1 AW/+45	9:1 AW/+45
VOC	**mg/kg initial oil**														
Propene	15.23	9.06	21.96	34.34	33.31	44.48	58.19	1.79	101.15	28.17	42.01	31.25	50.08	64.35	70.62
Dichlorodifluoromethane (CFC 12)	ND	ND	ND	2.79	ND	ND	ND	1.33	0.17	0.22	ND	0.30	ND	ND	ND
Chloromethane	0.83	0.59	ND	ND	0.58	1.28	0.77	0.16	0.57	ND	0.48	0.67	0.67	0.47	0.46
1,3-Butadiene	9.46	3.84	11.16	14.35	14.44	24.37	25.33	0.84	40.57	13.11	16.90	14.80	20.72	23.88	28.50
Ethanol	ND	ND	ND	ND	ND	ND	2.39	6.03	1.94	ND	ND	ND	ND	ND	2.77
Acetonitrile	2.00	2.25	ND	ND	5.42	8.46	3.80	3.14	ND	15.29	8.45	12.82	31.08	ND	ND
Acrolein	6.35	14.97	16.74	19.42	24.07	46.17	21.11	1.45	9.30	37.14	1.77	30.58	8.80	24.87	7.70
Acetone	ND	5.99	ND	ND	24.31	ND	7.18	7.84	11.16	ND	ND	10.06	8.93	ND	ND
Trichlorofluoromethane	ND	ND	ND	0.17	ND	0.13	ND	0.72	0.17	ND	ND	0.10	ND	ND	ND
Acrylonitrile	ND	1.12	ND	ND	ND	ND	ND	ND	ND	ND	ND	ND	ND	ND	ND
Methylene Chloride	ND	ND	ND	ND	0.96	1.67	0.63	5.55	0.68	1.75	1.54	3.06	4.53	6.57	4.70
Trichlorotrifluoroethane	ND	ND	ND	ND	ND	ND	ND	0.25	ND	ND	ND	ND	ND	ND	ND
Carbon Disulfide	31.70	10.73	37.35	4.20	5.14	31.38	4.83	ND	7.83	24.38	3.36	18.22	4.62	2.46	0.90
2-Butanone (MEK)	ND	0.47	2.47	0.68	ND	ND	0.71	0.25	1.19	ND	ND	1.19	0.83	ND	1.24
Ethyl Acetate	ND	ND	ND	ND	ND	ND	ND	8.93	ND	ND	ND	13.81	ND	ND	ND
n-Hexane	5.25	4.98	45.55	62.32	19.04	8.88	6.91	2.44	7.54	3.73	9.08	11.66	16.60	12.75	36.84
Tetrahydrofuran (THF)	ND	ND	ND	ND	ND	16.67	2.96	ND	ND	1.09	ND	ND	ND	ND	ND
Benzene	834.65	374.05	881.23	624.48	589.34	1410.38	597.97	28.57	633.63	1092.18	529.93	867.81	685.86	517.04	508.19
Carbon Tetrachloride	ND	ND	ND	ND	ND	ND	ND	0.23	ND	ND	ND	ND	ND	ND	ND
Cyclohexane	3.01	2.43	21.20	27.86	9.75	4.36	3.80	0.96	4.06	2.48	4.84	6.91	9.71	7.36	16.95
n-Heptane	5.46	3.65	34.59	39.68	16.85	6.80	5.49	1.45	5.75	4.37	7.53	10.85	15.54	11.94	25.42
Toluene	34.69	13.25	59.32	76.96	48.33	87.42	68.38	4.66	81.27	42.36	42.38	45.54	59.77	76.77	76.39
n-Butyl Acetate	ND	ND	ND	ND	ND	ND	ND	0.14	ND	ND	ND	ND	ND	ND	ND
n-Octane	3.79	1.87	15.62	16.88	10.35	3.85	3.38	0.66	4.06	3.93	5.15	8.29	12.82	8.85	13.10
Ethylbenzene	2.78	1.40	4.69	4.98	4.09	4.62	3.87	0.36	5.07	3.06	3.30	3.65	5.70	4.97	6.09
m,p-Xylenes	5.98	2.87	10.46	11.63	9.95	7.53	8.99	0.69	12.48	6.10	7.51	8.75	15.24	12.70	15.23
Styrene	37.85	26.20	21.20	26.17	20.46	46.17	37.30	1.93	43.95	44.42	23.05	27.62	31.08	29.85	31.58

o-Xylene	3.67	1.50	3.35	3.88	3.37	3.33	3.24	0.34	4.39	2.62	3.00	3.35	5.70	4.38	5.16
n-Nonane	2.00	1.03	5.47	5.99	4.57	2.18	2.25	0.35	3.13	3.57	3.53	6.41	10.36	5.57	6.09
Cumene	ND	ND	ND	ND	ND	ND	ND	ND	ND	ND	ND	ND	0.66	ND	0.49
alpha-Pinene	ND	ND	ND	ND	ND	ND	ND	0.11	ND	ND	ND	ND	ND	0.34	ND
n-Propylbenzene	ND	ND	ND	0.65	ND	ND	ND	ND	ND	ND	0.52	0.87	1.42	0.76	0.92
4-Ethyltoluene	ND	ND	ND	ND	ND	ND	ND	ND	0.68	ND	ND	ND	1.20	0.77	0.85
1,3,5-Trimethylbenzene	2.00	0.77	ND	0.64	ND	ND	0.77	ND	0.93	0.95	0.70	1.09	1.68	0.97	1.00
1,2,4-Trimethylbenzene	4.35	1.69	1.91	1.53	1.45	1.16	1.69	0.12	2.29	2.34	1.77	2.67	4.28	2.50	2.39
d-Limonene	ND	ND	ND	ND	ND	ND	ND	1.01	ND	ND	ND	ND	ND	ND	ND
Naphthalene	278.11	88.72	211.80	236.22	192.32	230.60	232.10	11.34	194.23	342.14	161.20	285.89	181.02	168.93	130.80

Table 4-9. Non-detectable VOCs in emissions from every test sample.

1,2-Dichloro-1,1,2,2-tetrafluoroethane	Vinyl Chloride
Bromomethane	Chloroethane
2-Propanol (Isopropyl Alcohol)	1,1-Dichloroethene
3-Chloro-1-propene (Allyl Chloride)	trans-1,2-Dichloroethene
1,1-Dichloroethane	Methyl tert-Butyl Ether
Vinyl Acetate	cis-1,2-Dichloroethene
Chloroform	1,2-Dichloroethane
1,1,1-Trichloroethane	1,2-Dichloropropane
Bromodichloromethane	Trichloroethene
1,4-Dioxane	Methyl Methacrylate
cis-1,3-Dichloropropene	4-Methyl-2-pentanone
trans-1,3-Dichloropropene	1,1,2-Trichloroethane
2-Hexanone	Dibromochloromethane
1,2-Dibromoethane	Tetrachloroethene
Chlorobenzene	Bromoform
1,1,2,2-Tetrachloroethane	Benzyl Chloride
1,3-Dichlorobenzene	1,4-Dichlorobenzene
1,2-Dichlorobenzene	1,2-Dibromo-3-
1,2,4-Trichlorobenzene	Hexachlorobutadiene

Table 4-10. Carbonyl emission factors in mg/kg initial oil.

	1:1 AW/90	**1:1 AW/+45**	**9:1 C**	**9:1 A/+45**	**9:1 W**	**9:1 AW/+45**	**4:1 C**	**4:1 A/+45**	**4:1 W**	**4:1 AW/+45**
Carbonyl	**mg/kg initial oil**									
Formaldehyde	193	344	390	173	160	222	216	214	208	195
Acetaldehyde	73	147	212	82	68	100	72	91	86	93
Acrolein	ND	ND	ND	ND	ND	ND	ND	ND	ND	ND
Acetone	146	169	607	107	109	179	126	107	107	100
Propionaldehyde	36	ND	49	ND	ND	40	36	26	ND	16
Crotonaldehyde	ND	ND	ND	ND	ND	ND	ND	ND	ND	ND
n-Butyraldehyde	ND	ND	ND	ND	ND	ND	18	20	20	27
Benzaldehyde	45	31	174	35	80	101	60	67	76	57
Isovaleraldehyde	26	ND	ND	16	39	ND	43	44	77	55
Valeraldehyde	ND	ND	149	ND	ND	ND	ND	ND	31	42
o-Tolualdehyde	ND	ND	241	ND	ND	ND	ND	ND	44	ND
m&p-Tolualdehyde	ND	ND	ND	ND	ND	ND	ND	ND	ND	ND
Hexaldehyde	718	1008	2081	1531	2479	ND	ND	ND	ND	ND
2,5-Dimethylbenzaldehyde	ND	ND	ND	ND	ND	1031	401	398	877	438

4.8 Polyaromatic Hydrocarbons

The lowest PAH emission factor was derived from the test configuration with a Boom Ratio of 1:1 with added air (Table 4-11 and Table 4-12, and Figure 4-15). Three replicate samples were collected for one of the test figurations (Boom Ratio 9:1, air and waves +45°) which showed a relative standard deviation of 35%. PAH_{16} values of 697 mg/kg oil initial obtained during testing of 1 m^2 oil slicks (Gullett et al., 2017) are much higher than those found here likely due to different oil and test conditions.

Table 4-11. PAH emission factors in mg/kg initial oil.

	Boom Ratio 1:1					Boom Ratio 4:1			
Targets	Control	Air	Waves	Air and Waves 90°	Air and Waves +45°	Control	Air +45°	Waves	Air and Waves +45°
	mg/kg initial oil					mg/kg initial oil			
Naphthalene	127.25	50.70	189.20	44.93	87.05	98.33	78.40	97.73	99.49
Acenaphthylene	40.41	17.36	60.66	17.26	26.66	33.55	26.36	32.27	30.86
Acenaphthene(CCC)	0.30	0.20	0.44	0.13	0.25	0.23	0.26	0.15	0.21
Fluorene	4.38	2.11	6.41	1.78	3.02	3.65	3.39	2.84	3.13
Phenanthrene	33.64	14.74	46.93	11.83	21.20	24.32	20.55	19.41	18.36
Anthracene	4.42	1.94	6.43	1.52	2.83	3.75	3.17	3.05	2.97
Fluoranthene(CCC)	24.82	10.66	35.99	8.80	15.00	17.64	14.08	18.07	16.85
Pyrene	23.49	10.46	34.43	8.49	14.35	16.80	13.58	17.26	16.38
Benzo(a)anthracene	3.86	1.42	5.80	1.08	2.33	2.74	2.59	3.11	2.94
Chrysene	4.37	1.57	6.68	1.27	2.86	3.23	2.89	3.60	3.33
Benzo(b)fluoranthene	4.11	1.53	6.14	1.25	2.54	2.87	2.33	2.98	2.85
Benzo(k)fluoranthene	5.33	2.24	8.66	1.65	3.35	4.06	3.54	4.53	4.33
Benzo(a)pyrene(CCC)	6.35	2.56	9.39	1.94	3.81	4.65	3.57	4.68	4.55
Indeno(1,2,3-cd)pyrene	6.70	2.91	9.83	2.16	4.04	4.82	3.80	5.02	4.65
Dibenz(a,h)anthracene	0.44	0.17	0.63	0.11	0.28	0.30	0.26	0.34	0.31
Benzo(ghi)perylene	5.57	2.68	8.26	2.04	3.37	4.11	3.07	4.12	3.79
SUM 16-EPA PAH	295.45	123.25	435.91	106.25	192.94	225.04	181.84	219.18	215.02

Table 4-12. PAH emission factors in mg/kg initial oil.

			Boom ratio 9:1			
				Air and Waves +45°		
	Control	Air +45°	Waves	Avg.	Stand. Dev.	RSD
Targets			**mg/kg initial oil**			%
Naphthalene	208.27	159.25	203.01	127.18	43.52	34
Acenaphthylene	65.02	52.21	66.26	41.66	13.79	33
Acenaphthene(CCC)	0.63	0.56	0.54	0.47	0.23	48
Fluorene	8.85	8.22	9.83	5.96	2.65	45
Phenanthrene	43.54	37.37	41.12	20.29	11.93	59
Anthracene	7.69	6.90	7.70	3.99	2.27	57
Fluoranthene(CCC)	31.44	24.17	28.71	17.52	4.96	28
Pyrene	31.28	24.67	28.71	17.66	4.90	28
Benzo(a)anthracene	7.61	5.46	6.60	4.23	1.50	35
Chrysene	8.16	5.73	7.11	4.66	1.78	38
Benzo(b)fluoranthene	6.26	4.15	5.43	3.34	1.24	37
Benzo(k)fluoranthene	9.10	6.48	7.88	4.87	1.57	32
Benzo(a)pyrene(CCC)	10.59	8.32	8.67	5.22	1.74	33
Indeno(1,2,3-cd)pyrene	9.56	6.83	7.89	5.03	1.55	31
Dibenz(a,h)anthracene	0.81	0.53	0.67	0.41	0.15	36
Benzo(ghi)perylene	7.38	5.40	6.12	3.98	1.16	29
SUM 16-EPA PAH	456.19	356.25	436.25	266.45	92.22	35

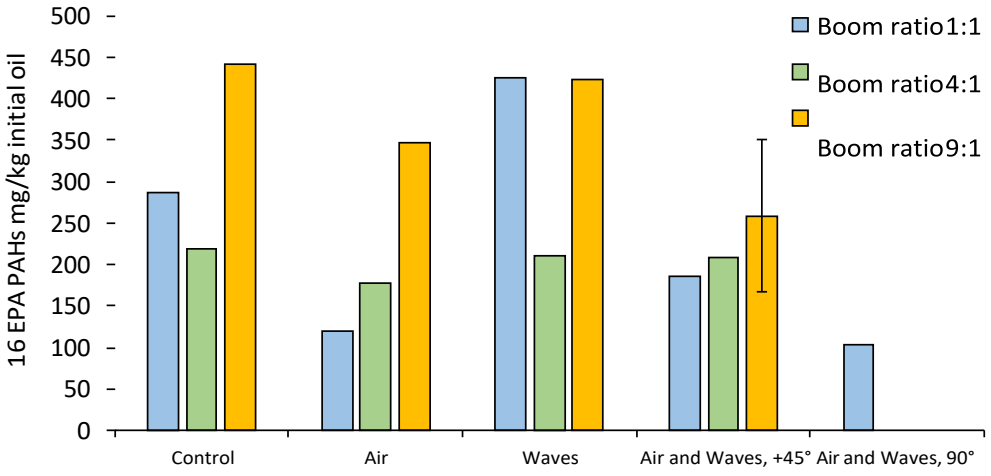

Figure 4-15. PAH emission factors for the different test configurations.

4.9 Polychlorinated Dibenzodioxins and Furans

The PCDD/PCDF emission factors for the control configurations were four to seven times higher than the other three configurations (air, waves, air and waves), even when factoring in the non-detected congeners or setting the non-detected congeners at the limit of detection (LOD) as shown in Table 4-13 and Figures 4-16 and 4-17. This high, average control value emission factor is due to a single, two-burn sample; the one other sample was a single burn and was in line with the rest of the tests. No reason for this large variance is apparent. The average control value is, however, consistent with the PCDD/PCDF reported earlier in Aurell et al., 2010 (Aurell and Gullett, 2010).

PCDDs/PCDFs were collected from the same configuration during multiple burns resulting in a single or duplicate sample for each of the test configurations. Not all seventeen TEQ congeners were detected in all samples. Fifteen and sixteen of seventeen TEQ congeners were detected in the control samples, sixteen of seventeen were detected in the air, and waves samples, while twelve to fifteen congeners were detected in the samples collected from the air and waves configurations.

Table 4-13. PCDD/PCDF emission factors.

Test Configuration	Burn No.	PCDD/PCDF Total ng/kg initial oil	PCDD/PCDF TEQ Total ND = 0 ng TEQ/kg initial oil	PCDD/PCDF TEQ Total ND = LOD ng TEQ/kg initial oil
Control 1:1	1	28.39	1.87	1.92
Control 4:1, 9:1	6, 10	289.78	3.09	3.25
Air 1:1 90°, 4:1 +45°, 9:1 +45°	2,7,11	30.44	0.64	0.70
Waves 1:1, 4:1, 9:1	3,8,12	36.19	0.69	0.76
Air and Waves 1:1 90°, 1:1 +45°, 4:1 +45°, 9:1 +45°	4,5,9,13	18.14	0.35	0.42
Air and Waves 4:1 -45°	14	8.78	0.20	0.41
Air and Waves 9:1 +45°	15,16	40.87	0.87	0.95

ND = Not detected. LOD = Limit of detection.

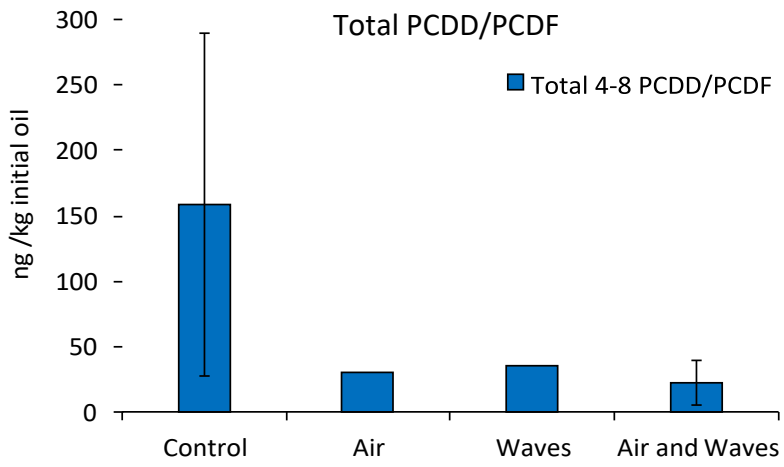

Figure 4-16. Total PCDD/PCDF emission factors.

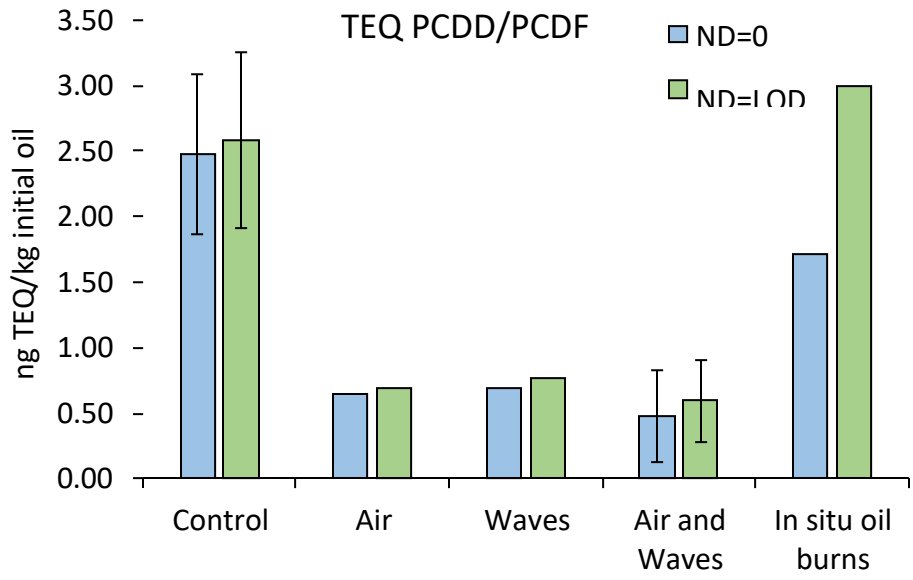

Figure 4-17. Comparison of PCDD/PCDF TEQ emission factor with Deepwater Horizon in situ oil burn data (Aurell et al., 2010 (Aurell and Gullett, 2010)).

4.10 Residue Analysis

As detailed in Chapter 3.11, post burn residue samples were collected and analyzed for monoaromatic hydrocarbons (i.e., alkanes, PAHs, total petroleum hydrocarbons, and BTEX).

4.10.1 Alkanes

- Total alkanes (sum of C10-C35 normal aliphatics, and branched alkanes [pristine and phytane]) ranged from 4.8 µg/mg of residue to 30.5 µg/mg for the various test

configurations as seen in as seen in Figure 4-18.

- On average, 18.5 µg/mg of alkanes remained in the burn residue. The raw crude oil contained 46.7 µg/mg total alkanes (Table 4-15), indicating a 60% reduction in the post-burn concentration, averaging across all treatments.
- The lighter, lower-boiling-point alkanes were preferentially removed, and the heavier, higher-boiling-point components were concentrated in the post-burn samples. In comparison to the raw crude oil, alkanes with 10 to 18 carbons (denoted as nC10-18 in Table 4-15) decreased by 83% on average post-burn, while nC19-27 decreased by 20% and the nC28-35 content remained almost constant.
- Boom Ratio of 4:1 had the highest alkanes concentration in the residues (22 ± 9 µg/mg, n=5) followed by 9:1 (20 ± 5 µg/mg, n=6) and 1:1 (13 ± 5 µg/mg, n=5).
- Waves treatment had the highest alkane residual concentration (23 ± 7 µg/mg, n=3) followed by Air and Waves (22 ± 6 µg/mg, n=7), Air (13 ± 0.4 µg/mg, n=3), and Control (10 ± 5 µg/mg, n=3)
- Nozzle Location of -45° had the highest alkane residual concentration (30 µg/mg; n=1), followed by +45° (20 ± 6 µg/mg, n=7), no nozzle (17 ± 9 µg/mg, n=6), and 90° (14 ± 0.1 µg/mg, n=2).

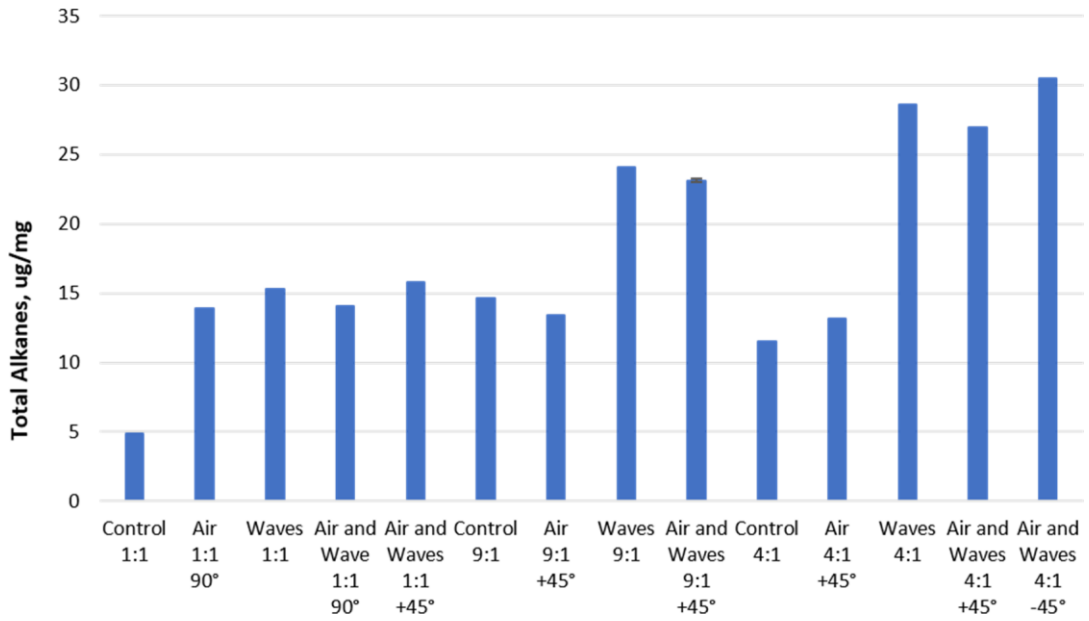

Figure 4-18. Residual total alkanes for each test configuration.

4.10.2 PAHs

- Total PAHs (sum of C0-C4 naphthalenes, C0-C4 phenanthrenes, C0-C3 fluorenes, C0-C4 dibenzothiophenes, C0-C4 naptha benzothiophenes, C0-C4 pyrenes and C0-C4 chrysenes) ranged from 2.1 µg/mg to 13.1 µg/mg for the various test configurations (Figure 4-19).
- The raw crude oil pre-burn Control contained 16.9 µg/mg total PAHs (Table 4-16). A 50% reduction in total PAHs was observed post burn on average. The more volatile 2-ring PAH compounds decreased by 74%, while the 3-ring compounds decreased by 30% and no significant change was observed with the 4-ring compounds concentration.

- Boom Ratio of 4:1 had the highest residual PAHs concentration (9.8 ± 3.6 µg/mg, n=5) followed by 9:1 (9.0 ± 2.1 µg/mg, n=6) and 1:1 (6.1 ± 2.3 µg/mg, n=5).
- Waves treatment had the highest total PAHs concentration (10.2 ± 2.6 µg/mg, n=3) followed by Air and Waves (10.0 ± 2.1 µg/mg, n=7), Air (6.3 ± 0.2 µg/mg, n=3) and Control (4.7 ± 2.3 µg/mg, n=3)
- Nozzle Location of -45° had the highest total PAHs concentration (13.1 µg/mg; n=1), followed by +45° (9.0 ± 2.2 µg/mg, n=7), no nozzle (7.4 ± 3.7 µg/mg, n=6) and 90° (6.7 ± 0.4 µg/mg, n=2).

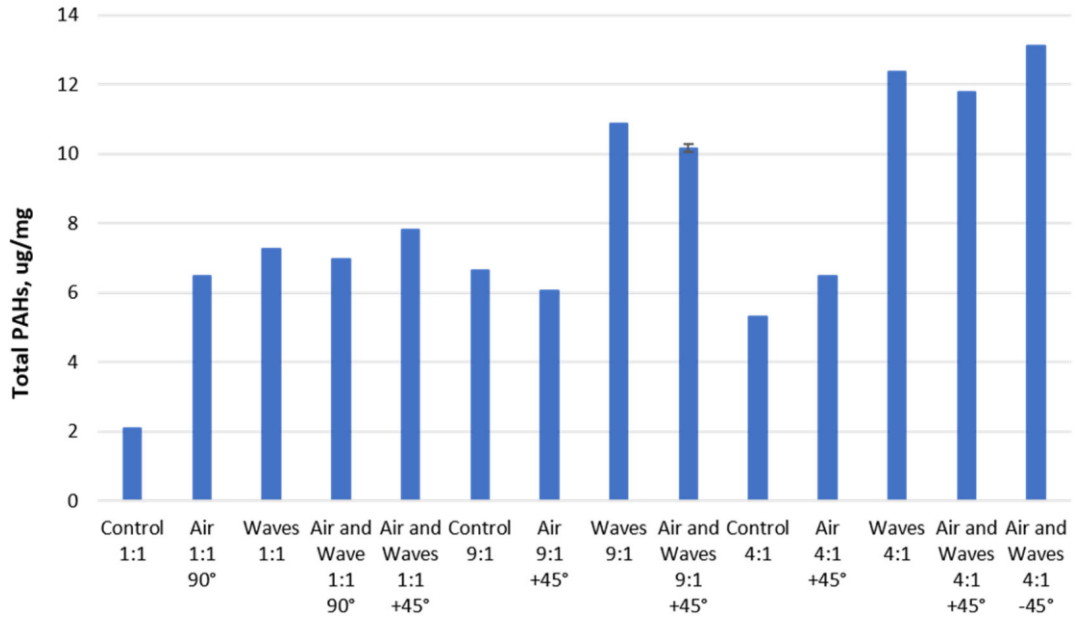

Figure 4-19. Residual total PAHs for each test configuration.

4.10.3 TPH

- Total petroleum hydrocarbons (TPH; as total extracted petroleum hydrocarbons) ranged from 0.08 g/g to 0.53 g/g for the various test configurations (Figure 4-20)
- On average, 0.3 g TPH per gram of post burn residue was detected (Table 4-16).
- Boom Ratio of 4:1 had the highest TPH concentration (0.37 ± 0.15 g/g, n=5) followed by 9:1 (0.33 ± 0.10 g/g, n=6) and 1:1 (0.22 ± 0.09 g/g, n=5).
- Air and Waves treatment had the highest TPH concentration (0.39 ± 0.10 g/g, n=7) followed by Waves (0.36 ± 0.07 g/g, n=3), Air (0.23 ± 0.01 g/g, n=3) and Control (0.16 ± 0.07 g/g, n=3)
- Nozzle Location of -45° had the highest TPH concentration (0.53 g/g; n=1), followed by +45° (0.34 ± 0.10 g/g, n=7), no nozzle (0.26 ± 0.13 g/g, n=6) and 90° (0.25 ± 0.02 g/g, n=2).

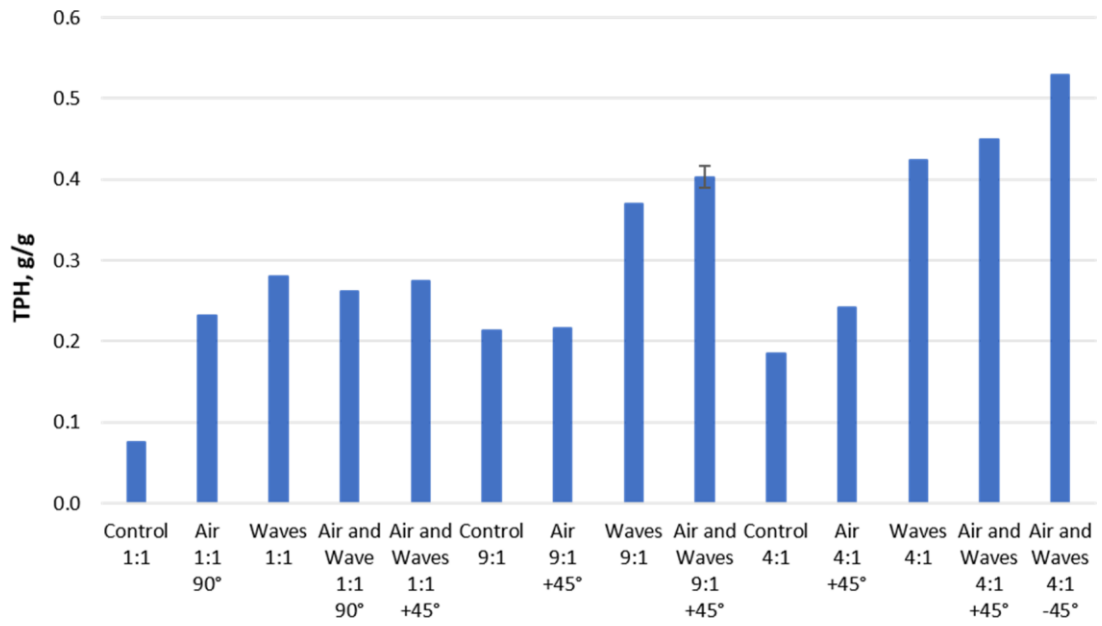

Figure 4-20. Residual TPH for each test configuration.

4.10.4 BTEX, Mass Loss, Combustion Efficiency, and Hydrocarbon Composition for each Test Configuration

- The total mass loss (from Section 4.1) and the BTEX, total alkanes, total PAHs and TPH results are summarized in Table 4-17 and reported graphically in Figure 4-21. Lower residual hydrocarbon concentrations are observed with increasing mass loss percent, indicating a more efficient burn (Figure 4-21).
- Boom Ratio of 4:1 had the highest burn residue hydrocarbon concentration, followed by 9:1 and 1:1. The highest mass loss was achieved for the 1:1 Boom Ratio (94.14 ± 1.55 %), followed by 9:1 (93.95 ± 4.52 %) and 4:1 (92.40 ± 4.03 %).
- Air and Waves treatment had the highest residual hydrocarbon concentration followed by Waves, Air, and Control. The highest mass loss was observed for the Control (97.00 ± 2.65 %), followed by Air (96.87 ± 1.65 %), Waves (91.87 ± 2.87 %) and Air and Waves (91.31 ± 2.52 %)
- Nozzle Location of -45° had the highest residual hydrocarbon concentration, followed by +45°, no nozzle, and 90°. The 90° nozzle treatment had the highest mass loss (94.95 ± 0.78 %), no nozzle (94.43 ± 3.74 %), +45° (93.01 ± 3.71 %), and -45° (88.80%).
- Analysis of TPH, Total PAHs, and BTEX emission factors versus MCE found only poor ($R^2 < 0.21$) correlations and are not shown here.

Table 4-14. Monoaromatic hydrocarbons (BTEX) concentration in raw crude oil and post-burn residuals for each test configuration.

Burn #	Test Condition	Configuration		Benzene		Toluene		Ethyl Benzene		m,p-Xylene		o-Xylene		Total BTEX
		Boom Ratio	Nozzle Location	*Avg.*	*Std. dev.*	*Avg.*	*Std. dev.*	*Avg.*	*Std. dev.*	*Avg.*	*Std. dev.*	*Avg.*	*Std. dev.*	*Avg.*
				ng/mg										
-	Raw Crude Oil	-	-	2071.12	96.33	4713.14	393.42	1572.06	56.49	5561.69	362.96	1985.43	123.34	15903
1	Control	1:1	No nozzle	<0.1	-	0.59	0.44	<0.1	-	<0.1	-	<0.1	-	0.59
2	Air	1:1	90°	2.82	0.23	18.00	3.94	0.73	0.94	2.89	3.79	2.37	1.88	24.43
3	Waves	1:1	No nozzle	7.24	1.46	29.59	6.16	5.75	1.13	23.95	3.96	10.63	3.22	66.53
4	Air and Waves	1:1	90°	10.05	1.72	30.13	6.91	7.73	3.12	25.98	12.70	11.17	4.59	73.89
5	Air and Waves	1:1	+45°	25.83	1.44	92.70	11.72	21.87	3.51	111.90	11.84	40.13	3.62	252.30
6	Control	9:1	No nozzle	1.46	0.39	15.98	2.23	5.15	2.55	1.61	1.49	20.69	6.79	23.67
7	Air	9:1	+45°	0.80	0.05	13.68	1.17	6.75	1.41	17.18	2.88	10.15	2.71	38.42
8	Waves	9:1	No nozzle	15.96	5.00	67.33	29.78	21.80	11.06	102.96	59.02	34.06	18.91	208.04
9	Air and Waves	9:1	+45°	15.86	2.30	66.47	23.07	26.63	11.41	106.61	51.76	38.83	19.25	215.57
10	Control	4:1	No nozzle	11.02	2.23	46.16	17.76	16.06	8.91	61.41	36.56	20.47	11.33	134.64
11	Air	4:1	+45°	15.89	2.10	63.77	13.13	19.98	6.05	74.58	21.50	22.86	8.16	174.22
12	Waves	4:1	No nozzle	18.47	0.44	64.02	3.68	20.03	1.63	90.49	9.36	30.95	1.33	193.01
13	Air and Waves	4:1	+45°	28.89	3.47	108.95	16.68	39.58	7.43	148.98	26.71	51.39	10.57	326.41
14	Air and Waves	4:1	-45°	28.58	3.24	139.99	24.51	62.97	12.73	236.53	44.93	88.80	16.45	468.06
15	Air and Waves	9:1	+45°	19.60	1.98	70.16	15.40	28.16	7.43	104.97	30.97	36.49	11.27	222.89
16	Air and Waves	9:1	+45°	18.89	5.48	77.43	22.56	32.01	11.16	121.17	39.89	43.16	14.32	249.50

Table 4-15. Composition of alkanes in raw crude oil and post-burn residuals for each test configuration.

Burn #	Date	Test Condition	Configuration		nC10-18		nC-19-27		nC28-35		Total Alkanes
			Boom Ratio	Nozzle Location	*Avg.*	*Std. Dev.*	*Avg.*	*Std. Dev.*	*Avg.*	*Std. Dev.*	*Avg.*
					µg/mg						
-	-	Raw crude oil	-	-	30.98		12.38		3.30		46.66
1	11/5/2018	Control	1:1	No nozzle	0.94	0.15	2.74	0.19	1.16	0.23	4.84
2	11/5/2018	Air	1:1	90°	3.00	0.21	7.48	0.24	3.44	0.10	13.92
3	11/5/2018	Waves	1:1	No nozzle	3.47	0.37	8.31	0.72	3.55	0.44	15.33
4	11/6/2018	Air and Waves	1:1	90°	3.40	0.07	7.64	0.24	3.01	0.15	14.05
5	11/6/2018	Air and Waves	1:1	+45°	4.22	0.26	8.32	0.68	3.28	0.39	15.83
6	11/7/2018	Control	9:1	No nozzle	3.25	0.85	8.31	1.31	3.11	0.44	14.67
7	11/7/2018	Air	9:1	+45°	2.54	0.04	7.45	0.39	3.40	0.16	13.39
8	11/7/2018	Waves	9:1	No nozzle	6.64	0.53	13.29	1.56	4.14	0.46	24.07
9	11/7/2018	Air and Waves	9:1	+45°	6.15	0.05	13.06	0.77	4.17	0.58	23.38
10	11/8/2018	Control	4:1	No nozzle	3.05	1.33	6.24	2.16	2.26	0.59	11.56
11	11/8/2018	Air	4:1	+45°	3.56	0.22	7.31	0.61	2.25	0.91	13.12
12	11/8/2018	Waves	4:1	No nozzle	9.03	1.61	15.08	2.72	4.48	1.19	28.59
13	11/8/2018	Air and Waves	4:1	+45°	8.97	0.51	13.95	0.76	4.01	0.99	26.93
14	11/8/2018	Air and Waves	4:1	-45°	11.84	0.47	15.13	0.72	3.52	0.58	30.48
15	11/9/2018	Air and Waves	9:1	+45°	7.09	0.38	12.35	0.85	3.61	0.70	23.04
16	11/9/2018	Air and Waves	9:1	+45°	7.17	1.07	12.26	1.50	3.53	0.49	22.96

Table 4-16. Composition of PAHs in raw crude oil and post-burn residuals for each test configuration.

Burn #	Date	Test Condition	Configuration		2-ring compounds		3-ring compounds		4-ring compounds		Total PAHs
			Boom Ratio	Nozzle Location	*Avg.*	*Std. Dev.*	*Avg.*	*Std. Dev.*	*Avg.*	*Std. Dev.*	*Avg.*
					µg/mg						
-	-	Raw crude oil	-	-	8.98		6.44		1.44		16.87
1	11/5/2018	Control	1:1	No nozzle	0.38	0.05	1.24	0.11	0.48	0.03	2.09
2	11/5/2018	Air	1:1	90°	1.50	0.12	3.62	0.07	1.35	0.08	6.47
3	11/5/2018	Waves	1:1	No nozzle	1.78	0.17	4.12	0.30	1.35	0.11	7.25
4	11/6/2018	Air and Waves	1:1	90°	1.82	0.10	3.80	0.17	1.35	0.09	6.97
5	11/6/2018	Air and Waves	1:1	+45°	2.06	0.17	3.95	0.31	1.81	0.05	7.82
6	11/7/2018	Control	9:1	No nozzle	1.37	0.34	3.72	0.53	1.53	0.32	6.63
7	11/7/2018	Air	9:1	+45°	1.23	0.02	3.42	0.17	1.41	0.17	6.07
8	11/7/2018	Waves	9:1	No nozzle	3.00	0.27	5.70	0.49	2.17	0.25	10.87
9	11/7/2018	Air and Waves	9:1	+45°	2.82	0.08	5.70	0.41	1.89	0.03	10.40
10	11/8/2018	Control	4:1	No nozzle	1.38	0.54	2.99	0.96	0.93	0.21	5.30
11	11/8/2018	Air	4:1	+45°	1.71	0.09	3.62	0.19	1.15	0.01	6.48
12	11/8/2018	Waves	4:1	No nozzle	4.03	0.68	6.79	1.20	1.56	0.26	12.37
13	11/8/2018	Air and Waves	4:1	+45°	3.77	0.25	6.16	0.24	1.86	0.22	11.79
14	11/8/2018	Air and Waves	4:1	-45°	4.65	0.22	6.74	0.30	1.70	0.27	13.10
15	11/9/2018	Air and Waves	9:1	+45°	3.10	0.16	5.52	0.39	1.57	0.24	10.18
16	11/9/2018	Air and Waves	9:1	+45°	3.03	0.44	5.36	0.65	1.52	0.14	9.91

Table 4-17. Summary of hydrocarbon composition vs. percent loss in post-burn residue.

Burn #	Date	Test Condition	Boom Ratio	Nozzle Location	Mass loss (%)	BTEX (ng/mg)	Total Alkanes (ug/mg)	Total PAHs (ug/mg)	TPH (g/g)
1	11/5/2018	Control	1:1	No nozzle	94.3	0.6	4.8	2.1	0.075
2	11/5/2018	Air	1:1	90°	95.5	24.4	13.9	6.5	0.231
3	11/5/2018	Waves	1:1	No nozzle	91.5	66.5	15.3	7.3	0.280
4	11/6/2018	Air and Waves	1:1	90°	94.4	73.9	14.0	7.0	0.262
5	11/6/2018	Air and Waves	1:1	+45°	95.0	252.3	15.8	7.8	0.275
6	11/7/2018	Control	9:1	No nozzle	99.6	23.7	14.7	6.6	0.213
7	11/7/2018	Air	9:1	+45°	98.7	38.4	13.4	6.1	0.216
8	11/7/2018	Waves	9:1	No nozzle	94.9	208.0	24.1	10.9	0.369
9	11/7/2018	Air and Waves	9:1	+45°	89.2	215.6	23.4	10.4	0.371
10	11/8/2018	Control	4:1	No nozzle	97.1	134.6	11.6	5.3	0.184
11	11/8/2018	Air	4:1	+45°	96.4	174.2	13.1	6.5	0.242
12	11/8/2018	Waves	4:1	No nozzle	89.2	193.0	28.6	12.4	0.424
13	11/8/2018	Air and Waves	4:1	+45°	90.5	326.4	26.9	11.8	0.450
14	11/8/2018	Air and Waves	4:1	-45°	88.8	468.1	30.5	13.1	0.529
15	11/9/2018	Air and Waves	9:1	+45°	89.5	222.9	23.0	10.2	0.420
16	11/9/2018	Air and Waves	9:1	+45°	91.8	249.5	23.0	9.9	0.416

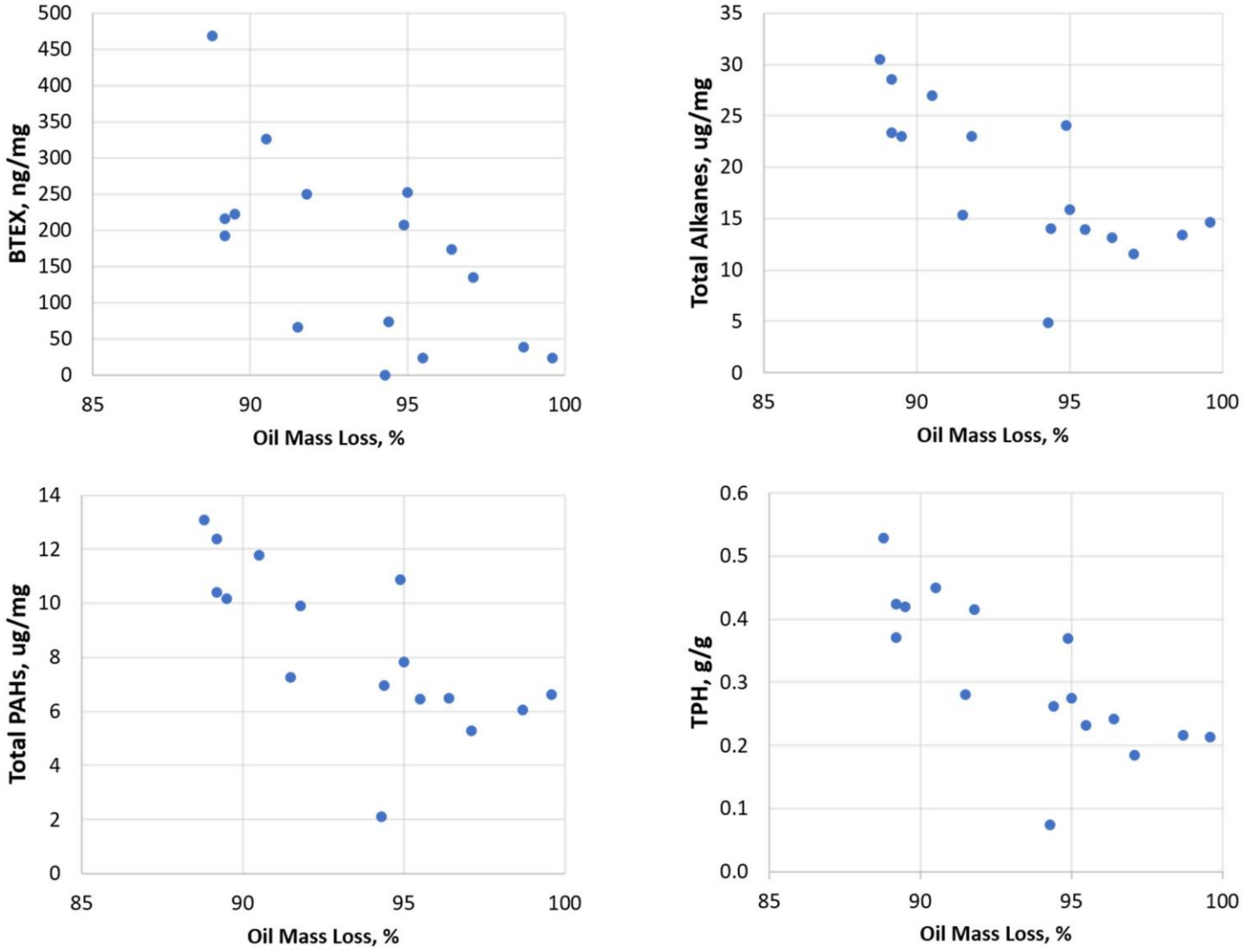

Figure 4-21. Hydrocarbon composition vs. percent loss in post-burn residue.

4.10.5 Water Samples

In addition to the burn residue sample, a one-liter water sample was collected from the tank at the end of each burn and analyzed for BTEX, alkanes, PAHs and TPH, the results of which are summarized in Table 4-18.

Table 4-18. BTEX, total alkanes, total PAHs and TPH in the water sample.

Burn Number	Date	Test Condition	Configuration		BTEX	Total Alkanes	Total PAHs	TPH
			Boom Ratio	Nozzle location	*ng/L*	*µg/L*	*µg/L*	*mg/L*
1	11/5/2018	Control	1:1	No nozzle	74.3	5.9	13.6	1.049
2	11/5/2018	Air	1:1	90°	287.5	7.9	19.5	0.938
3	11/5/2018	Waves	1:1	No nozzle	177.1	18.9	20.1	1.101
4	11/6/2018	Air and Waves	1:1	90°	376.9	3.3	7.8	0.663
5	11/6/2018	Air and Waves	1:1	+45°	532.6	3.3	7.7	0.870
6	11/7/2018	Control	9:1	No nozzle	368.0	263.7	107.9	5.758
7	11/7/2018	Air	9:1	+45°	590.7	70.3	48.4	2.530
8	11/7/2018	Waves	9:1	No nozzle	214.0	38.3	32.8	1.278
9	11/7/2018	Air and Waves	9:1	+45°	160.1	14.9	33.6	1.743
10	11/8/2018	Control	4:1	No nozzle	300.5	8.4	15.7	0.693
11	11/8/2018	Air	4:1	+45°	408.8	3.4	8.5	0.768
12	11/8/2018	Waves	4:1	No nozzle	982.5	6.8	22.0	0.852
13	11/8/2018	Air and Waves	4:1	+45°	4319.9	3.9	16.9	0.797
14	11/8/2018	Air and Waves	4:1	-45°	13073.6	81.5	132.2	4.516
15	11/9/2018	Air and Waves	9:1	+45°	1302.2	118.8	76.6	2.698
16	11/9/2018	Air and Waves	9:1	+45°	598.3	23.8	39.4	1.199

5 CONCLUSIONS

Oil mass loss ranged from 88.8% to 99.6%. The three-run average Control oil mass loss was 97%, a value greater than 12 of the 13 remaining runs in which waves and air were introduced. The Air tests had virtually the same oil weight loss as the Control at 96.87%. The three Waves-only tests resulted in an average mass loss of 91.9%; this value was virtually unchanged with the addition of air (91.3%, n=3). The presence of Waves, regardless of Air or Boom Ratio condition, always lowered the oil weight loss.

MCE calculated using gas and particle carbon averaged 0.89 and ranged from 0.85 to 0.93. Higher Boom Ratios have higher MCE values than lower Boom Ratios and higher oil weight loss, but only in the absence of waves. The highest MCE, 0.92, was observed at the highest Boom Ratio, 9:1. This is possibly due to more efficient air penetration into the flame zone due to the thinner oil slick configuration. High MCE values can still be associated with lower mass loss fractions (Figure 4-5) depending on other conditions. Residue emission factors (the mass concentration per mass of residue) declined with increasing oil mass loss but no such correlation was found with MCE values.

The particle number concentration was dominated by particles < 100 nm. The particle size distributions generally did not change throughout the burn period. Emission factors ($PM_{2.5}$) show a strong ($R^2 = 0.84$) negative correlation with MCE. The run with the highest MCE value resulted in $PM_{2.5}$ emission factors about three times lower than the lowest MCE runs. The MCE values decline with the burn; $PM_{2.5}$ samples collected in the second half of the burns had higher emission factors. $PM_{2.5}$ emission factors showed no trend with oil mass loss. Like $PM_{2.5}$, VOC emission factors showed a strong negative trend with increasing MCE.

6 REFERENCES

40 CFR Part 50, Appendix L, 1987. Reference method for the determination of particulate matter as PM2.5 in the Atmosphere. https://www.gpo.gov/fdsys/pkg/CFR-2014-title40-vol2/pdf/CFR-2014-title40-vol2-part50-appL.pdf, Accessed February, 2019.

U.S. EPA Test Method 0023a. SW-846 (NTIS PB88-239223), 1996.

U.S. EPA Compendium Method TO-11A, 1999a. Determination of Formaldehyde in Ambient Air Using Adsorbent Cartridge Followed by High Performance Liquid Chromatography (HPLC). https://www3.epa.gov/ttnamti1/files/ambient/airtox/to-11ar.pdf, Accessed July 25, 2016.

U.S. EPA Compendium Method IO-3.3, 1999b. Determination of metals in ambient particulate matter using X-Ray Fluorescence (XRF) Spectroscopy. http://www.epa.gov/ttnamti1/files/ambient/inorganic/mthd-3-3.pdf, Accessed February 13, 2019.

U.S. EPA Compendium Method TO-9A, 1999c. Determination of polychlorinated, polybrominated and brominated/chlorinated dibenzo-p-dioxins and dibenzofurans in ambient air. http://www.epa.gov/ttnamti1/files/ambient/airtox/to-9arr.pdf, Accessed February 13, 2019.

U.S. EPA Compendium Method TO-15, 1999d. Determination of volatile organic compounds (VOCs) in air collected in specially-prepared canisters and analyzed by gas chromatography/mass spectrometry (GC/MS). http://www.epa.gov/ttnamti1/files/ambient/airtox/to-15r.pdf, Accessed February 13, 2019.

NIOSH Method 5040, 1999e. Elemental Carbon (Diesel Particulate). https://www.cdc.gov/niosh/docs/2003-154/pdfs/5040.pdf

U.S. EPA Method 8270D (SW-846), 2007. Semivolatile Organic Compounds by Gas Chromatography/Mass Spectrometry (GC/MS). http://www.epa.gov/osw/hazard/testmethods/sw846/pdfs/8270d.pdf, Accessed April 24, 2015.

U.S. EPA Method 524.3, 2009. Measure of purgeable organic compounds in water by capillary column gas chromatography/mass sepectrometry. https://www.nemi.gov/methods/method_summary/10417/, Accessed February 13, 2019.

U.S. EPA Method 25C, 2017a. Determination of nonmethane organic compounds (NMOC) in landfill gases. https://www.epa.gov/sites/production/files/2017-08/documents/method_25c.pdf, Accessed February 12, 2019.

U.S. EPA Method 3A, 2017b. Determination of oxygen and carbon dioxide concentrations in emissions from stationary sources (instrumental analyzer procedure). https://www.epa.gov/sites/production/files/2017-08/documents/method_3a.pdf, Accessed February 12, 2019.

U.S. EPA Method 8015D, n.d. Nonhalogenated organics using GC/FID. https://www.epa.gov/sites/production/files/2015-12/documents/8015d_r4.pdf, Accessed February 13, 2019.

Agency., U.S.E.P., February 2007. Method 8290A. Polychlorinated dibenzo-p-dioxins (PCDDs) and polychlorinated dibenzofurans (PCDFs) by high-resolution gas chromatography/high-

resolution mass spectrometry (HRGC/HRMS). In Test Methods for Evaluating Solid Waste, Physical/Chemical Methods; SW-846. Washington, D.C., Revision 1 www.epa.gov/wastes/hazard/testmethods/sw846/pdfs/8290a.pdf.

Aurell, J., Gullett, B.K., 2010. Aerostat Sampling of PCDD/PCDF Emissions from the Gulf Oil Spill In Situ Burns. Environ Sci Technol 44, 9431-9437.

Gullett, B.K., Aurell, J., Holder, A., Mitchell, W., Greenwell, D., Hays, M., Conmy, R., Tabor, D., Preston, W., George, I., Abrahamson, J.P., Vander Wal, R., Holder, E., 2017. Characterization of emissions and residues from simulations of the Deepwater Horizon surface oil burns. Marine Pollution Bulletin 117, 392-405.

Gullett, B.K., Hays, M.H., Tabor, D., Vander Wal, R., 2016. Characterization of the Particulate Emissions from the BP Deepwater Horizon Spill Surface Oil Burns. Marine Pollution Bulletin 107, 216-223.

Khan, B., Hays, M.D., Geron, C., Jetter, J., 2012. Differences in the OC/EC Ratios that Characterize Ambient and Source Aerosols due to Thermal-Optical Analysis. Aerosol Science and Technology 46, 127-137.

Koseki, H., 2000. Large Scale Pool Fires: Results Of Recent Experiments. Fire Safety Science 6, 115-132.